National Library
of Canada

Bibliothèque nationale
du Canada

Canadian Theses Service

Service des thèses canadiennes

Ottawa, Canada
K1A 0N4

NOTICE

The quality of this microform is heavily dependent upon the quality of the original thesis submitted for microfilming. Every effort has been made to ensure the highest quality of reproduction possible.

If pages are missing, contact the university which granted the degree.

Some pages may have indistinct print especially if the original pages were typed with a poor typewriter ribbon or if the university sent us an inferior photocopy.

Reproduction in full or in part of this microform is governed by the Canadian Copyright Act, R.S.C. 1970, c. C-30, and subsequent amendments.

AVIS

La qualité de cette microforme dépend grandement de la qualité de la thèse soumise au microfilmage. Nous avons tout fait pour assurer une qualité supérieure de reproduction.

S'il manque des pages, veuillez communiquer avec l'université qui a conféré le grade.

La qualité d'impression de certaines pages peut laisser à désirer, surtout si les pages originales ont été dactylographiées à l'aide d'un ruban usé ou si l'université nous a fait parvenir une photocopie de qualité inférieure.

La reproduction, même partielle, de cette microforme est soumise à la Loi canadienne sur le droit d'auteur, SRC 1970, c. C-30, et ses amendements subséquents.

NL-339 (r. 88/04) c

Canada

UNIVERSITY OF ALBERTA

Slenderness Effects in Eccentrically Loaded Masonry Walls

by

Mohammad Abdul Muqtadir

A THESIS
SUBMITTED TO THE FACULTY OF GRADUATE STUDIES AND
RESEARCH IN PARTIAL FULFILMENT OF THE REQUIREMENTS
FOR THE DEGREE OF DOCTOR OF PHILOSOPHY

DEPARTMENT OF CIVIL ENGINEERING

EDMONTON, ALBERTA
Spring, 1991

National Library of Canada
Bibliothèque nationale du Canada

Canadian Theses Service
Service des thèses canadiennes

Ottawa, Canada
K1A 0N4

The author has granted an irrevocable non-exclusive licence allowing the National Library of Canada to reproduce, loan, distribute or sell copies of his/her thesis by any means and in any form or format, making this thesis available to interested persons.

The author retains ownership of the copyright in his/her thesis. Neither the thesis nor substantial extracts from it may be printed or otherwise reproduced without his/her permission.

L'auteur a accordé une licence irrévocable et non exclusive permettant à la Bibliothèque nationale du Canada de reproduire, prêter, distribuer ou vendre des copies de sa thèse de quelque manière et sous quelque forme que ce soit pour mettre des exemplaires de cette thèse à la disposition des personnes intéressées.

L'auteur conserve la propriété du droit d'auteur qui protège sa thèse. Ni la thèse ni des extraits substantiels de celle-ci ne doivent être imprimés ou autrement reproduits sans son autorisation.

ISBN 0-315-66828-8

Canadä

UNIVERSITY OF ALBERTA
RELEASE FORM

NAME OF AUTHOR: MOHAMMAD ABDUL MUQTADIR

TITLE OF THESIS: SLENDERNESS EFFECTS IN ECCENTRICALLY LOADED MASONRY WALLS

DEGREE: DOCTOR OF PHILOSOPHY

YEAR THIS DEGREE GRANTED: SPRING 1991

Permission is hereby granted to the University of Alberta Library to reproduce single copies of this thesis and to lend or sell such copies for private, scholarly or scientific research purposes only.

The author reserves other publication rights, and neither the thesis nor extensive extracts from it may be printed or otherwise reproduced without the author's written permission.

(signed)

PERMANENT ADDRESS:
2200 Roche Court, Apt. 907
Mississauga, Ontario
L5K 3Z6

Date : April 24, 1991.

UNIVERSITY OF ALBERTA

FACULTY OF GRADUATE STUDIES AND RESEARCH

The undersigned certify that they have read, and recommend to the Faculty of Graduate Studies and Research for acceptance, a thesis entitled "SLENDERNESS EFFECTS IN ECCENTRICALLY LOADED MASONRY WALLS" submitted by MOHAMMAD ABDUL MUQTADIR in partial fulfillment of the requirements for the degree of DOCTOR OF PHILOSOPHY in Civil Engineering.

Dr. J. Warwaruk (Supervisor)

Dr. J. G. MacGregor

Dr. A. E. Elwi

M. Hatzinikolas
Dr. M. A. Hatzinikolas

F.E. Hicks
Dr. F. Hicks

JSKennedy
Dr. J. S. Kennedy

Dr. J. Glanville (External Examiner)

Date : April 11 1991

To Ammi and Abba

who are an inspiring example to me due to their courageous spirit and loving sacrifice.

ABSTRACT

Slender Masonry walls are analyzed as beam-columns using the Column Deflection Curve Method and Newmark's Numerical Method. The Load-Moment-Curvature based analytical model is verified using experimental data and differential equation solutions.

The variation of EI values is studied for different combinations of axial load and bending moment. Simple equations for EI values are proposed as a function of load and moment over the cross section. The Moment Magnifier Method using these new EI values is found to give results similar to the analytical model. This new approach is demonstrated to be better than the current approach in the CSA standard CAN3-S304-M84 and therefore can be used as a simple design procedure.

The analytical model developed in this study can be used to generate behavioural information for cases where no experimental data is currently available and thus facilitate in the development of the limit states design method for slender masonry walls.

ACKNOWLEDGEMENTS

I wish to express my gratitude to my supervisor Prof. J. Warwaruk for his valuable suggestions and unstinted support throughout the period of my study. I shall always treasure his advice about matters both academic and personal.

My heartfelt thanks are extended to Dr. M. A. Hatzinikolas, Director Prairie Masonry Research Institute for his constant encouragement and his keen interest in my project.

I deeply appreciate the advice and assistance I received from Prof. J. Longworth during the early phase of my research.

I am thankful for the financial assistance I received from the the Civil Engineering Department of the University of Alberta, Natural Science and Engineering Research Council, Prairie Masonry Research Institute and the Edward Sim Memorial Scholarship Fund.

I am grateful to my brother M. A. Saleem for being a source of inspiration to me since childhood and for encouraging me to pursue graduate studies in Canada.

Throughout the course of my research I was fortunate to have the invaluable support of my parents, Abbu and Mummy in India and members of my family in USA and Saudi Arabia.

Finally, I wish to thank my wife Rafath, for her patience and understanding during my studies. She has been a comforting companion and has always walked spiritedly beside me towards the fulfilment of our dreams.

TABLE OF CONTENTS

Chapter Page

1. Introduction 1
   1.1 Objective and Scope of the Thesis 3
   1.2 Organization of the Thesis 4
2. Literature Review 5
   2.1 Introduction 5
   2.2 Experimental Studies on Slender Masonry Walls 5
   2.3 Analytical Methods for Slender Walls 8
   2.4 Code Procedures for the Design of Slender Walls 10
      2.4.1 The Reduction Factors Method 11
      2.4.2 The Moment Magnifier Method 12
      2.4.3 The Displacement Method 15
3. Behaviour of Masonry under Eccentric Compression.... 16
   3.1 Introduction 16
   3.2 Axial and Eccentric Failures 16
   3.3 Failure Criterion of Masonry in Eccentric Compression 17
   3.4 Stress-Strain Relationship 19
   3.5 Strength Interaction Diagrams 20
4. Analysis Methods for Slender Masonry Walls 27
   4.1 Introduction 27
   4.2 Development of Analysis Methods 27
   4.3 Development of Load-Moment-Curvature Relationship 29
   4.4 Column Deflection Curve Method 31

4.4.1 Computation of CDCs.. 31
4.4.2 Application of CDC Technique........................ 33
4.5 Newmark's Numerical Method.................................. 34
4.6 Unwinding Phenomenon.. 37
5. Verification of the Analysis Method.................................. 45
5.1 Introduction.. 45
5.2 Comparison with an Exact Solution......................... 45
5.3 Experimental Verification.. 46
6. Development of Approximate Method.............................. 58
6.1 Introduction.. 58
6.2 Development of Approximate Method..................... 58
6.3 Evaluation of EI from P-M-Φ 62
6.4 Simplified Method to Calculate Flexural Rigidity..... 65
6.5 Assessment of Accuracy of EI Values..................... 69
6.6 Parametric Study... 71
6.6.1 Summary of Approximate for Slender Walls 72
6.7 Comparison with Tests.. 74
6.8 Assessment of Approximate Method........................ 76
7. Summary, Conclusions and Recommendations............... 127
7.1 Summary.. 127
7.2 Conclusions.. 127
7.3 Recommendations for Future Research.................. 129
References 130

Appendix

A. Listing of the Program using CDC Method.............. 135
B. Listing of the Program using Newmark's Numerical Method.. 146

LIST OF TABLES

Table Page

3.1 Prism Tests Under Eccentric Compression by Drysdale 21

3.2 Prism Tests Under Eccentric Compression by Hatzinikolas... 22

3.3 Prism Tests Under Eccentric Compression by Fattal... 22

LIST OF FIGURES

Figure Page

3.1 Eccentric Compressive Strength vs Prism Strength 23

3.2 Eccentric Compressive Strength vs Unit Strength 23

3.3 Assesment of Proposed Stress Strain Parameters Wall HC3 24

3.4 Assesment of Proposed Stress Strain Parameters Wall HC5 24

3.5 Comparison of New Criteria with Experiments by Drysdale (NB190) 25

3.6 Comparison of New Criteria with Experiments by Drysdale (NB140) 25

3.7 Comparison of New Criteria with Experiments by Drysdale (NB190NG) 26

3.8 Comparison of New Criteria with Experiments by Drysdale (NB140NG) 26

4.1 Masonry Wall Cross-section used in the Analysis 38

4.2 P-M-Φ Relationships for Reinforced Masonry 39

4.3 Use of Column Deflection Curves.. 40

4.4 Newmark's Numerical Procedure to Calculate Deflections ... 41

4.5 Concentration Formulae for Parabolic Distribution 42

4.6 Flow Chart for Column Deflection Curve Method 43

4.7 Flow Chart for Newmark's Numerical Method 44

5.1 A Comparison of Stress Strain Curves 50

5.2 Comparison with Angervo's Solution, H/t=12, t= 7.6 in 50

5.3 Comparison with Angervo's Solution, H/t=15, t= 7.6 in 51

5.4 Comparison with Angervo's Solution, H/t=22, t= 7.6 in 51

5.5 Plain Masonry Walls in Single Curvature Bending $e_2/e_1 = 1.0$, H/t = 14 , H = 105 in. 52

5.6 Plain Masonry Walls in Single Curvature Bending $e_2/e_1 = 0.0$, H/t = 18 , H = 137 in. 52

5.7 Plain Masonry Walls in Single Curvature Bending $e_2/e_1 = -1.0$, H/t = 18 , H = 137 in. 53

5.8 Reinforced Walls in Single Curvature Bending $e_2/e_1 = 1.0$, H/t =14 , H =105 in., As=3.0 Sq.in. 53

5.9 Reinforced Walls in Single Curvature Bending $e_2/e_1 = 1.0$, H/t =16 , H =122 in., As=3.0 Sq.in. 54

5.10 Reinforced Walls in Single Curvature Bending $e_2/e_1 = 1.0$, H/t =18 , H =137 in., As=3.0 Sq.in. 54

5.11 Reinforced Walls in Single Curvature Bending $e_2/e_1 = 1.0$, H/t =24 , H =183 in., As=3.0 Sq.in. 55

5.12 Reinforced Walls in Single Curvature Bending e_2/e_1 = 1.0, H/t =18 , H =137 in., As=1.32 Sq.in. 55

5.13 Reinforced Walls in Single Curvature Bending e_2/e_1 = 1.0, H/t =18 , H =137 in., As=0.33 Sq.in. 56

5.14 Reinforced Walls in Double Curvature Bending e_2/e_1 =-1.0, H/t =18 , H =137 in., As=0.33 Sq.in. 56

5.15 Deflection histories indicating unwinding of a reinforced wall e_2/e_1 =-1.0, H/t =18 , H =137 in., ... 57

6.1 Variation of Flexural Rigidityfor Fully Bedded Plain Masonry Walls 77

6.2 Variation of Flexural Rigidityfor Face-shell Bedded Plain Masonry Walls 78

6.3 Variation of Flexural Rigidityfor Reinforced Walls As = Balanced Reinforcement 79

6.4 Variation of Flexural Rigidityfor Reinforced Walls As = 0.5 * Balanced Reinforcement 80

6.5 Variation of Flexural Rigidityfor Reinforced Walls As = Minimum Reinforcement 81

6.6 Evaluation of Flexural Rigidityfor Fully Bedded Plain Masonry, P/Po = 0.1 82

6.7 Evaluation of Flexural Rigidityfor Fully Bedded Plain Masonry, P/Po = 0.2 82

6.8 Evaluation of Flexural Rigidityfor Fully Bedded Plain Masonry, P/Po = 0.3 83

6.9 Evaluation of Flexural Rigidityfor Fully Bedded Plain Masonry, P/Po = 0.4 83

6.10 Evaluation of Flexural Rigidityfor Fully Bedded Plain Masonry, P/Po = 0.5 84

6.11 Evaluation of Flexural Rigidityfor Fully Bedded Plain Masonry, P/Po = 0.6 84

6.12 Evaluation of Flexural Rigidityfor Fully Bedded Plain Masonry, P/Po = 0.7 85

6.13 Evaluation of Flexural Rigidityfor Fully Bedded Plain Masonry, P/Po = 0.8 85

6.14 Evaluation of Flexural Rigidityfor Faceshell Bedded Plain Masonry, P/Po = 0.1 86

6.15 Evaluation of Flexural Rigidityfor Faceshell Bedded Plain Masonry, P/Po = 0.2 86

6.16 Evaluation of Flexural Rigidityfor Faceshell Bedded Plain Masonry, P/Po = 0.3 87

6.17 Evaluation of Flexural Rigidityfor Faceshell Bedded Plain Masonry, P/Po = 0.4 87

6.18 Evaluation of Flexural Rigidityfor Faceshell Bedded Plain Masonry, P/Po = 0.5 88

6.19 Evaluation of Flexural Rigidityfor Faceshell Bedded Plain Masonry, P/Po = 0.6 88

6.20 Evaluation of Flexural Rigidityfor Faceshell Bedded Plain Masonry, P/Po = 0.7 89

6.21 Evaluation of Flexural Rigidityfor Faceshell Bedded Plain Masonry, P/Po = 0.8 89

6.22 Evaluation of Flexural Rigidityfor Reinforced Masonry As = Balanced Reinforcement, P/Po = 0.1 90

6.23 Evaluation of Flexural Rigidityfor Reinforced Masonry As = Balanced Reinforcement, P/Po = 0.2 90

6.24 Evaluation of Flexural Rigidityfor Reinforced Masonry As = Balanced Reinforcement, P/Po = 0.3 91

6.25 Evaluation of Flexural Rigidityfor Reinforced Masonry As = Balanced Reinforcement, P/Po = 0.4 91

6.26 Evaluation of Flexural Rigidityfor Reinforced Masonry As = Balanced Reinforcement, P/Po = 0.5 92

6.27 Evaluation of Flexural Rigidityfor Reinforced Masonry As = Balanced Reinforcement, P/Po = 0.6 92

6.28 Evaluation of Flexural Rigidityfor Reinforced Masonry As = Balanced Reinforcement, P/Po = 0.7 93

6.29 Evaluation of Flexural Rigidityfor Reinforced Masonry As = Balanced Reinforcement, P/Po = 0.8 93

6.30 Evaluation of Flexural Rigidityfor Reinforced Masonry As = 0.5 * Balanced Reinforcement, P/Po = 0.1 94

6.31 Evaluation of Flexural Rigidityfor Reinforced Masonry As = 0.5 * Balanced Reinforcement, P/Po = 0.2 94

6.32 Evaluation of Flexural Rigidityfor Reinforced Masonry As = 0.5 * Balanced Reinforcement, P/Po = 0.3 95

6.33 Evaluation of Flexural Rigidityfor Reinforced Masonry As = 0.5 * Balanced Reinforcement, P/Po = 0.4 95

6.34 Evaluation of Flexural Rigidityfor Reinforced Masonry As = 0.5 * Balanced Reinforcement, P/Po = 0.5 96

6.35 Evaluation of Flexural Rigidityfor Reinforced Masonry As = 0.5 * Balanced Reinforcement, P/Po = 0.6 96

6.36 Evaluation of Flexural Rigidityfor Reinforced Masonry As = 0.5 * Balanced Reinforcement, P/Po = 0.7 97

6.37 Evaluation of Flexural Rigidityfor Reinforced Masonry As = 0.5 * Balanced Reinforcement, P/Po = 0.8 97

6.38 Evaluation of Flexural Rigidityfor Reinforced Masonry As = Minimum Reinforcement, P/Po = 0.1 98

6.39 Evaluation of Flexural Rigidityfor Reinforced Masonry As = Minimum Reinforcement, P/Po = 0.2 98

6.40 Evaluation of Flexural Rigidityfor Reinforced Masonry As = Minimum Reinforcement, P/Po = 0.3 99

6.41 Evaluation of Flexural Rigidityfor Reinforced Masonry As = Minimum Reinforcement, P/Po = 0.4 99

6.42 Evaluation of Flexural Rigidityfor Reinforced Masonry As = Minimum Reinforcement, P/Po = 0.5 100

6.43 Evaluation of Flexural Rigidityfor Reinforced Masonry As = Minimum Reinforcement, P/Po = 0.6 100

6.44 Evaluation of Flexural Rigidityfor Reinforced Masonry As = Minimum Reinforcement, P/Po = 0.7 101

6.45 Evaluation of Flexural Rigidityfor Reinforced Masonry As = Minimum Reinforcement, P/Po = 0.8 101

6.46 Comparison of Analysis Methods for Faceshell Bedded Plain Masonry Wall, H/t = 15, e_2/e_1 = 1.0 102

6.47 Comparison of Analysis Methods for Faceshell Bedded Plain Masonry Wall, H/t = 20, e_2/e_1 = 1.0 102

6.48 Comparison of Analysis Methods for Faceshell Bedded Plain Masonry Wall, H/t = 25, e_2/e_1 = 1.0 103

6.49 Comparison of Analysis Methods for Faceshell Bedded Plain Masonry Wall, H/t = 30, e_2/e_1 = 1.0 103

6.50 Comparison of Analysis Methods for Faceshell Bedded Plain Masonry Wall, H/t = 15, e_2/e_1 = 0.0 104

6.51 Comparison of Analysis Methods for Faceshell Bedded Plain Masonry Wall, H/t = 20, e_2/e_1 = 0.0 104

6.52 Comparison of Analysis Methods for Faceshell Bedded Plain Masonry Wall, H/t = 25, e_2/e_1 =0.0 105

6.53 Comparison of Analysis Methods for Faceshell Bedded Plain Masonry Wall, H/t = 30, e_2/e_1 = 0.0 105

6.54 Comparison of Analysis Methods for Faceshell Bedded Plain Masonry Wall, H/t = 15, e_2/e_1 =-1.0 106

6.55 Comparison of Analysis Methods for Faceshell Bedded Plain Masonry Wall, H/t = 20, e_2/e_1 =-1.0 106

6.56 Comparison of Analysis Methods for Fully Bedded Plain Masonry Wall, H/t = 25, e_2/e_1 = -1.0 107

6.57 Comparison of Analysis Methods for Fully Bedded Plain Masonry Wall, H/t = 30, e_2/e_1 = -1.0 107

6.58 Comparison of Analysis Methods for Fully Bedded Plain Masonry Wall, H/t = 15, e_2/e_1 = 1.0 108

6.59 Comparison of Analysis Methods for Fully Bedded Plain Masonry Wall, H/t = 20, e_2/e_1 = 1.0 108

6.60 Comparison of Analysis Methods for Fully Bedded Plain Masonry Wall, H/t = 25, e_2/e_1 = 1.0 109

6.61 Comparison of Analysis Methods for Fully Bedded Plain Masonry Wall, H/t = 30, e_2/e_1 = 1.0 109

6.62 Comparison of Analysis Methods for Fully Bedded Plain Masonry Wall, H/t = 15, e_2/e_1 = 0.0 110

6.63 Comparison of Analysis Methods for Fully Bedded Plain Masonry Wall, H/t = 20, e_2/e_1 = 0.0 110

6.64 Comparison of Analysis Methods for Fully Bedded Plain Masonry Wall, H/t = 25, e_2/e_1 = 0.0 111

6.65 Comparison of Analysis Methods for Fully Bedded Plain Masonry Wall, H/t = 30, e_2/e_1 = 0.0 111

6.66 Comparison of Analysis Methods for Fully Bedded Plain Masonry Wall, H/t = 15, e_2/e_1 =-1.0 112

6.67 Comparison of Analysis Methods for Fully Bedded Plain Masonry Wall, H/t = 20, e_2/e_1 =-1.0 112

6.68 Comparison of Analysis Methods for Fully Bedded Plain Masonry Wall, H/t = 25, e_2/e_1 = -1.0 113

6.69 Comparison of Analysis Methods for Fully Bedded Plain Masonry Wall, H/t = 30, e_2/e_1 = -1.0 113

6.70 Comparison of Analysis Methods for Fully Grouted Reinforced Masonry Wall, H/t = 15, e_2/e_1 = 1.0 114

6.71 Comparison of Analysis Methods for Fully Grouted Reinforced Masonry Wall, H/t = 20, e_2/e_1 = 1.0 114

6.72 Comparison of Analysis Methods for Fully Grouted Reinforced Masonry Wall, H/t = 25, e_2/e_1 = 1.0 115

6.73 Comparison of Analysis Methods for Fully Grouted Reinforced Masonry Wall, H/t = 30, e_2/e_1 = 1.0 115

6.74 Comparison of Analysis Methods for Fully Grouted Reinforced Masonry Wall, H/t = 15, e_2/e_1 = 0.0 116

6.75 Comparison of Analysis Methods for Fully Grouted Reinforced Masonry Wall, H/t = 20, e_2/e_1 = 0.0 116

6.76 Comparison of Analysis Methods for Fully Grouted Reinforced Masonry Wall, H/t = 25, e_2/e_1 = 0.0 117

6.77 Comparison of Analysis Methods for Fully Grouted Reinforced Masonry Wall, H/t = 30, e_2/e_1 = 0.0 117

6.78 Comparison of Analysis Methods for Fully Grouted Reinforced Masonry Wall, H/t = 15, e_2/e_1 =-1.0 118

6.79 Comparison of Analysis Methods for Fully Grouted Reinforced Masonry Wall, H/t = 20, e_2/e_1 =-1.0 118

6.80 Comparison of Analysis Methods for Fully Grouted Reinforced Masonry Wall, H/t = 25, e_2/e_1 =-1.0 119

6.81 Comparison of Analysis Methods for Fully Grouted Reinforced Masonry Wall, $H/t = 30$, $e_2/e_1 = -1.0$ 119

6.82 Tests on Plain Masonry Walls in Single Curvature Bending $e_2/e_1 = 1.0$, $H/t = 14$, $H = 105$ in. 120

6.83 Tests on Plain Masonry Walls in Single Curvature Bending $e_2/e_1 = 0.0$, $H/t = 18$, $H = 137$ in. 120

6.84 Tests on Plain Masonry Walls in Single Curvature Bending $e_2/e_1 = -1.0$, $H/t = 18$, $H = 137$ in. 121

6.85 Tests on Reinforced Walls in Single Curvature Bending $e_2/e_1 = 1.0$, $H/t = 14$, $H = 105$ in., $As = 3.0$ Sq.in. 121

6.86 Tests on Reinforced Walls in Single Curvature Bending $e_2/e_1 = 1.0$, $H/t = 16$, $H = 122$ in., $As = 3.0$ Sq.in. 122

6.87 Tests on Reinforced Walls in Single Curvature Bending $e_2/e_1 = 1.0$, $H/t = 18$, $H = 137$ in., $As = 3.0$ Sq.in. 122

6.88 Tests on Reinforced Walls in Single Curvature Bending $e_2/e_1 = 1.0$, $H/t = 24$, $H = 183$ in., $As = 3.0$ Sq.in. 123

6.89 Tests on Reinforced Walls in Single Curvature Bending $e_2/e_1 = 1.0$, $H/t = 18$, $H = 137$ in., $As = 1.32$ Sq.in. 123

6.90 Tests on Reinforced Walls in Single Curvature Bending $e_2/e_1 = 1.0$, $H/t = 18$, $H = 137$ in., $As = 0.33$ Sq.in. 124

6.91 Tests on Reinforced Walls in Double Curvature Bending $e_2/e_1 = -1.0$, $H/t = 18$, $H = 137$ in., $As = 0.33$ Sq.in. 124

6.92 Assessment of Code Procedures for Faceshell Bedded Plain Masonry Wall, $H/t = 15$, $e_2/e_1 = 1.0$ 125

6.93 Assessment of Code Procedures for Faceshell Bedded Plain Masonry Wall, $H/t = 20$, $e_2/e_1 = 1.0$ 125

6.94 Assessment of Code Procedures for Fully Bedded Plain Masonry Wall, $H/t = 20$, $e_2/e_1 = 1.0$ 126

6.95 Assessment of Code Procedures for Fully Bedded Reinforced Masonry Wall, $H/t = 20$, $e_2/e_1 = 1.0$ 126

LIST OF SYMBOLS

A_s	Area of steel
B_1	Width of flange
B_2	Web thickness
C_e	Eccentricity Coefficient
C_m	$0.6 + 0.4M_1/M_2$. not less than 0.4
C_s	Slenderness Coefficient
e_1	Smaller vertical eccentricity at lateral supports
e_2	Larger vertical eccentricity at lateral supports
e_c	Normalized flexural rigidity at cracking=$(EI)_c/(EI)_o$
EI	Flexural Rigidity
$(EI)_c$	Flexural rigidity at cracking
$(EI)_i$	Initial flexural rigidity
$(EI)_u$	Flexural rigidity at ultimate
E_i	Initial tangent modulus of elasticity for masonry due to uniform strain resulting from axial load only
e_i	Normalized Initial Flexural rigidity = E_iI_o/E_oI_o
E_o	Modulus of Elasticity at zero strain
e_u	Normalized flexural rigidity at ultimate=$(EI)_u/E_oI_o$
f'_e	Compressive strength of masonry prism under eccentric load
f'_m	Prism strength under concentric axial load
f'_u	Compressive strength of the masonry unit
h	Wall height
I_1, I_2	Moments of inertia of the end sections, cracked or

	uncracked corresponding to e_1 and e_2
$I_{cr.}$	Moment of inertia of the cracked transformed section corresponding to the pure moment capacity
$I_{eff.}$	Effective Moment of inertia of the section
I_n	Moment of inertia of the uncracked net section
I_o	Gross Moment of inertia = I_n
I_u	Moment of inertia of the cross-section at ultimate
k	Effective length factor to account for boundary conditions
M	Moment
m	Normalized Moment = M/M_u
M_1	Smaller end moment acting on the wall
M_2	Larger end moment
M_c	Cracking moment
M_o	Maximum moment imposed by external forces
M_u	Maximum moment which the cross-section can resist
n	Number of Iteration
P	Axial load on the wall
P_b	Balanced Load
P_{cr}	Critical load = $\pi^2EI/(kh)^2$
P_o	Pure axial capacity of the cross-section
R	Compressive Edge Strain / Ultimate Strain = $2\,\varepsilon_a/\varepsilon_o$
T	Actual thickness of masonry cross-section
t	Effective thickness
$T1$	Thickness of the flange
w	Displacement
w'	Slope
w''	Curvature

α	Ratio of cracking moment (M_c) to ultimate moment (M_u)
Δx	Incremental wall height
ε	Strain
ε_a	Uniform strain due to axial load P only
ε_o	Ultimate Strain
ϕ	Curvature
σ	Stress
θ	P/P_o

CHAPTER 1

INTRODUCTION

Masonry has been used by man since time immemorial but with the advent of concrete and steel as viable construction materials it was relegated to the background. It is only in the latter half of this century that masonry has regained its popularity because of its aesthetically pleasing appearance and economy of construction. However, design methods continue to be empirical in nature. Gradually engineering and scientific attention is being focused on masonry. Designers are seeking rational design methods for masonry to be able to use it with confidence. Research in structural masonry in the last few decades has led to improved understanding but many questions still remain unanswered.

Due to improvements in material properties and new building techniques there is an increased usage of tall and slender walls. They are found to be very suitable for apartment buildings, office complexes, schools, warehouses and shopping plazas. In spite of the development in masonry the current design code (CSA Standard CAN3-S304-M84 "Masonry Design for Buildings") has stringent requirements for the design of slender walls.

Studies carried out by Yokel (1971), Drysdale (1976), Turkstra (1976), Hatzinikolas (1978), ACI Southern California Chapter (1981) and others have increased the understanding of the performance of slender masonry walls in compression and out of plane bending. This has led to some revisions of the slender wall design methods in building codes.

In order to develop a reliable design procedure for slender masonry walls, all parameters affecting their capacity need to be investigated. Large numbers of experiments are required to arrive at statistically useful conclusions. Unfortunately, not enough experimental data for slender walls have been reported. It is difficult to study the behavior of slender walls under various load combinations and bedding conditions since full scale wall tests are very expensive and time consuming. In these circumstances an analytical model can be developed to generate behavioral information about the effect of different parameters on the capacity of slender walls.

Prior to introduction of the present code CAN3-S304-M84, analysis of slenderness effects in masonry was limited to the traditional reduction factors approach in which axial capacity is reduced by factors corresponding to eccentricity of load and slenderness. The introduction of the moment magnifier method in CAN3-S304-M84 is an attempt to rationally model the behavior of slender masonry walls. However, the moment magnifier method in the code uses effective rigidity values based on very simplified assumptions. Moment of inertia at the ends is calculated as cracked or uncracked based on end eccentricities. For walls bent in single curvature, moment of inertia at mid-height is assumed equal to zero. In between a linear variation of moment of inertia is assumed. For walls in double curvature, moment of inertia at quarter points along the height is taken as zero and at mid-height it is taken as gross moment of inertia. From such distributions an effective moment of inertia is calculated and multiplied with a constant modulus of elasticity to determine the effective rigidity. The code procedures are reviewed in detail in the next chapter on literature review.

In order to successfully apply the moment magnifier method, more precise calculation of the effective rigidity is required by properly accounting for the material non-linearity and cracking of the cross-section. It is difficult to estimate these effects by simple procedures as they are coupled with the magnitude as well as eccentricity of the load.

1.1 Objective and Scope of the Thesis

The purpose of this investigation is to understand the behavior of eccentrically loaded slender masonry walls. It is the objective in this thesis to develop a rational analysis method which will properly account for the non-linearities due to material behavior and cracking of the cross-section. The method accounts for both material and stability failures and successfully predicts available experimental results.

Following a verification of the analytical model, the behavior of plain and reinforced slender walls with various grouting and bedding conditions are studied under different loading conditions. Current design methods are assessed.

As a result of the above studies on the behavior of slender masonry walls, suggestions are made for modifications to the current design methods.

1.2 Organization of the Thesis

Chapter two reviews the literature concerning the analysis methods for slender masonrywalls including approximate methods and the current code procedures given in CAN3-S304-M84. Previous experimental investigations on slender masonry walls are also reviewed. In chapter three material behavior of block masonry in terms of stress-strain characteristics and failure criteria under eccentric compression are studied. A new criterion for eccentric failure based on unit strength rather than prism strength is used. Chapter four deals with the analytical method developed in this study based on load-moment-curvature relationships. Verification of the analytical model for plain and reinforced walls under various loading conditions is carried out in chapter five. A simple design method is developed in chapter six. Based on a parametric study this simple design method is shown to be conservative for most of the cases studied. Advantages and limitations of the approximate method are discussed. Superiority of this new approach is demonstrated by comparing it with other approximate methods.

Finally in chapter seven, a brief summary of the results of the study, the final conclusions along with recommendations for future research are presented.

CHAPTER 2

LITERATURE REVIEW

2.1 Introduction

Codes in many developed countries, including Canada, still follow the working stress design method for design of structural masonry. Not enough experimental and analytical work has been carried out to allow a well accepted limit states design approach for masonry, similar to that used for reinforced concrete and structural steel.

The present CSA code, CAN3-S304-M84 uses an empirical approach for the design of slender masonry walls. Over the years this approach has been demonstrated by different investigators to be quite conservative. There have been recent attempts to incorporate rational methods of design for slender walls.

In this chapter all the important experimental and analytical investigations carried out to study slender masonry walls are reviewed, with emphasis on the presently available design methods in the CSA standard CAN3-S304-M84.

2.2 Experimental Studies on Slender Masonry Walls

Research work for modern engineered masonry started in the latter half of this century in North America and Europe. The Swiss were first to demonstrate the potential of masonry by using it in multistoreyed load bearing construction after an extensive experimental program carried out in the 1950s at Swiss Federal

Institute of Technology.

In North America the Structural Clay Products Institute (1969) carried out a series of tests on brick walls to study the effects of slenderness and eccentricity on the axial load carrying capacity of walls. Walls with different slenderness (h/t ratios) and varying eccentricities (e/t ratios) were tested. Based on the test results, empirical equations to account for the reduction in capacity corresponding to each of these factors were developed and these equations formed the basis for the reduction factors approach for design.

Extensive analytical and experimental studies on brick and block walls were reported by Yokel (1971). A total of 192 plain and reinforced walls were tested under eccentric axial load and lateral loads. Walls with widths from 2 ft. to 4 ft. and heights up to 20 ft. were tested. In the experiments, masonry under eccentric load was observed to sustain significantly higher compressive stresses than obtained under concentric axial loads. This increase of strength under eccentric load as compared to axial load was attributed to a strain gradient effect over the cross section. This experimental work forms the basis of a proposed load-moment interaction diagram and its modification for slenderness using a moment magnifier approach.

Drysdale (1976) carried out tests on plain and reinforced concrete masonry walls under eccentric vertical loads and/or lateral loads. Test results were compared with design methods available in the CSA Code. Code procedures were found to be too conservative. Variability of safety in the CSA reduction factors approach under various loading conditions was demonstrated by examples using a virtual eccentricity concept.

Fattal and Cattaneo (1976) continued the previous work by Yokel (1971) and tested 95 prisms and 56 brick, block and composite walls under different combinations of transverse loads and eccentric or concentric axial loads. Strain gradient effects and wall capacities were investigated.

Cranston and Roberts (1976) tested eccentrically loaded plain block walls and couplet specimens. Additional tests were reported on reinforced block walls under simulated lateral loads. Vertical loads were applied on horizontally placed walls simply supported at two ends and free along the other two edges. Based on the tests it was concluded that design procedures using permissible stresses result in uneconomical design.

Hatzinikolas (1978) carried out large scale experimental studies on 68 plain and reinforced concrete full-scale masonry walls. Walls with different slenderness and different eccentricities were tested under pin-ended conditions. Load conditions were chosen to cover both single and double curvature bending. The effect of main and joint reinforcement was studied experimentally. Effective rigidity values were suggested based on the cracked moment of inertia of the cross-section. The level of cracking was established depending on the eccentricity over the cross-section. For double curvature bending, critical load values were determined from a stepped column by assuming cracking in a portion of the wall. These effective rigidity and critical load values were used in the moment magnifier method which was proposed for the design of slender masonry walls.

Amrhein (1981) tested 30 reinforced slender walls under simulated axial and lateral loads. In these experiments load deflection behavior of panels was studied. The observed load deflection characteristics can be approximated by three straight lines corresponding respectively to uncracked, cracked and post-yielding stages. These reinforced walls exhibited better flexural performance than similar unreinforced plain walls. Based on the observations, it was recommended that the severe (h/t) restriction in the code for slender walls could be relaxed. However, the tests revealed the need for the inclusion of deflection limits in the design codes.

Suwalski (1986) tested 12 full scale slender walls under eccentric load to verify a finite element model developed to study slender masonry walls.

2.3 Analytical Methods for Slender Walls

Early studies on the analysis of masonry walls were based on the solution of a basic differential equation for a beam-column using various assumptions regarding material behavior. Assumptions made included linear elastic behavior or elastic-plastic behavior with no tensile strength or limited tensile strength.

Strength and load deflection behavior of masonry walls was investigated as far back as 1954 by Angervo (1954) and by Chapman and Slatford (1957) by solving the basic differential equation assuming elastic behavior and no tensile strength. Similar solutions were proposed later by Yokel (1971) and Risagar (1970). Angervo (1954) also solved the differential equations using nonlinear stress strain diagrams. His solution properly predicted material and stability failures for solid rectangular cross-sections. Solutions were provided in terms of charts and tables for different slenderness ratios. In 1971 Sahlin (1971) carried out a parametric study using a solution similar to Angervo's (1954) linear elastic solution. It was suggested that for slenderness ratios (h/t) less than 30, capacity is a stress problem and for slenderness ratio above 30, buckling failure governs.

Numerical methods available for slender steel and concrete members were extended by Chen (1973), Drysdale (1976) and Ojinaga (1976) by incorporating a material model for masonry.

Chen and Atsuta (1973) carried out a nonlinear analysis based on load moment-curvature relationships assuming an elastic-plastic behavior and zero tensile strength for masonry.

Ojinaga (1976) analyzed solid walls, masonry with a small percentage of voids using a load-moment-curvature based analysis procedure. Linear elastic behavior of masonry was assumed and modulus of elasticity was calculated using a best fit for the experimental data.

Drysdale (1976) used a finite strip method to study plain and reinforced masonry walls. The height of the wall was divided into several segments and the cross section was divided into strips through the thickness of the wall. Internal and external forces were balanced using the incremental iterative procedure.

Nathan (1985) used the column deflection curve method to predict material and stability failures of reinforced and prestressed concrete walls by generating a series of column deflection curves. Recently, a finite element method was used by Suwalski (1986) to study slender wall behavior.

Irrespective of the analysis method used, the results very much depended on the choice of an appropriate material model for masonry. Hence for a clear understanding of the behavior of slender walls, a proper material model must be assumed and an analysis method should be chosen to properly predict both material and stability failures. The analysis method should be able to cover a wide range of loading conditions from symmetric single curvature to antisymmetric double curvature loading. For the case of antisymmetric double curvature bending, a special failure mode where the deflected shape unwinds from a double to a single curvature mode has to be considered. This unwinding phenomenon has been observed in experiments on slender walls and columns by Hatzinikolas (1978) in masonry, by Young (1973) in steel and by MacGregor (1966) in reinforced concrete. The chosen analytical method should also be able to properly predict this unwinding phenomenon.

2.4 Code Procedures for the Design of Slender Walls

To determine the capacity of a wall, the two most important factors are slenderness and eccentricity of the load. Traditionally these two factors have been accounted for in the code procedures by reducing the axial capacity in the presence of eccentricity and slenderness. The reduction coefficients are empirical in nature. In addition to the reduction factors approach, the present CSA code allows the design of slender walls using the moment magnifier method or the displacement method. Following is a review of all the available procedures in the code.

2.4.1 The Reduction Factors Method

Reduction factors were developed by empirical or semi empirical methods to account for slenderness and eccentricity of the load. Eccentric vertical loads and the lateral loads when present along with an axial load are reduced to an equivalent concentric force and a bending moment or to an equivalent vertical force and eccentricity. The design of the cross section is based on this resultant vertical load and an equivalent or virtual eccentricity.

Coefficients developed for slenderness and eccentricity were based on experiments carried out by the Structural Clay Products Institute (SCPI). They are widely in use in codes without any further experimental or analytical verification.

CSA standard CAN3-S304-M84 uses the equations developed by SCPI. The slenderness coefficient C_s and the eccentricity coefficient C_e are computed using the following equations.

$$C_s = 1.2 - (h/t)\,(5.75 + (1.5 + e_1/e_2)^2)/300 < 1.0 \tag{2.1}$$

$$C_e = 1.3/(1+6e/t) + (e/t - 1/20)(1 - e_1/e_2)/2 \quad \text{for } t/20 < e < t/6 \tag{2.2}$$

$$C_e = 1.95\,(1/2 - e/t) + (e/t - 1/20)(1 - e_1/e_2)/2 \quad \text{for } t/6 < e < t/3 \tag{2.3}$$

where

e_1 = Smaller vertical eccentricity at lateral supports
e_2 = Larger vertical eccentricity at lateral supports
e = Maximum eccentricity anywhere along the height
h = Effective height
t = Effective thickness

The wall capacity is calculated as the capacity of a short axially loaded wall multiplied by C_s and C_e.

When the applied eccentricity is greater than t/3, then both the axial load and bending moment are modified by the coefficient C_s and the code requires the assessment of interaction between axial load and bending moment based on a transformed section analysis. However, most of the designers choose the simpler and more conservative unity interaction equation between the axial load and bending moment.

2.4.2 The Moment Magnifier Method

In this method primary moments due to an eccentric vertical load or due to lateral loads are increased by a factor to account for secondary bending. The magnification factor is closely approximated by $1/(1-P/P_{cr})$. This solution is true for symmetric single curvature bending when the two end moments are equal. To account for unsymmetric bending corresponding to unequal end moments a factor C_m is applied to arrive at the equivalent maximum moment. The effect of different boundary conditions is taken care of by choosing an appropriate effective height of the wall. The effective rigidity EI used to calculate P_{cr} should include the effect of cracking of the cross section. Different investigators have suggested different methods to arrive at an estimate of the effective rigidity.

The moment magnifier method has been successfully applied to steel and reinforced concrete beam columns. Yokel and Dikkers (1971) suggested a similar approach for masonry walls using the following equations.

$$M = M_o (C_m/(1 - P/P_{cr})) \tag{2.4}$$

where

M_o = Maximum moment imposed by external forces

C_m = $0.6 + 0.4M_1/M_2$ not less than 0.4

M_1 = Smaller end moment acting on the wall

M_2 = Larger end moment

P_{cr} = Critical load = $\pi^2 EI/(kh)^2$

h = Wall height

k = Effective length factor to account for boundary conditions

EI = $E_i I_n$ / 3.5 for plain masonry

EI = $E_i I_n$ / 2.5 for reinforced masonry.

E_i = Initial tangent modulus of elasticity for masonry

I_n = Moment of inertia of the uncracked net section.

Hatzinikolas (1978) suggested a modified approach with an alternate procedure to calculate effective rigidity. For plain walls or for reinforced walls with eccentricity less than t/3, moment of inertia was calculated as

$$I = 8\,(0.5 - e/t)^3\, I_o \tag{2.5}$$

For reinforced walls with e greater than t/3

$$I = (0.5 - e/t)\, I_o \quad > 0.1 I_o \tag{2.6}$$

The Moment magnifier method in the CSA standard CAN3-S304-M84 was developed by Ojinaga and Turkstra (1980). They suggested the following method for the calculation of the effective moment of inertia. For plain masonry

$$I_{eff.} = (I_1 + I_2)/4 \qquad 0 < e_1/e_2 < 1.0 \qquad (2.7)$$

$$I_{eff.} = \text{Lesser of } (I_1 + I_o)/4 \text{ and } (I_2 + I_o)/4 \qquad -1 < e_1/e_2 < 0 \qquad (2.8)$$

For reinforced masonry

$$I_{eff.} = (I_1 + 2I_{cr.} + I_2)/4 \qquad 0 < e_1/e_2 < 1.0 \qquad (2.9)$$

$$I_{eff.} = \text{lesser of } (I_1 + 2I_{cr.} + I_o)/4 \text{ and } (I_2 + 2I_{cr.} + I_o)/4 \qquad -1 < e_1/e_2 < 0 \qquad (2.10)$$

I_1, I_2 = Moments of inertia of the end sections, cracked or uncracked corresponding to e_1 and e_2

I_o = Moment of inertia of the uncracked section

$I_{cr.}$ = Moment of inertia of the cracked transformed section corresponding to the pure moment capacity

The moment of inertia as calculated above is multiplied by a constant modulus of elasticity to get EI.

The January 1988 Amendment to CAN3-S304-M84 further reduces EI as calculated above to 0.25EI.

2.4.3 The Displacement Method

This iterative method which is also in CAN3-S304-M84 was initially proposed by Ojinaga and Turkstra (1980). However, in the code it is given as a one step procedure. The effective flexural rigidity (EI) is calculated as in the moment magnifier method. Then the displacement at mid height is calculated using the EI values. Additional secondary moment equal to the force multiplied by the displacement is then added to the initial moment and the capacity of the cross section is checked.

In their present form both the Moment magnifier method and the Displacement method have limited application because they incorporate flexural rigidity values based on simplified assumptions.

CHAPTER 3

BEHAVIOR OF MASONRY UNDER ECCENTRIC COMPRESSION

3.1 Introduction

In this chapter the relevant material properties of masonry are examined. Differences between axial and eccentric failure mechanisms are clearly pointed out. A stress-strain relationship representative of the eccentric failure mechanism is proposed. A new criterion is suggested for eccentric failure and its superiority over the currently used criterion is demonstrated by comparisons with experimental results.

3.2 Axial and Eccentric Failures

The compressive strength of masonry prisms under axial load (f'_m) depends on many factors such as unit strength, mortar strength, joint thickness, reinforcement and workmanship. The primary mode of failure under axial loading is tensile splitting of the masonry assemblage. This is attributed to the differences in physical properties of mortar and masonry units. The most widely accepted explanation of this phenomenon is due to Hilsdorf (1967). Hilsdorf's approach is based on the assumption that masonry units behave in accordance with a modification of Mohr's theory of failure. A perfect bond is assumed between mortar and unit. As the vertical load increases, the mortar expands laterally more than the masonry units and gives rise to tensile stresses in the units. This lateral expansion leads to the confinement of mortar because a perfect bond is assumed between mortar and masonry units. The strength of mortar increases due to this confinement. The lateral tensile stresses developed in the units lead to the tensile splitting of the assembly. Recently, alternative explanations for this phenomenon have been offered by Shrive (1982), using a finite element analysis and by Yao (1989), using the theory of elasticity.

It is well known that the failure mode under eccentric load is distinctly different from the tensile splitting failure under axial load. Under eccentric compression failure occurs mainly by crushing on the compression side of the prism. Masonry under eccentric compression is observed to develop significantly higher compressive stresses than obtained under axial load. This apparent increase in compressive strength is traditionally attributed to a strain gradient effect across the cross section. Research carried out by Yokel and Dikkers (1971), Drysdale and Hamid (1983) led to the development of a factor to account for the strain gradient effect. This factor is a function of eccentricity of the load and is widely accepted at present. The S304-M84 code recognizes this apparent increase in strength and includes a factor of 1.3 in the calculation of an eccentricity coefficient. However, the basis of this correlation is questionable because two entirely different failure mechanisms are involved, and a criterion for eccentric failure needs to be developed independent of the strength under axial load which corresponds to tensile splitting.

3.3 Failure Criterion of Masonry in Eccentric Compression

Hatzinikolas (1980) and Yao (1989) have independently proposed an alternate eccentric failure criterion based on compressive strength of masonry unit (f_u), rather than prism strength (f_m) and strain gradient effect. According to this criterion, eccentrically loaded masonry walls fail when the compressive strength of masonry units is reached. This criterion is derived from the observation that the failure mode of a masonry unit tested alone closely resembles the failure of the unit in an eccentrically loaded prism. It was also observed by Yao (1989) that the joint conditions i.e. the joint thickness and the type of mortar, do not have significant effects on the eccentric compressive strength of a masonry prism.

In order to examine the validity of the alternate approach it was compared with experimental data from three sources, Fattal (1976), Hatzinikolas (1978) and Drysdale (1983). This data set correspond to a total of 73 masonry prisms tested to failure under eccentric loads. The data is tabulated in table 3.1 to table 3.3. For each of the prisms eccentric compressive strength (f'_e), masonry unit strength (f_u), and the prism strength (f_m) was reported. For comparison, eccentric compressive strength was plotted against unit strength and prism strength separately in Figure 3.1 and Figure 3.2. A best fit line using the least squares fit was derived in each case. Coefficients of determination calculated were 0..501 for the case of unit strength and 0..403 for the the second case of prism strength. A line with a correlation coefficient closer to one indicates a better representation of the experimental data. These best fit lines were then compared with the two criteria based on (f_u), and the current design basis of ($1.3f_m$). Such a comparison confirmed that the alternate approach based on (f_u) indeed achieves a better agreement than the former criteria.

3.4 Stress-Strain Relationship

Studies on the material behavior of masonry have concentrated on the response of prisms under axial load. Stress-strain relationships and compressive strength (f_m) thus obtained correspond to tensile splitting. This data cannot be directly used to study behavior of masonry walls under eccentric compression. According to the experimental data from Suwalski (1986) and Yao (1989) masonry exhibits a nonlinear stress-strain relationship.

Wall tests under eccentric loads carried out by Hatzinikolas (1978) showed that the ultimate compressive strains in masonry reached up to 0.0028. Further prism tests by Suwalski (1986) and Yao (1989) under eccentric load show that masonry can sustain strains of 0.003. Along with this observation about ultimate compressive strain of masonry, its brittle nature and the resemblance in compressive behavior of masonry blocks and plain concrete, the following parabolic stress-strain relationship is proposed to represent the behavior of masonry under eccentric compression.

$$\sigma = f_u \left(2.0(\varepsilon/\varepsilon_0) - (\varepsilon/\varepsilon_0)^2 \right) \qquad (3.1)$$

where σ = stress, ε = strain and $\varepsilon_0 = 0.0028$

In order to study the adequacy of the above stress-strain parameters, full-scale wall test data under eccentric load from Hatzinikolas (1978) was used. Test data for the two cases Wall HC3, a plain wall and Wall HC5 a grouted wall were specially chosen because the strain distributions at different levels of axial load were known. To satisfy equilibrium, the stresses over the cross-section when integrated must be equal to the applied vertical load. Therefore, at different stages of load application, the experimentally recorded strain distribution and the above stress strain parameters, were used to establish the stress distribution across the cross-section. Load was obtained by integrating the stress over the cross section. The loads thus calculated, for different stages of loading compared well with the applied loads recorded in the experiments. The comparisons shown in Fig. 3.3 and Fig. 3.4, confirm the adequacy of the above stress-strain parameters.

3.5 Strength Interaction Diagrams

Strength Interaction diagrams were developed by using the the nonlinear stress strain relationship discussed in the previous section. Failure is assumed to occur when masonry reaches its ultimate compressive strain of 0.0028. Masonry is assumed to have zero tensile strength. Depth of the neutral axis was varied and a linear strain distribution was assumed across the depth of the cross-section. In each case the stress distribution was determined from the stress-strain relationship. Axial load and bending moment were determined by integrating the stresses over the cross-section.

Test results on eccentrically loaded prisms Drysdale (1983) were compared with the interaction curves in Fig 3.5 to Fig. 3.8. Except for a few points test results compared favorably with the interaction curves.

Table 3.1 Prism Tests under eccentric compression by Drysdale

	Prism Strength	Unit Strength	Eccentric Compr. Strength
	f'm (ksi)	f'u (ksi)	f'e (ksi)
1	3.611	3.640	4.060
2	3.611	3.640	4.031
3	3.611	3.640	3.915
4	2.088	3.640	2.958
5	2.088	3.640	3.611
6	2.088	3.640	4.350
7	2.045	3.640	2.755
8	2.045	3.640	3.625
9	2.045	3.640	5.133
10	2.233	3.640	3.509
11	2.233	3.640	4.075
12	2.233	3.640	4.365
13	2.610	2.480	2.813
14	2.610	2.480	2.886
15	2.610	2.480	2.436
16	1.595	2.480	2.349
17	1.595	2.480	2.987
18	1.595	2.480	3.654
19	4.336	4.050	4.930
20	4.336	4.050	5.090
21	4.336	4.050	4.771
22	2.175	4.050	2.770
23	2.175	4.050	4.771
24	2.175	4.050	5.162
25	3.016	2.930	3.741
26	3.016	2.930	3.640
27	3.016	2.930	3.640
28	2.045	2.930	2.915
29	2.045	2.930	3.538
30	2.045	2.930	4.684
31	2.364	3.220	2.770
32	2.364	3.220	2.552
33	2.364	3.220	3.060
34	2.103	3.220	3.045
35	2.103	3.220	3.306
36	2.103	3.220	3.176
37	1.537	2.450	3.335
38	1.537	2.450	2.204
39	1.537	2.450	2.378
40	3.451	3.420	3.843
41	3.451	3.420	3.785
42	3.451	3.420	3.422
43	2.001	3.420	2.291
44	2.001	3.420	3.335
45	2.001	3.420	4.510
46	3.132	3.390	3.016
47	3.132	3.390	3.393
48	3.132	3.390	3.263
49	1.653	3.390	2.059
50	1.653	3.390	2.857
51	1.653	3.390	3.625

Table 3.2 Prism Tests under eccentric compression by Hatzinikolas

	Prism Strength	Unit Strength	Eccentric Compr. Strength
	f'm (ksi)	f'u (ksi)	f'e (ksi)
1	1.900	1.950	2.630
2	1.900	1.950	3.190
3	1.900	1.950	2.430
4	1.900	1.950	2.890
5	1.900	1.950	3.850
6	1.650	1.950	2.590
7	1.650	1.950	2.420
8	1.650	1.950	2.250
9	1.650	1.950	2.540
10	1.650	1.950	2.250

Table 3.3 Prism Tests under eccentric compression by Fattal

	Prism Strength	Unit Strength	Eccentric Compr. Strength
	f'm (ksi)	f'u (ksi)	f'e (ksi)
1	1.405	2.210	1.778
2	1.405	2.210	1.300
3	1.405	2.210	2.371
4	1.405	2.210	2.109
5	1.405	2.210	1.996
6	1.405	2.210	2.146
7	1.405	2.210	1.801
8	1.405	2.210	1.843
9	1.405	2.210	1.797
10	1.405	2.210	1.611
11	1.405	2.210	1.994
12	1.405	2.210	1.761

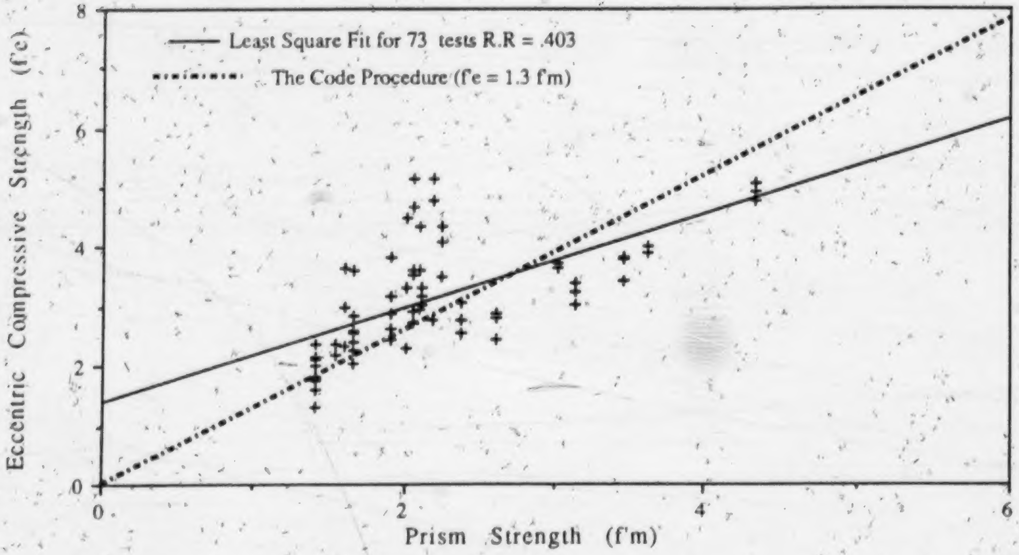

Fig.3.1 Eccentric Compressive Strength vs Prism Strength (f'm)

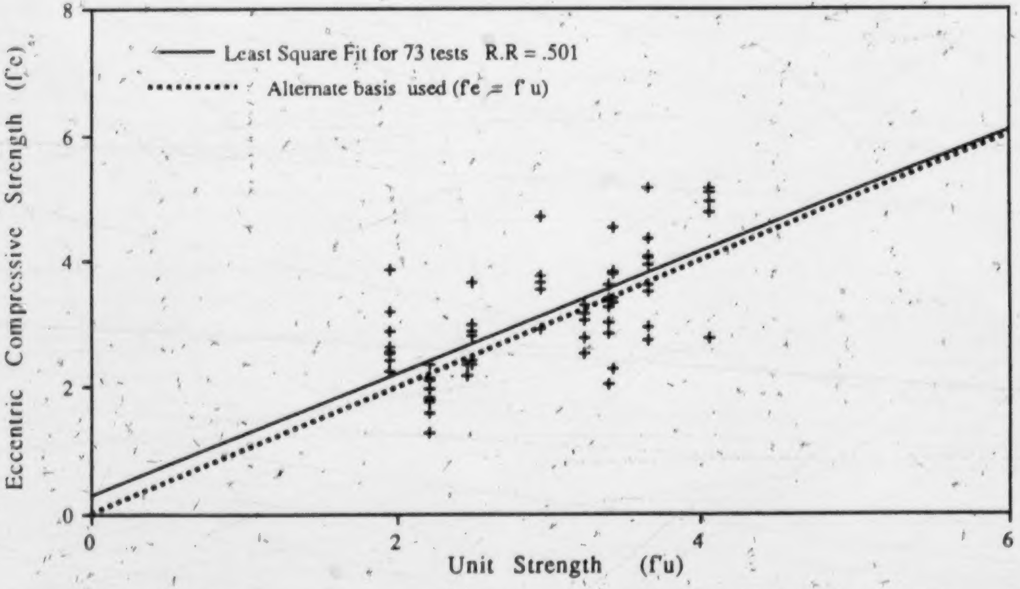

Fig.3.2 Eccentric Compressive Strength vs Unit Strength(f'u)

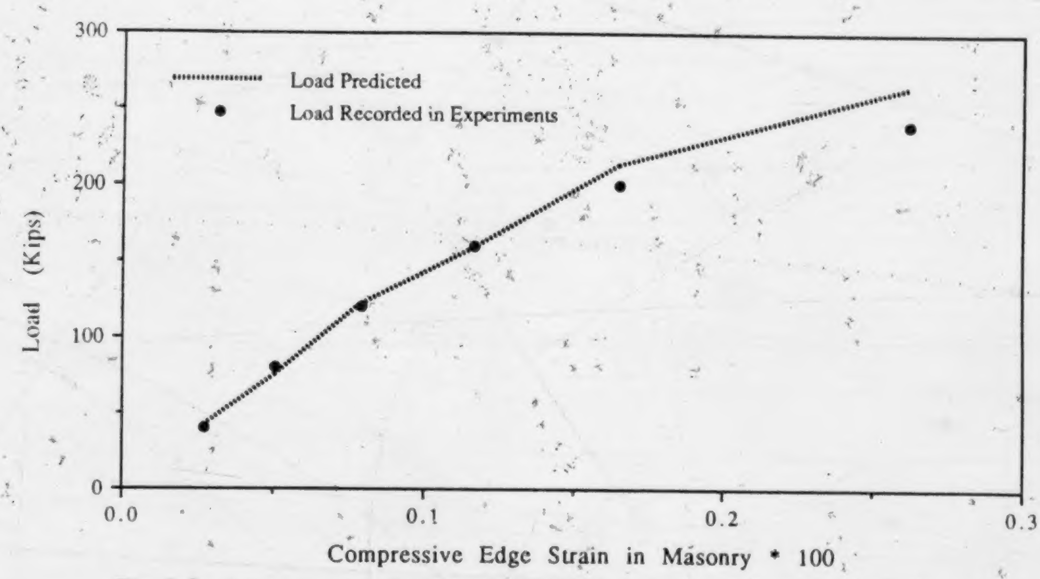

Fig.3.3 Assesment of Proposed Stress Strain Parameters using strain distributions on wall HC3, experiments by Hatzinikolas

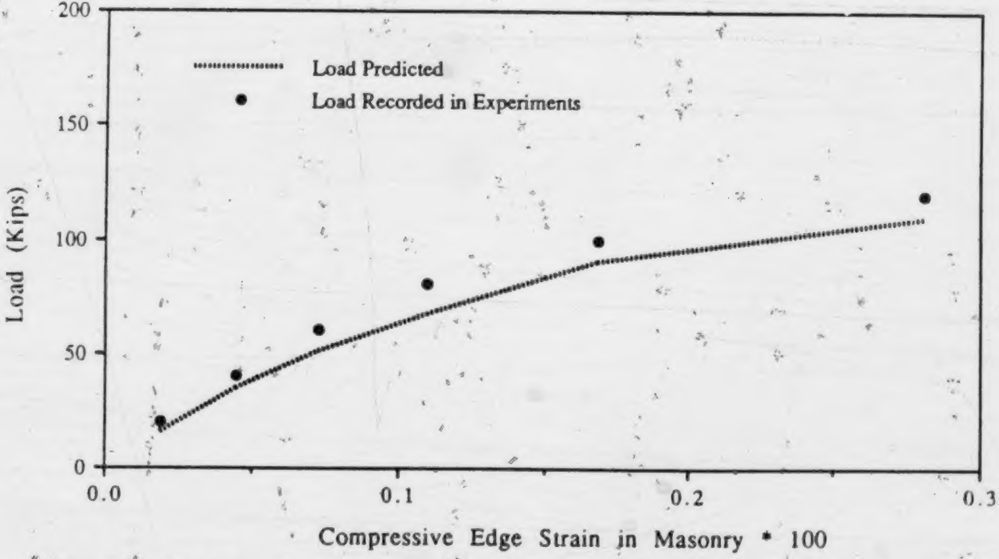

Fig.3.4 Assesment of Proposed Stress Strain Parameters using strain distributions on Wall HC5, experiments by Hatzinikolas

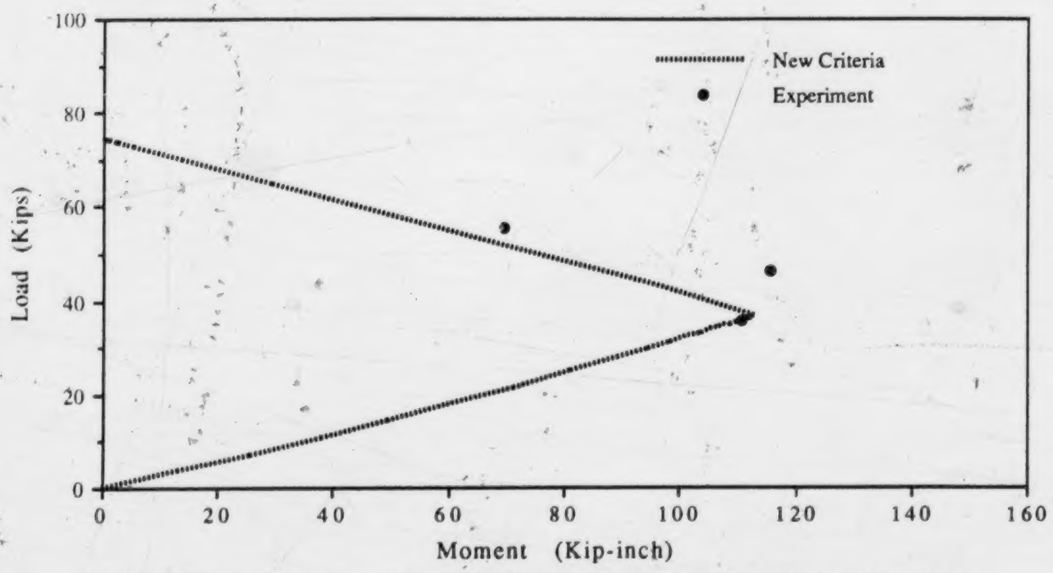

Fig.3.5 Comparison of New Criteria with Experiments by Drysdale, Face shell bedded masonry, Normal Blocks (NB190)

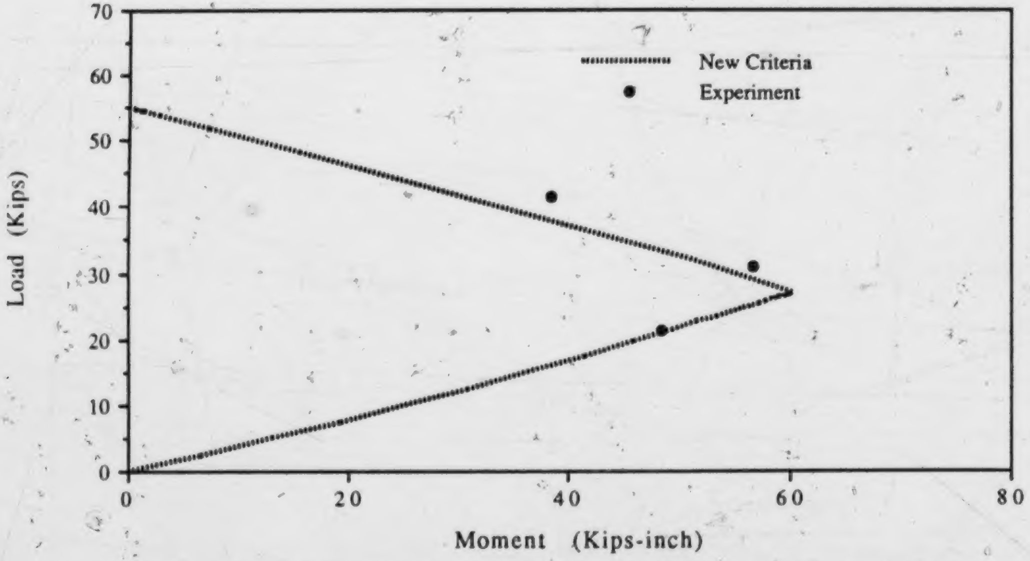

Fig.3.6 Comparison of New Criteria with Experiments by Drysdale Face shell bedded masonry, Normal blocks (NB140)

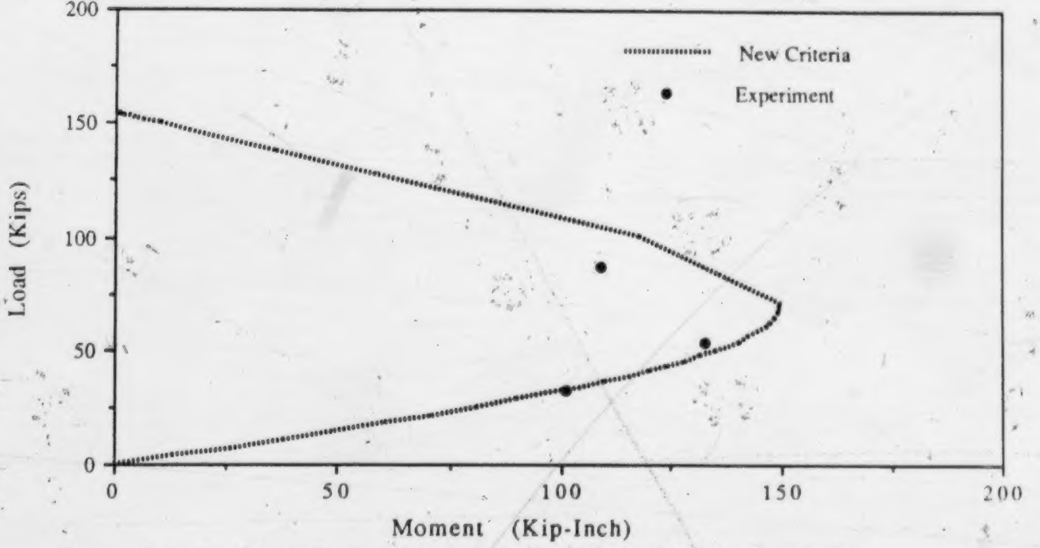

Fig.3.7 Comparison of New Criteria with Experiments by Drysdale
Fully grouted Masonry, Normal Blocks and Normal Grout (NB190NG)

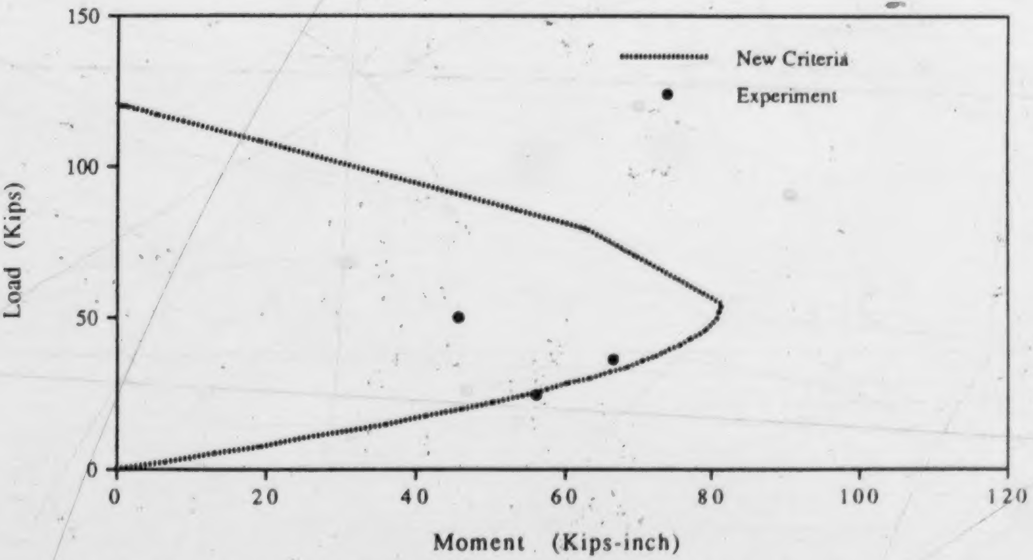

Fig.3.8 Comparison of New Criteria with Experiments by Drysdale
Fully Grouted Masonry, Normal Blocks and Normal Grout (NB140NG)

CHAPTER 4

ANALYSIS METHODS FOR SLENDER MASONRY WALLS

4.1 Introduction

This chapter deals with the adaptation of analysis methods to account for slenderness effects using load-moment-curvature relationships. The two analysis methods (Column Deflection Curve Method and Newmark's Numerical Method) are based on iterative procedures which properly account for material and stability failures. The steps of the analysis methods and convergence criteria used are discussed in detail. For walls initially bent in double curvature a failure possibility which corresponds to unwinding from a double to a single curvature mode is also included in the Newmark's Numerical Method.

4.2 Development of Analysis Methods

A rational analysis method is developed in this chapter to properly account for the non-linearities due to material behavior and cracking of the cross-section. The method is suitable for analysis of slender concrete masonry walls under in-plane compression combined with out-of-plane bending. This method properly predicts material and stability failures. The cross section chosen is such that masonry walls with various bedding and grouting conditions can be analyzed using this method.

For equal end eccentricities and single curvature bending, the Column Deflection Curve (CDC) method is used because of its simplicity of application. For the case of unequal end eccentricities and for the case of double curvature bending, a more versatile method using Newmark's Numerical Procedure is used to compute failure loads for walls treated as beam-columns.

The general differential equation for a beam-column with flexural rigidity EI is

$$(EIw'')'' + Pw'' = q(x) \tag{4.1}$$

where w is the deflection from the thrust line, at a distance x along the thrust line, P is the axial load and q(x) is the distributed load along x.

For beam-columns with only axial loads and end moments the differential equation becomes

$$(EIw'')'' + Pw'' = 0 \tag{4.2}$$

For the elastic case a general solution can be found because EI does not change. However, for masonry E changes because of the nonlinearity of the stress strain relationship and I changes because of cracking of the cross section. When both E and I change, numerical methods such as CDC method and Newmark's Numerical Method are used to solve the differential equation.

The applied moment that a cross section can resist is a function of axial load, curvature, material properties, geometry and level of cracking of the cross section. For a given axial load acting over the cross-section, a relationship between moment and curvature can be developed by considering all these factors. Such a

Load-Moment-Curvature relationship is used to identify curvatures corresponding to bending moments along the height of the wall. Since the effects of changing flexural rigidity (EI) are properly accounted for in the development of a load-moment-curvature relationship, an analysis method using the load-moment-curvature relationship accounts for the nonlinearity of stress strain and cracking of the cross-section. The first step in such an analysis method is the development of Load-Moment-Curvature relationships.

4.3 Development of Load-Moment-Curvature Relationships

A Load-Moment-Curvature relationship is developed corresponding to a given axial load. In order to analyze different types of masonry cross-sections, a cross-section in the form of an I-section is chosen as shown in Fig. 4.1 with reinforcement placed in the middle of the web. By specifying the web thickness (B_2) and the area of reinforcement (A_s), a variety of cross-sections corresponding to different grouting and bedding conditions were studied. For $B_2 = B_1$ and $A_s=0$, this cross-section represents fully bedded and fully grouted plain masonry wall. If B_2 and A_s are both equal to zero, the cross-section corresponds to the case of faceshell bedded ungrouted masonry. For partially or fully grouted reinforced walls, B_1 and A_s are accordingly chosen. Realizing the fact that the contribution of grout will be less than the units in resisting load and moments, the area of grout, i.e. thickness of web, is reduced by a ratio of grout strength to unit strength. Load-moment-curvature relationships are developed using the following steps.

1. A value of target load P is chosen.
2. Initial values for compressive edge strain and curvature are selected which establish the neutral axis location and strain distribution over the cross-section.
3. The stress distribution is determined using the non-linear stress-strain relationship proposed in Chap. 3.
4. The axial load corresponding to this stress distribution is calculated by integrating the stress over the cross-section.
5. The calculated load is compared with the target load of step 1. If required, compressive edge strain is varied and steps 3 and 4 are repeated. This iteration is continued until the difference between the target and calculated load is one percent (or less) of the target load.
6. If the curvature reaches a value such that the load cannot be matched without exceeding ultimate strain then material failure is assumed and computations are stopped.
7. The above procedure is repeated for different values of curvature to obtain a complete load-moment-curvature relationship.

Typical Load-moment-curvature relationships developed for reinforced walls are shown in Figure 4.2

4.4 Column Deflection Curve Method

A column of any arbitrary length under the action of a given axial load, P, may occupy an infinite number of equilibrium configurations. A particular configuration is uniquely defined by the load and some parameter such as the end slope. Such a configuration is called as Column Deflection Curve (CDC). A series of CDCs are shown are shown in Figure 4.3.

Von Karaman (1910) was the first to recognize that the deflected axis of any beam column can be represented by a portion of the CDC. He used this concept to obtain the maximum strength of rectangular steel beam-columns subjected to axial loads and small eccentricities. Since then many researchers Chwalla (1934), Horne (1956), Ellis (1958) and Ojalvo (1960) have used this concept to solve various beam-column problems. More recently the CDC technique has been successfully applied to steel and reinforced concrete respectively by Galambos (1968) and Nathan (1972,1985). The practical aspect of the CDC approach is that once a set of deflection curves are obtained then the complete in-plane load-deflection curve for different beam-columns can be evaluated. In the following sections, development of CDCs are discussed first, then the method to solve various beam-columns is illustrated.

4.4.1 Computation of CDCs

CDCs are constructed numerically. A given CDC can give information about various combinations of end moments. The construction method for CDCs is as follows.

1. If the displacement of a CDC from the thrust line is $w(x)$, at a distant x along the thrust line, then expansion of $w(x)$ in a Taylor's series about a point x_o, leads to

$$w(x_o + \Delta x) = w(x_o) + w'(x_o)\Delta x + 1/2\ w''(x_o)\Delta x^2 + \ldots$$

where primes indicate differentiation with respect to x. Also, w' is the slope θ and w'' is the curvature ϕ. If the series is truncated after three terms, the displacement is given by

$$w(x_o + \Delta x) = w(x_o) + \theta(x_o)\Delta x + 1/2\ \phi(x_o)\Delta x^2 \qquad (4.3)$$

2. Similarly, by expanding w' about x_o and after truncation the slope is obtained as

$$\theta(x_o + \Delta x) = \theta(x_o) + \phi(x_o)\Delta x \qquad (4.4)$$

The truncation of the equations is equivalent to assuming a constant curvature between x_o and $(x_o + \Delta x)$. For a given value of axial load P, a curve of moment versus curvature is constructed as explained in the previous section. If all the quantities of interest are known or assumed at x_o, by using the above equations all quantities of interest at $(x_o + \Delta x)$ can be calculated. This process is repeated until one quarter wavelength is reached. Using the deflection values for one quarter wavelength, a complete CDC is obtained for the particular value of end slope and thrust P.

4.4.2 Application of CDC Technique to Masonry Walls

In this study the CDC method because of its simplicity of application is used for the special case of equal end eccentricities and single curvature bending.

As shown in Figure 4.3, starting at mid height of the wall with slope equal to zero and moment equal to that causing material failure, the CDC is generated by successive integration of the differential equation by assuming constant curvature within each short segment as explained in the previous section. The integration is continued until the end of the wall is reached or to a point when deflection becomes zero indicating the completion of one quarter wavelength of CDC. The starting moment at mid-height of the wall is then reduced in small steps of 5% of the ultimate moment and new CDCs are obtained. After obtaining all CDCs, the CDC giving the greatest eccentricity at the end of the column is determined. As shown in the Figure 4.3, this either corresponds to material failure at mid-height, for wall with height H_c or it corresponds to instability failure, for wall with height L_c. Such calculations provide just one point on a load-moment interaction curve for a given length of column. By repeating this process for different levels of axial load, a complete load-moment interaction diagram corresponding to the chosen length and cross section of the wall is obtained. Such an interaction diagram can be directly used for the identification of maximum sustainable end moments for any given axial load.

4.5 Newmark's Numerical Method

For walls subjected to unequal end moments Newmark's Numerical Technique is used to find the equilibrium position of masonry walls. At a given axial load moment is applied in increments, and for each increment several iterations are required to converge to a stable configuration starting from an initial deflection surface.

The wall is modelled as a sequence of short segments of length equal equal to Δx as shwon in Figure 4.4. The performance of a wall is approximated by the behavior of these small segments tied together at their end nodes by the known relationships of moment and curvature. Because the member is divided into segments, curvatures are concentrated at the nodes. The concentrated curvature values at nodes were determined by assuming a parabolic distribution of curvature. The concentration formulae are shown in Figure 4.5. The length of the subdivisions is chosen to be five percent of the wall height to reduce error.

For the calculations of deflections, starting with the concentrated curvatures at the nodes, slope along the height is estimated by integrating curvatures and a deflected surface is then found by integrating slope along the height. A linear variation of the deflection is then added to correct any end conditions such as zero deflections at supports. As a result the member is merely translated as a rigid body so that no changes in relative slopes or deflections between nodes are incurred.

In the iterative procedure moment is applied in steps. The magnitude of the moment increments must not be too large in order to limit the error of approximating the load-displacement curve. The smaller the increment, the more accurately will the failure load be determined. Considering these factors, the increment of moment at each step was taken as five percent of the ultimate moment capacity of the cross section.

An initial deflection surface is used to commence the iterative procedure. The surface used is the theoretical deflected shape neglecting P-Δ effects. Since the procedure iterates to the equilibrium position, this initial deflection curve does not affect the final deflected shape.

The analysis method calculates deflections, slopes along the member, the ultimate moment, and type of failure. For material failure, the position along the member where it occurs is also determined.

The following are the criteria for convergence and failure used in the analysis.

1. If the deflection surface in the nth iteration is very close to the deflection surface in the next iteration, or

$$\frac{\text{Sum of Deflections at the nodes}(n-1)}{\text{Sum of Deflections at the nodes}(n)}$$

is between 0.99 and 1.01 then convergence has been reached.

2. Material failure occurs when maximum compressive strain is reached at one edge of the wall. During the calculation this will be seen as an attempt to apply a moment larger than the cross section capacity.
3. If calculations proceed such that the material failure does not occur and convergence is not being achieved, then stability failure at any iteration n is investigated as follows.

   If

   $$\frac{\text{Sum of Deflections at the nodes }(n-2)}{\text{Sum of Deflections at the nodes }(n-1)} = P$$

   $$\frac{\text{Sum of Deflections at the nodes }(n-1)}{\text{Sum of Deflections at the nodes }(n)} = Q$$

   If Q is found to be greater than P, it indicates that the deflections are diverging and therefore stability failure occurs because solution will not converge to a stable position.
4. For stability failure, a limit of 50 iterations is set after which instability was assumed. This limit of 50 iterations is more than twice the usual number of iterations needed for convergence.

The flow charts for the CDC method and the Newmark's Numerical Procedure are shown in Figures 4.6 and in Figure 4.7 respectively.

4.6 Unwinding Phenomenon

For walls initially bent in double curvature, a special failure possibility must be considered. This corresponds to unwinding from a double to a single curvature mode. Experimental studies on walls initially bent in double curvature have indicated that the ultimate failure occurs in a deflected shape which closely resembles the half sine wave or single curvature mode.

A design recommendation should consider all the failure modes; therefore this unwinding phenomenon is accounted for in this analysis procedure. Theoretically, unwinding occurs at higher axial loads due to the magnification of small initial imperfections of the single curvature type. Therefore, the deflected shape just before failure closely resembles that of a single curvature mode. In the analysis procedure a small sinusoidal initial imperfection of H/1000 at mid-height is assumed. This imperfection of H/1000 is chosen to be less than the minimum eccentricities in the Canadian code: 0.01t or 25mm for masonry members and 15mm+0.03t for reinforced concrete members. Along with applied loads and such an initial imperfection, the iterative procedure using Newmark's Numerical Method indeed exhibited unwinding phenomenon. Inspection of the deflected shape just before failure showed the wall bent mainly in single curvature mode. Unwinding leads to a large reduction of capacities at higher axial loads.

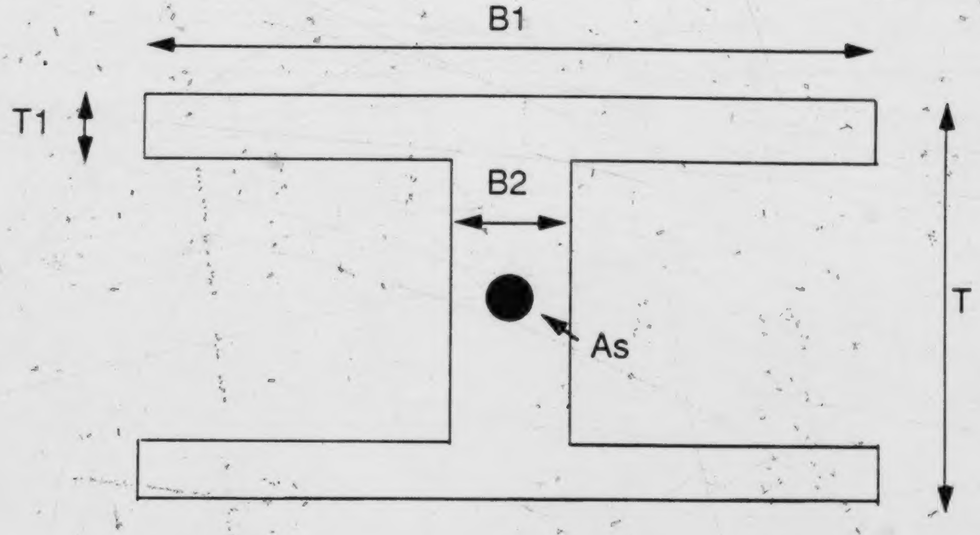

Figure 4.1 Masonry Wall Cross-section used in the analysis

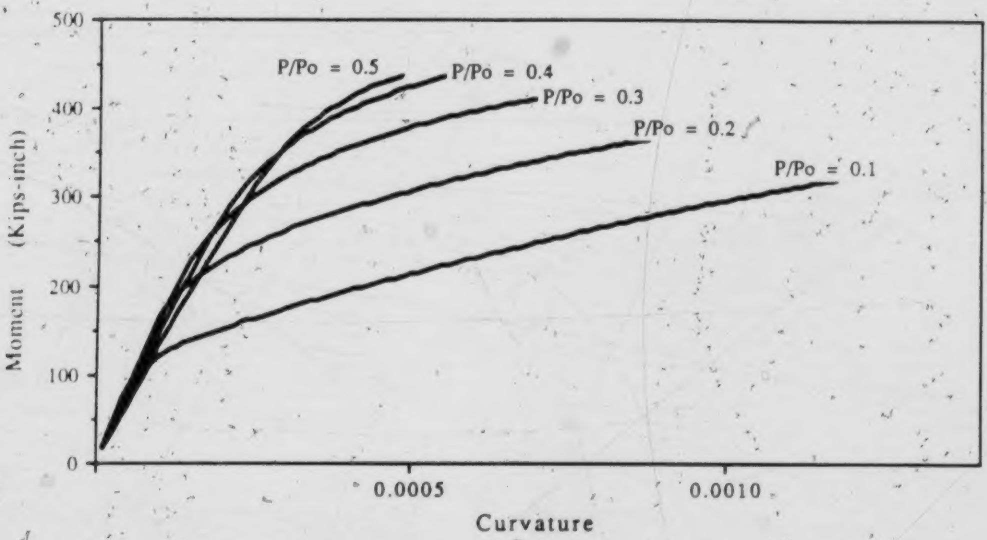

Figure 4.2 Moment Curvature Relationships for reinforced masonry walls As = Balanced reinforcement/2

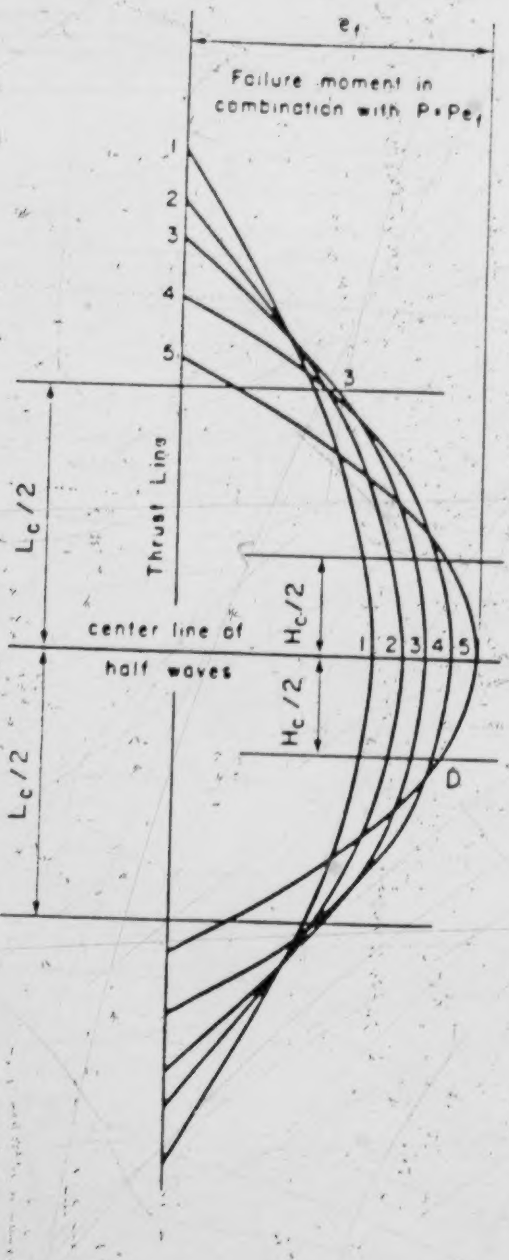
e_f
Failure moment in combination with P=Pe_f
1
2
3
4
5
3
Thrust Line
L_c/2
H_c/2
center line of half waves
1 2 3 4 5
H_c /2
L_c/2
D

Figure 4.3 Use of Column Deflection Curves

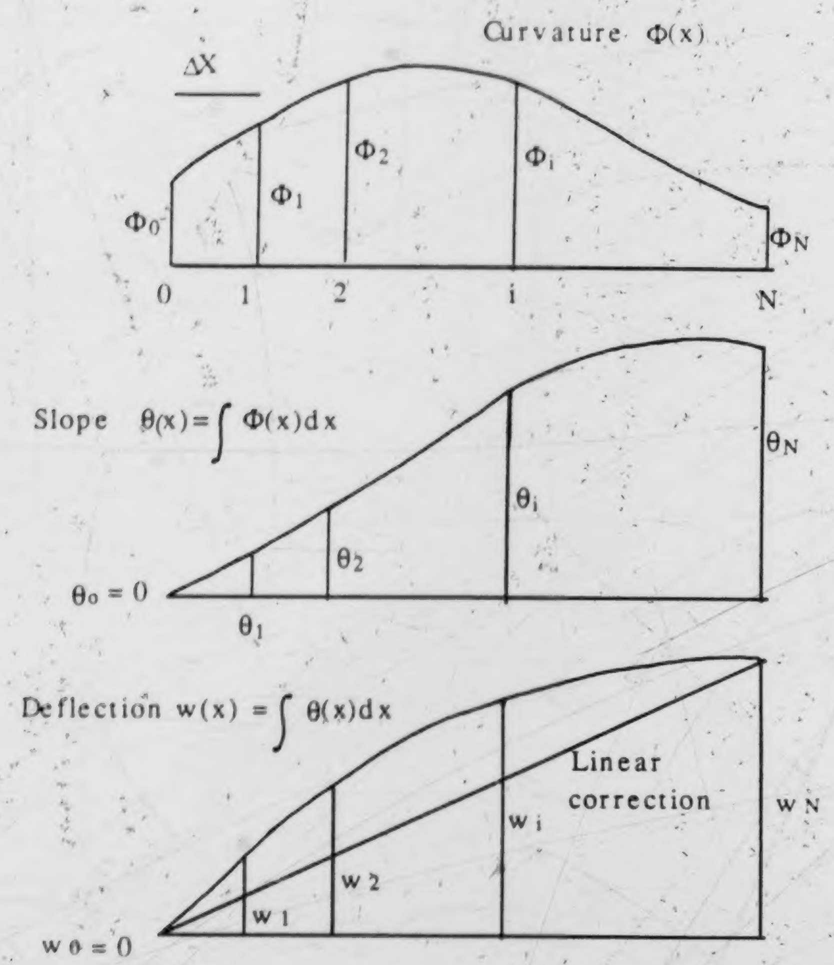
Curvature $\Phi(x)$
ΔX
Φ_0
Φ_1
Φ_2
Φ_i
Φ_N
0
1
2
i
N
Slope $\theta(x)=\int \Phi(x)dx$
θ_N
θ_i
θ_2
$\theta_o = 0$
θ_1
Deflection $w(x) = \int \theta(x)dx$
Linear correction
w_N
w_i
w_2
w_1
$w_0 = 0$

Corrected deflections $= y_i = w_i - \frac{i}{N} w_N$

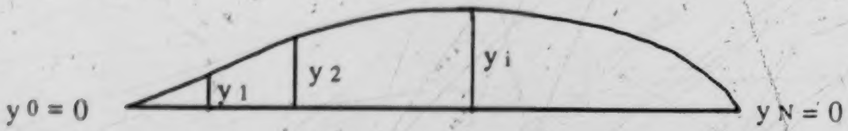
$y_0 = 0$
y_1
y_2
y_i
$y_N = 0$

Figure 4.4 Newmark's Numerical Procedure to calculate deflections

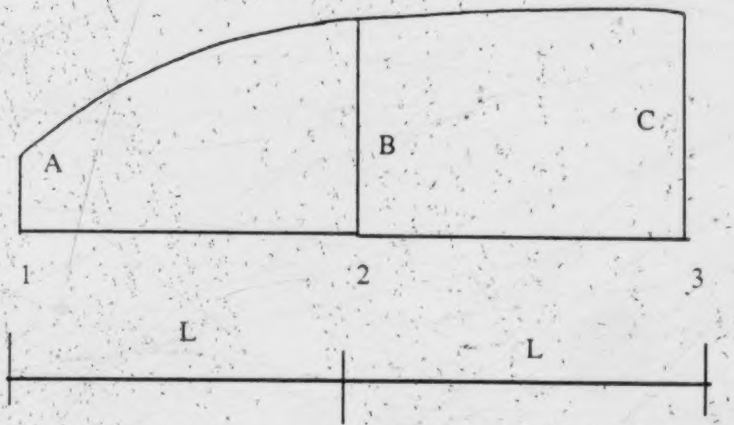

Parabolic Distribution of Curvature

Concentrated value of Curvature at Node 1 = L (7A + 6B - C)/24

Concentrated value of Curvature at Node 3 = L (7C + 6B - A)/24

Concentrated value of Curvature at Node 2 = L (A + 10B + C)/12

Figure 4.5 Concentration Formulae for Parabolic Distribution from Lind (1975)

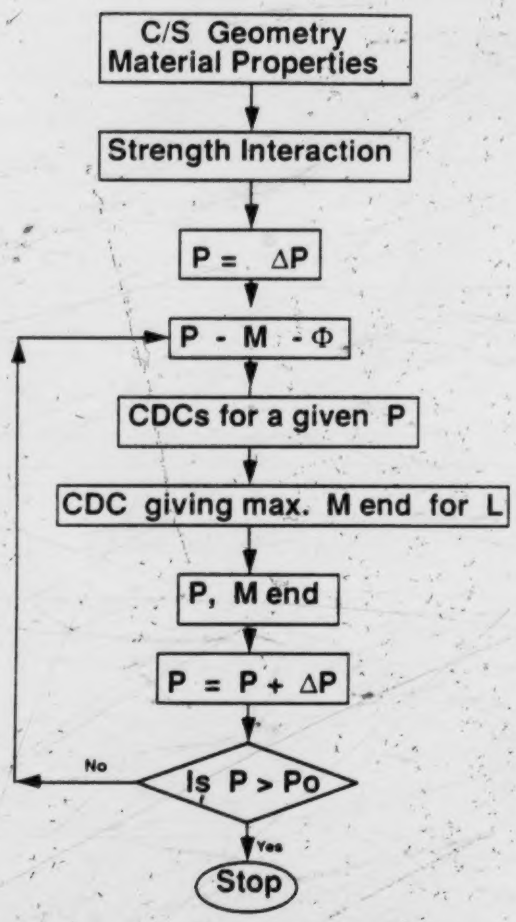
C/S Geometry
Material Properties
Strength Interaction
P = ΔP
P - M - Φ
CDCs for a given P
CDC giving max. M end for L
P, M end
P = P + ΔP
Is P > Po
No
Yes
Stop

Figure 4.6 Flow chart for Column Deflection Curve Method

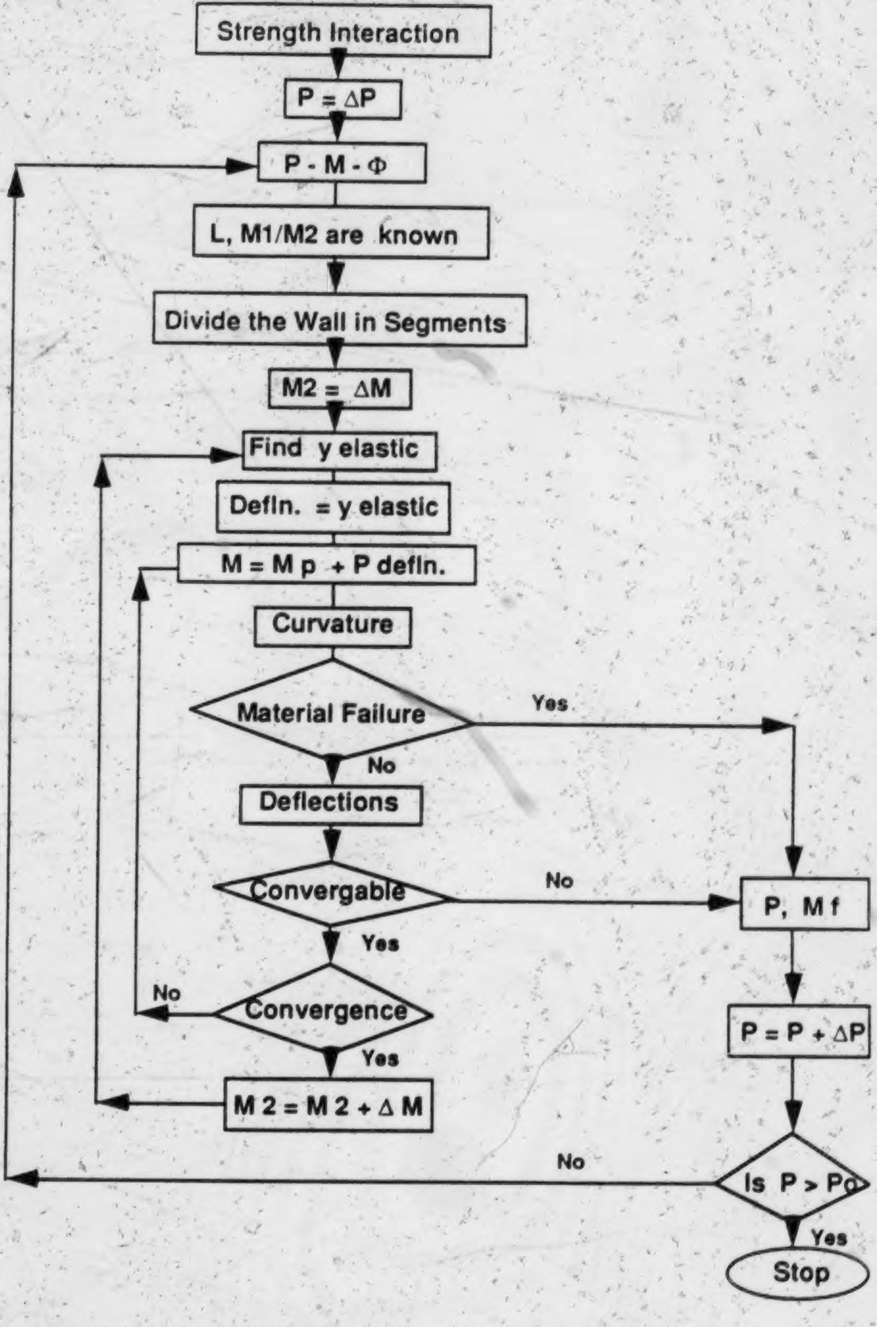
Strength Interaction
P = ΔP
P - M - Φ
L, M1/M2 are known
Divide the Wall in Segments
M2 = ΔM
Find y elastic
Defln. = y elastic
M = M p + P defln.
Curvature
Material Failure
Yes
No
Deflections
Convergable
No
Yes
No
Convergence
Yes
M 2 = M 2 + Δ M
P, M f
P = P + ΔP
No
Is P > Po
Yes
Stop

Figure 4.7 Flow chart for Analysis Method using Newmark's Numerical Procedure

CHAPTER 5

VERIFICATION OF ANALYSIS METHOD

5.1 Introduction

In this chapter the analysis method developed to account for slenderness effects is verified by comparing it with experimental and other analytical results. A special case corresponding to a slender wall with rectangular cross section has been solved in close form by Angervo (1954). A comparison with such an exact solution is made to assess the numerical accuracy of the computer program. Verification of the analysis method is carried out by using experimental data available from previous tests conducted at the University of Alberta by Hatzinikolas (1978). Experiments were carried out for both plain and reinforced slender walls under different bending configurations and for varying slenderness ratios.

5.2 Comparison with an Exact Solution

Angervo (1954) solved the case of an eccentrically compressed homogeneous pillar with a rectangular cross section. Solutions were found by using linear as well as non-linear stress strain diagrams. Solutions were provided in the form of charts which can be used to determine capacity under different eccentricities and for a variety of slenderness ratios. The non-linear stress-strain diagram used by Angervo is of the form

$$\sigma = \frac{f'_u}{k_2}\left(1 - \frac{1}{\sqrt{2k_1\frac{\varepsilon}{\varepsilon_o} + 1}}\right) \qquad (5.1)$$

By varying the constants k_1 and k_2 different parabolic stress-strain curves were studied. The case of $k_1 = -1.00$ and $k_2 = 0.423$ resemble very closely the following stress strain diagram used in this study.

$$\sigma = f'_u\left[2\frac{\varepsilon}{\varepsilon_o} - \left(\frac{\varepsilon}{\varepsilon_o}\right)^2\right] \qquad (5.2)$$

A comparison of the two stress strain diagrams is shown in Fig. 5.1. For the case of rectangular walls subjected to symmetric single curvature bending, the solutions obtained by Angervo were compared with the solution obtained with the analysis method using the CDC approach discussed in the previous chapter. The same parameters were used as input to the two methods. The resulting solutions are compared in Fig. 5.2 to 5.4 corresponding to slenderness ratios of 12, 15 and 22 respectively. Such a comparison indicates reasonably good agreement between the two solutions and therefore provides a satisfactory analytical verification of the analysis method developed in this study.

5.3 Experimental Verification

Extensive experimental studies were carried out on masonry walls at the University of Alberta by Hatzinikolas(1978).

Hatzinikolas' experiments included the testing of 78 full-scale walls. Variables introduced were different bedding and grouting conditions and the effect of main and joint reinforcement. Wall heights varied from 92 inches to 168 inches which correspond to (H/t) ratio of 12 to 22 respectively. These results are found to be very useful and have been used by many investigators to assess slender wall design methods.

The analytical solution which uses the CDC approach for symmetric single curvature bending with $e_2/e_1 = 1.0$ and the Newmark's Numerical Method for all other cases is compared with experimental data in Fig. 5.5 to Fig. 5.14. Fig 5.5 to Fig 5.7 correspond to plain walls and the remaining figures correspond to reinforced walls.

Fig. 5.5 is for plain walls in single curvature bending. The wall height is 105 in. which corresponds to an H/t ratio of 13.77. That these walls exhibit brittle behavior is obvious by a limited $(e/t)_{max}$ ratio. Experimental results are reasonably well predicted by the analysis method.

In Fig. 5.6 the case of unequal end eccentricities is studied with $e_2/e_1 = 0.0$, i.e. the load at one of the ends is concentric. The brittle nature of the wall is exhibited by a rather limited $(e/t)_{max}$ ratio. Comparing this with the previous case of symmetric single curvature bending, the wall is stronger in this form of loading because the primary and secondary moments do not occur at the same point along the wall. In this case also, the analysis method predicted experimental results reasonably well.

In Fig. 5.7 the analytical and experimental results were studied for the case of double curvature bending with an e_2/e_1 ratio of -1. Experimental studies have indicated that the ultimate failure occurs by unwinding from a double to a single curvature mode. The analysis method also consistently exhibited unwinding phenomenon. Analysis indicated that the deflected shape just before ultimate failure resembled very closely a half sine wave or single curvature mode. A typical deflection history indicating the unwinding phenomenon for a reinforced wall is shown in Fig. 5.15. At lower axial loads the analysis showed that the failure occurs by exceeding the moments near the ends. Experiments also indicated a crushing failure at the ends for low axial loads and high moments.

In Fig. 5.9 to Fig. 5.13 reinforced walls under single curvature bending were studied. In all these walls ductile behavior is exhibited by a higher $(e/t)_{max}$ ratio. An increase in slenderness resulted in a reduction of capacity as expected. P/P_o vs e/t curves corresponding to higher values of slenderness lie inside the curves for lower slenderness. The analysis method predicted experimental results reasonably well for all these cases.

In Fig. 5.14 reinforced walls in double curvature bending were studied. The analysis method predicted a ductile behavior for the wall. Again, as for plain walls in double curvature bending, unwinding occurred from a double to a single curvature mode prior to the ultimate failure. Experimental results in this case were found to be higher than analytical results.

In summary, the analysis method predicted experimental results reasonably well. The method has a rational basis and uses a realistic stress-strain diagram. Both material and stability failures are properly predicted using this method. Besides calculating ultimate load and moment, the method can be used to determine wall deflections along the height for any stage of loading before failure.

In view of the advantages of the analysis method it is used in the following chapter to study the behavior of plain and reinforced walls with different grouting and bedding conditions and to develop an approximate method for slender masonry walls.

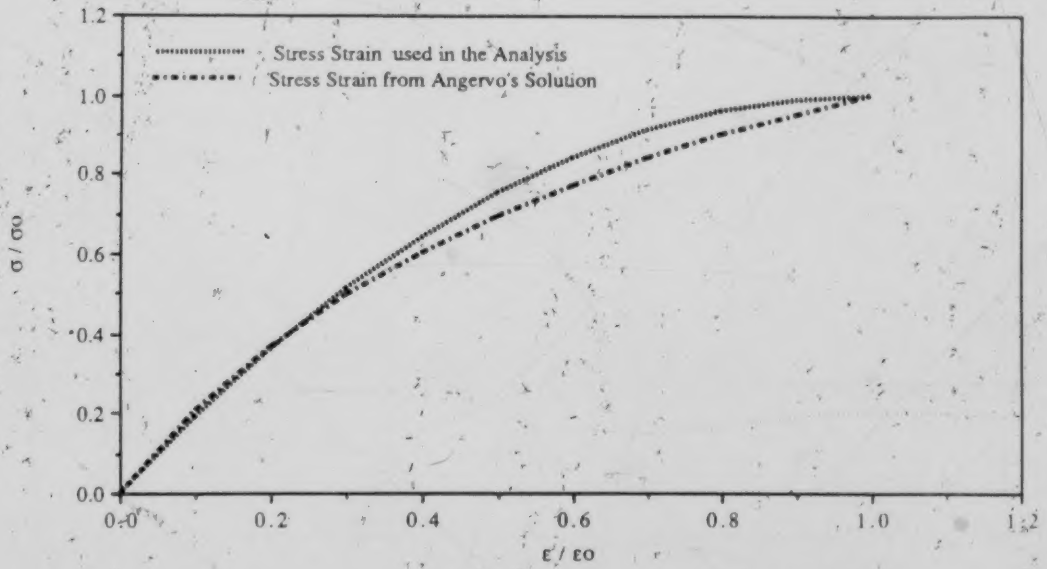

Fig.5.1 A Comparison of Stress Strain Curves

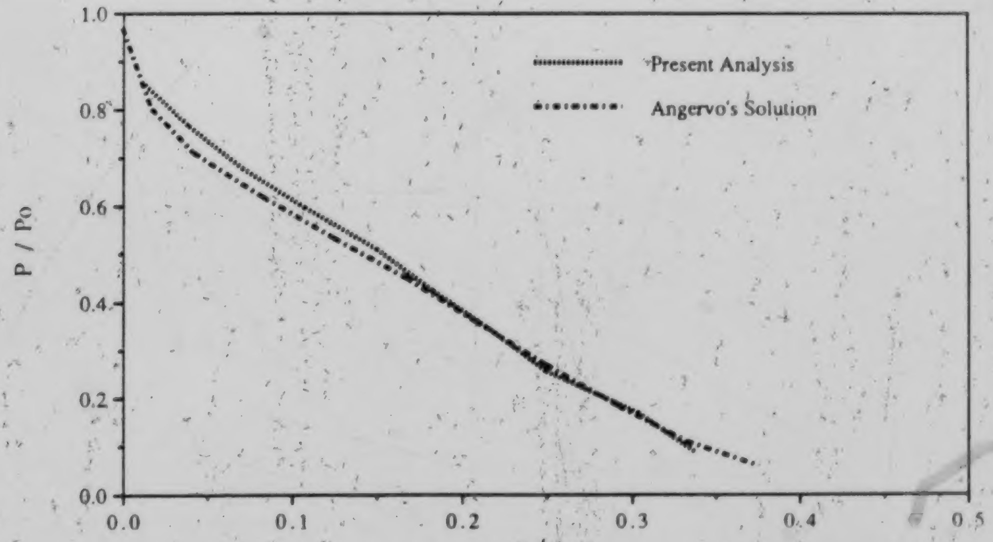

Fig.5.2 Comparison with Angervo's Solution
H/t = 12, t= 7.6 inches

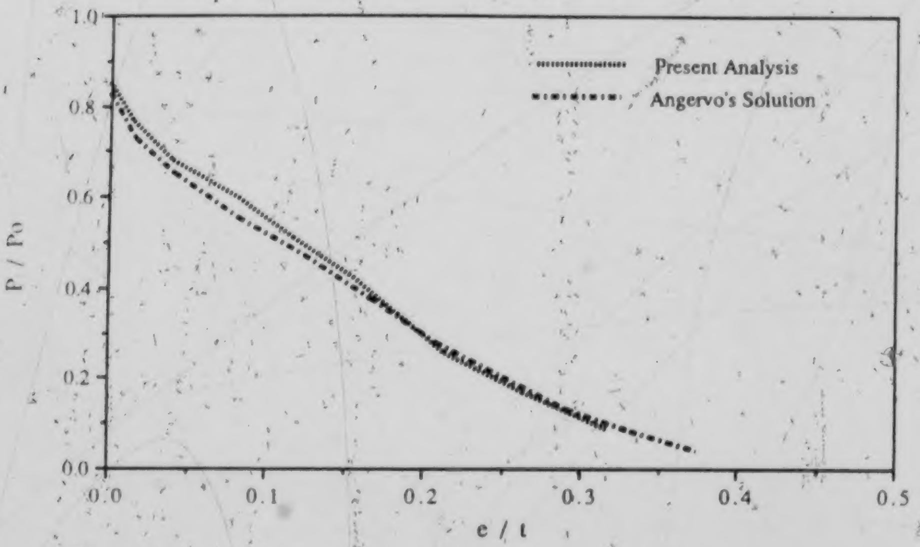

Fig.5.3 Comparison with Angervo's Solution
H/t = 15, t= 7.6 in.

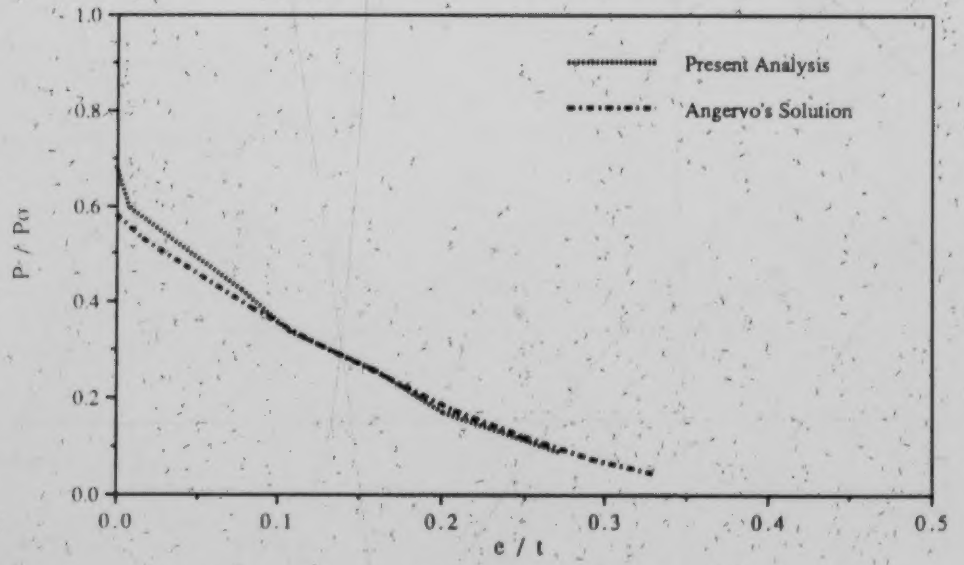

Fig.5.4 Comparison with Angervo's Solution
H/t = 22, t=7.6 in.

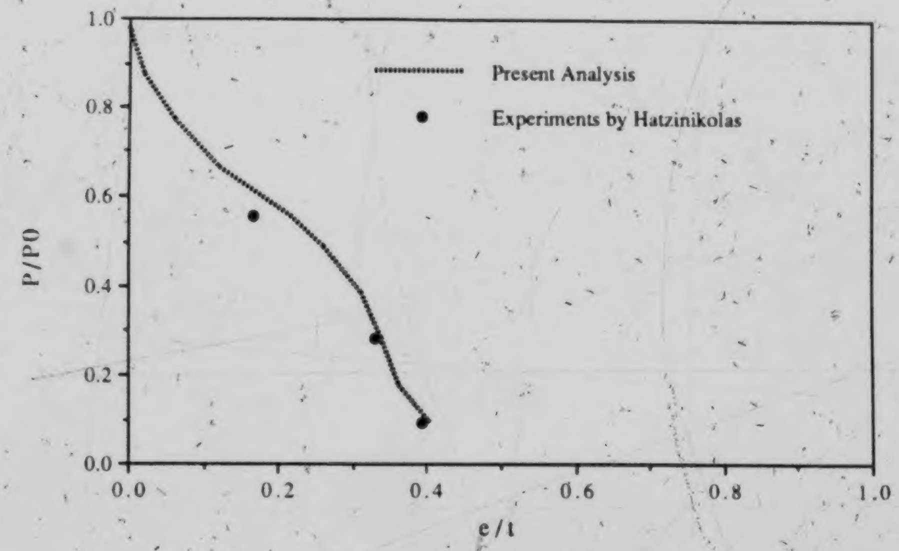

Fig.5.5 Plain Masonry Walls in single curvature bending
e2/e1 = 1.0, H/t = 13.77, H 105 in.

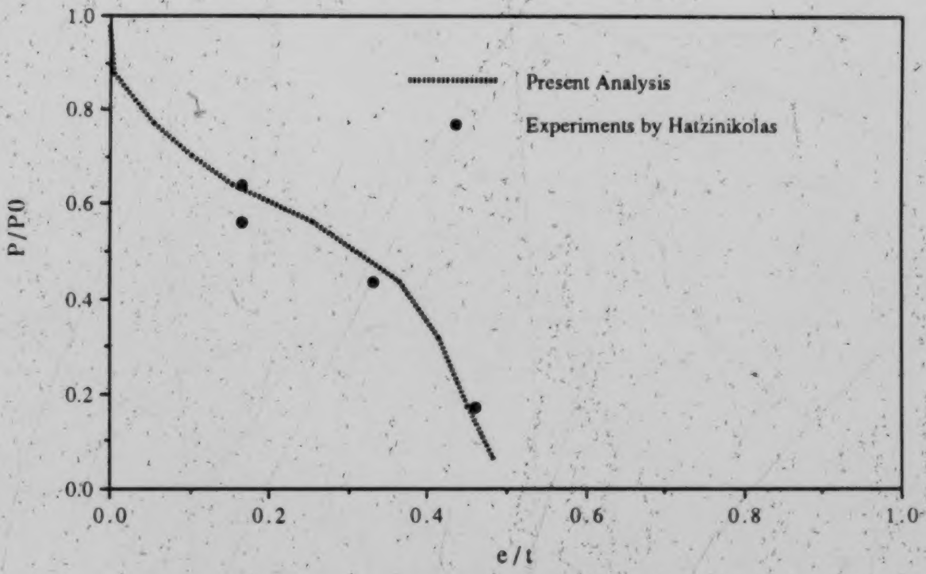

Fig.5.6 Plain Walls in Single Curvature Bending
e2/e1 = 0.0, H/t = 18, H=137 in.

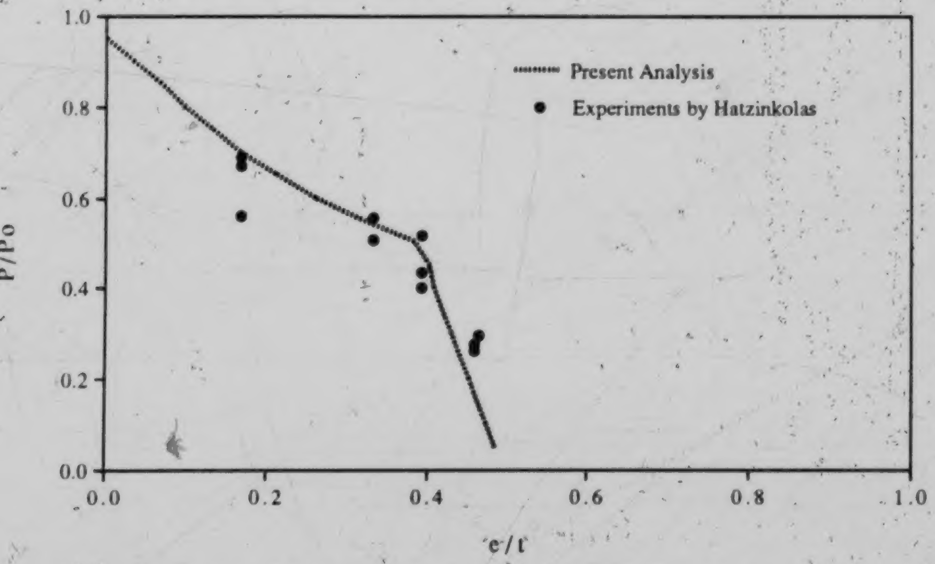

Fig.5.7 Plain Walls in Double Curvature Bending
e2/e1 = -1.0, H/t = 14, H=105 in.

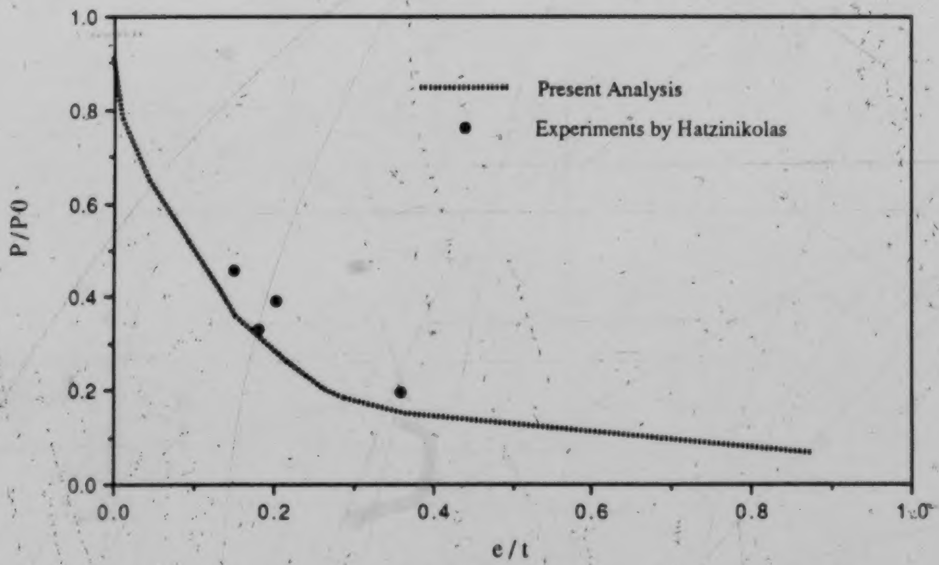

Fig. 5.8 Reinforced Walls in Single Curvature Bending
e2/e1 = 1.0, H/t =14, H=105 in.

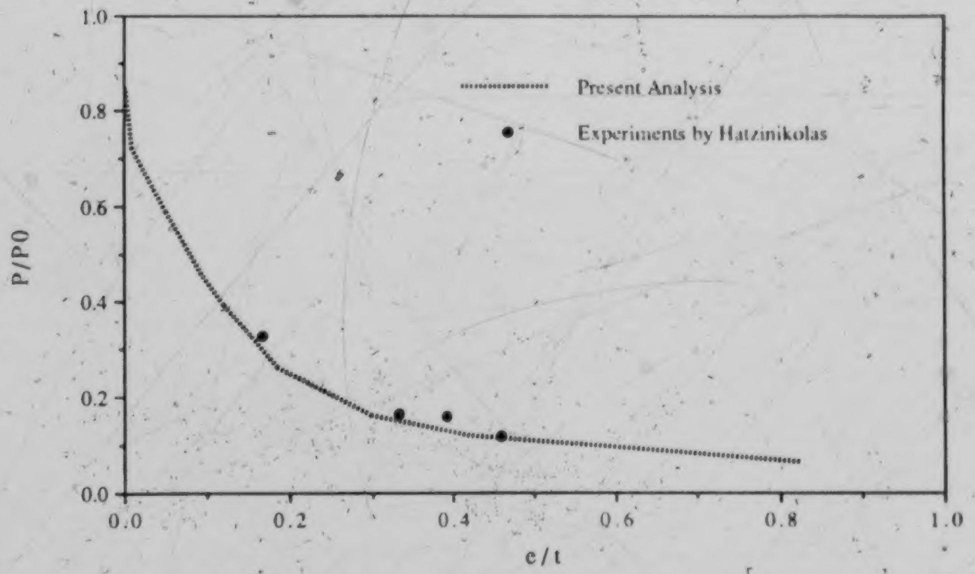

Fig.5.9 Reinforced Walls in Single Curvature Bending
e2/e1=1.0, H/t=16, H=122 in., As=3.0 in.sq.

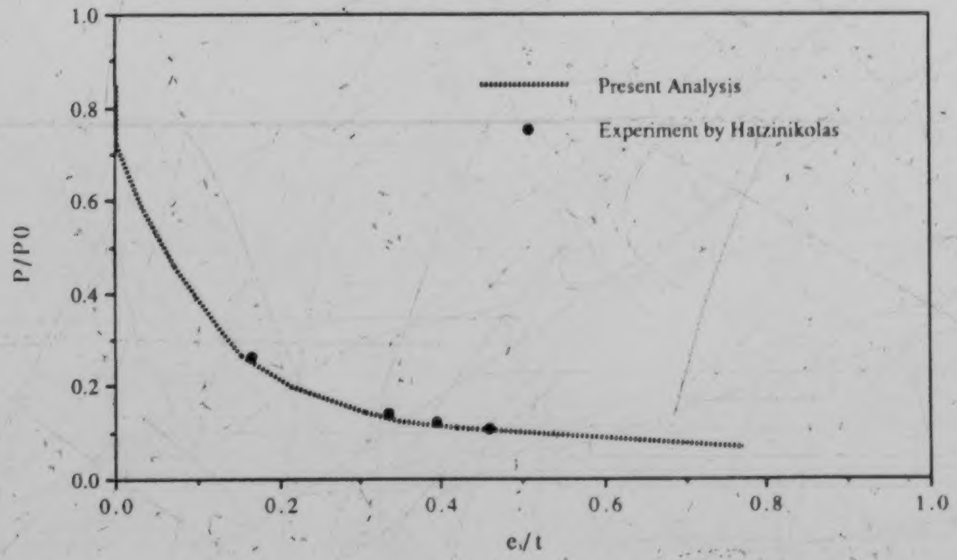

Fig.5.10 Reinforced Walls in Single Curvature Bending
e2/e1=1.0, H/t=18, H=137 in., As=3.0 in.sq.

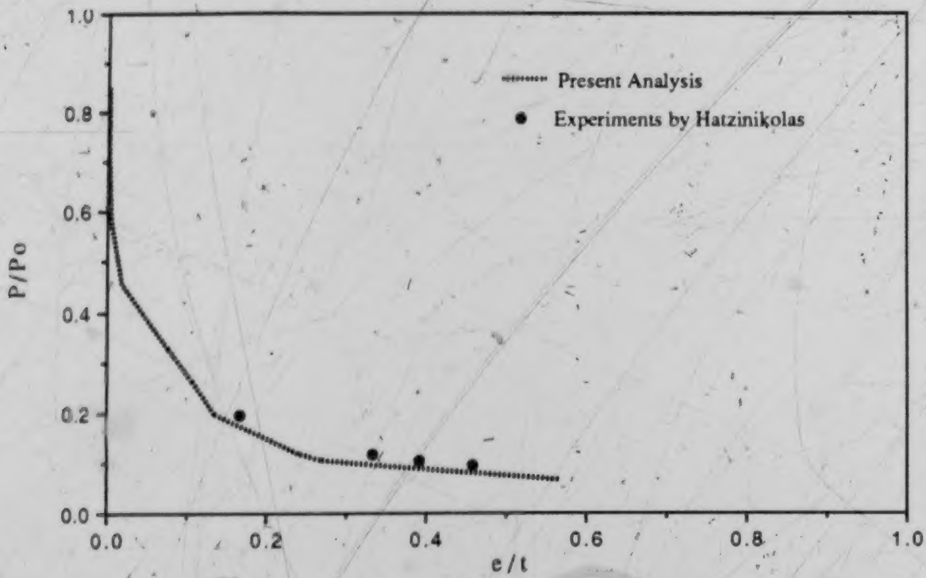

Fig.5.11 Reinforced Walls in Single Curvature Bending
e2/e1=1.0, H/t=24, H=183 in., As=3.0 in.Sq.

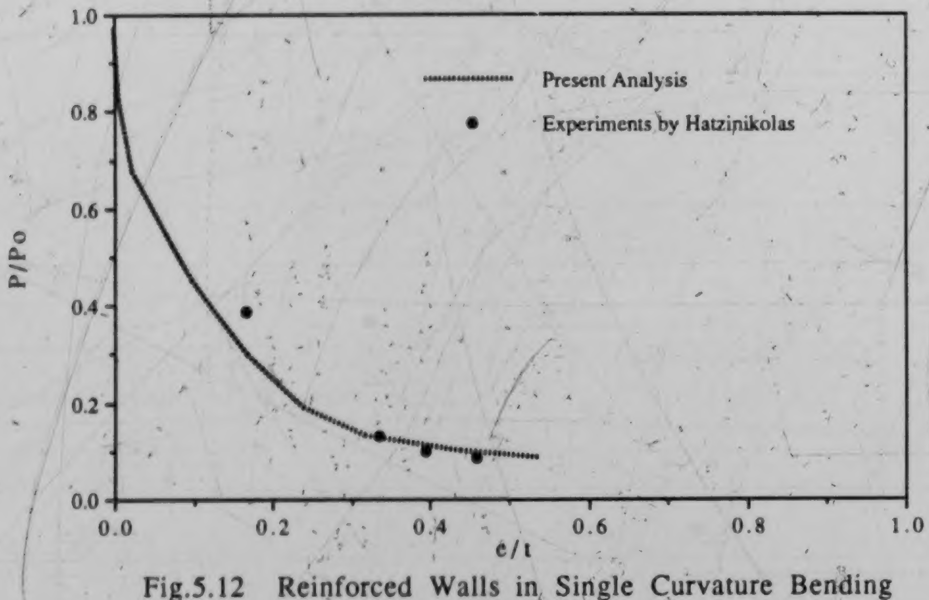

Fig.5.12 Reinforced Walls in Single Curvature Bending
e2/e1=18, H/t=18, H=137 in., As=1.32 in.Sq.

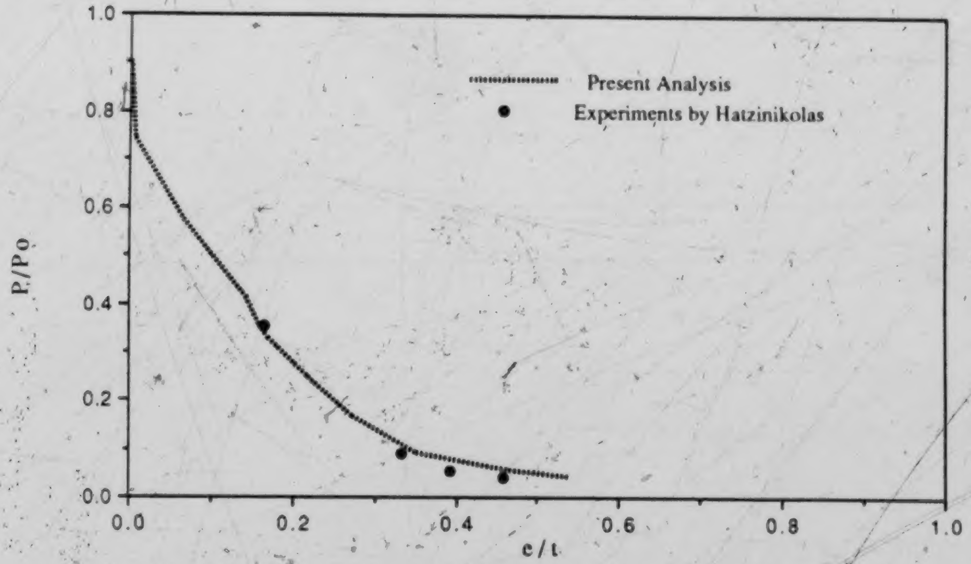

Fig.5.13 Reinforced Walls in Single Curvature Bending
e2/e1=1.0, H/t=18, H=137 in., As=.33 in.Sq.

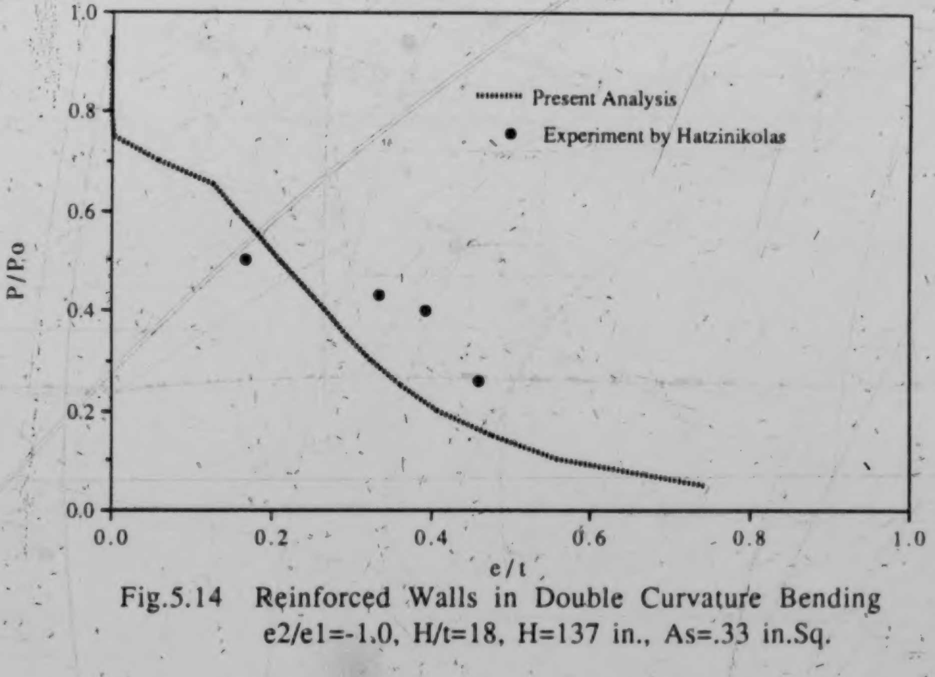

Fig.5.14 Reinforced Walls in Double Curvature Bending
e2/e1=-1.0, H/t=18, H=137 in., As=.33 in.Sq.

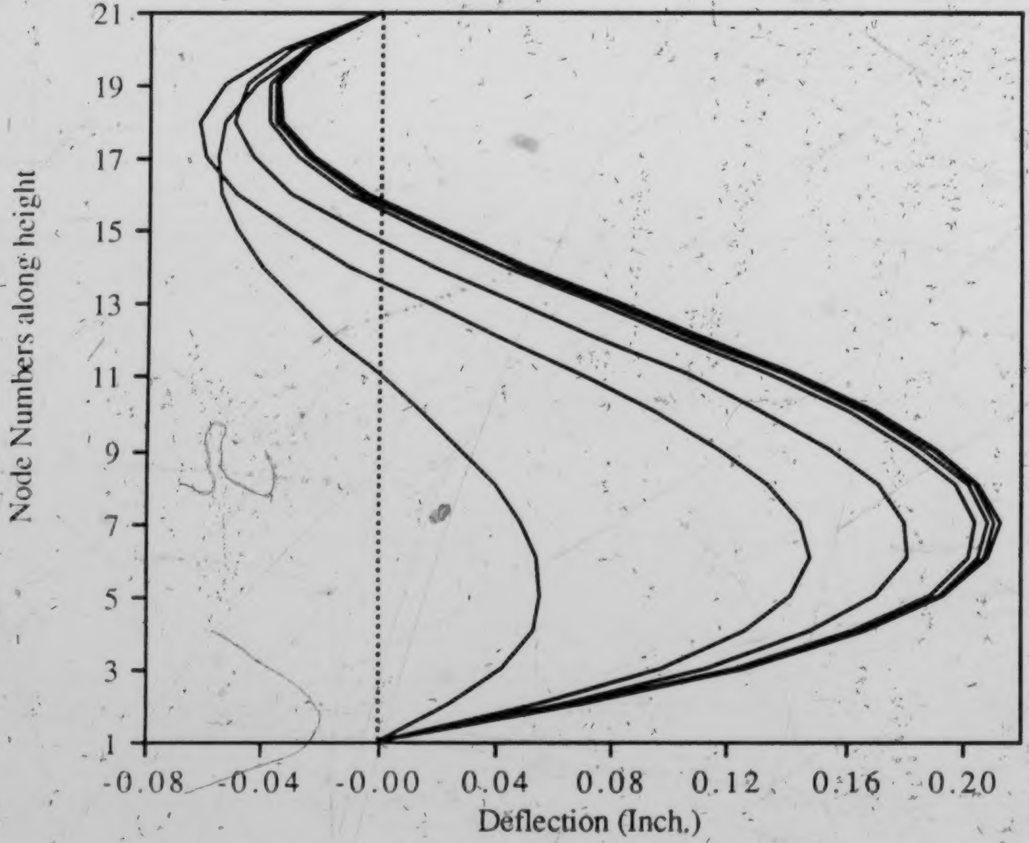

Fig. 5.15 Deflection histories indicating unwinding of a reinforced wall, As= .33 in. Sq., H/t = 18, e1/e2 = -1, P = 350 Kips, M/Mu = 0.9

CHAPTER 6

DEVELOPMENT OF APPROXIMATE METHOD

6.1 Introduction

This chapter deals with the development of an approximate analysis method for slender masonry walls. The aim is to propose a simple procedure suitable for design office use. The procedure should have a rational basis, must be conservative and should be able to predict results similar to those of a reasonably accurate computer based detailed analysis.

Among all the approximate methods for slender walls, the Moment Magnifier method is the most rational. The Moment Magnifier method gives very good results if Flexural Rigidity (EI) can be correctly predicted. In this chapter, after a review of approximate methods, thevariation of (EI) values is studied by varying both bending moment and axial load for different types of cross sections. A simplified procedure to calculate EI values is then proposed. Finally, the Moment Magnifier method is used by incorporating these EI values. A parametric study is carried out to study the validity of this new approach by comparing it with the moment-curvature based analysis method. Superiority of this new approach is demonstrated by comparing it with experiments and with the approximate methods in the code.

6.2 Development of Approximate Method

Walls have been used traditionally to resist axial loads. Therefore, to determine wall capacity a simple equation was used.

$$P = A_n f_m \tag{6.1}$$

where f_m is the allowable compressive stress and A_n is the effective area of cross section. When it was found that high slenderness and eccentric application of load lead to considerable reductions in capacity, it was necessary to incorporate these effects into the equation for wall capacity. The simplest approach was to introduce reduction factors corresponding to slenderness and eccentricity. Consequently, the equation for wall capacity took the present form of

$$P = C_s C_e A_n f_m \tag{6.2}$$

In CSA S304 the coefficients C_s and C_e are determined by equations which depend on the relative eccentricity ratio (e_2/e_1), the eccentricity ratio (e_1/t) and slenderness ratio (H/t). The basis of these equations is the experimental work on solid brick walls carried out by the Structural Clay Products Institute (1969). These equations inappropriately form the basis of design for brick as well as block walls in the present Canadian code. This approach based on empirical rules has been extensively used because it produced safe and very conservative designs. However, the validity of such an approach as a design procedure is questionable because it neither properly considers applied loading nor the structural response.

Only very recently, the Moment Magnifier method has been included as an additional design procedure in CSA S304. The Moment Magnifier method is a popular approximate method for analysis and design of both reinforced concrete and steel slender members under combined loading.

There have been several attempts to use the Moment Magnifier method for slender masonry walls. When it is applied to masonry, serious theoretical and practical difficulties arise in the estimation of the flexural rigidity (EI). The flexural rigidity is an important factor as it establishes the magnified moment. In order to successfully apply the Moment Magnifier method, the material nonlinearity and cracking of the cross section have to be considered in evaluating effective rigidity. It is difficult to estimate these effects by simple procedures as they are coupled with the magnitude of axial load and bending moment acting on the cross-section.

The present Moment Magnifier method in the CSA S304 is based on an assumed distribution of rigidity along the height depending on the ratio of end eccentricities. Linear stress-strain behaviour is assumed. At the ends the moment of inertia is calculated as cracked or uncracked depending on applied end eccentricities. For walls bent in single curvature, the moment of inertia at mid-height is assumed equal to zero. In between a linear variation of moment of inertia is assumed. For walls bent in double curvature bending, the moment of inertia at quarter points along the height is taken as zero and at mid height the moment of inertia is taken equal to the gross moment of inertia. From such distributions average effective moment of inertia is calculated and multiplied by a constant modulus of elasticity to get an effective rigidity (EI) for the wall. The distribution of moment of inertia assumed in the calculation process is very approximate and does not have a rational basis.

The January 1988 amendment to CSA S304 reduces $(EI)_{eff.}$ as calculated above to $0.25(EI)_{eff.}$. Hence these provisions grossly underestimate the effective rigidity of a cross section.

A load-moment-curvature based analytical method was used in chapter 4 which provides a very good estimation of wall capacity because it properly takes into account the varying flexural rigidity (EI) corresponding to a load and moment over the cross-section by the use of P-M-Φ relationships. The development of P-M-Φ relationships takes into account factors like load, moment, material behaviour and geometry of the cross section in the calculations.

Accordingly, the Moment Magnifier method can be applied with success to slender masonry walls if one can calculate (EI) values similar to those calculated by a reasonable load-moment-curvature relationship. In an attempt to propose rational (EI) values, the variation of (EI) is initially studied by varying the bending moment at a given axial load. A procedure to calculate (EI) using load-moment-curvature relationships is presented below.

6.3 Evaluation of EI from P-M- Φ relationships

For a given load P, moment-curvature relationships can be developed as explained in section 4.2. For a linear elastic case, the curvature is given by the ratio of moment and Effective flexural rigidity (EI). Consequently (EI) can be calculated as

$$EI = \frac{M}{\phi} \tag{6.3}$$

For a P-M-Φ relationship derived using nonlinear stress-strain behaviour and by accounting for the cracking of the cross-section, EI corresponding to a given moment, M can be calculated as

$$(EI)_M = \frac{dM}{d\phi} \tag{6.4}$$

This gives the variation of EI at a given load as the moment varies from zero to the ultimate moment.. The ultimate moment corresponding to an axial load is known from a load-moment-curvature relationship or can be readily obtained from a strength interaction diagram. An interaction diagram is developed using the geometry of the cross section and the stress-strain relationship. Compressive edge strain is kept constant and equal to ultimate strain ε_0 and the depth to the neutral axis is varied to achieve various strain distributions. Corresponding stress distributions are calculated using the stress strain relationship from which load and moment is calculated by integration over the cross section. A plot of such pairs of load and moment is referred to as a strength interaction diagram. A balanced condition corresponds to the simultaneous attainment of compression and tension failure strains in the cross section. Axial load calculated for this condition is termed as balanced load. For an axial load less than the balanced load ultimate failure occurs as a tensile failure and for a load greater than balanced load, ultimate failure occurs by a compression failure.

The variation of (EI) is studied for three types of walls: plain walls fully-bedded, plain walls with face-shell bedding and reinforced walls. In each case axial load is varied and results are plotted in figures 6.1 to 6.5 after normalizing (EI) with $(EI)_o$ and moment (M) with ultimate moment (M_u). In each case normalized flexural rigidity (e) is plotted as a function of normalized moment (m). They are defined as follows

$$e = \frac{EI}{E_o\, I_o} \qquad (6.5)$$

$$m = \frac{M}{M_u} \qquad (6.6)$$

Where I_o is gross moment of inertia of the cross section and E_o is the slope of stress strain diagram at zero strain.

The Flexural rigidity plots were observed to have a few distinct characteristics. A variation of (EI) was markedly different for two different cases.

1. Load less than balanced load:

In this case, ultimate failure condition being a tensile one, the location of the beginning of cracking and a following sudden deterioration of flexural rigidity was observed. When the moment equals zero, EI is the product of the gross moment of inertia and E corresponds to the uniform strain over the cross section. As the moment increases, EI varies slightly to a point when applied moment equals the cracking moment. This occurs when strain on the tension face of wall is reduced to zero. Immediately after cracking, flexural rigidity is reduced sharply as the moment approaches ultimate moment.

2. Load greater than balanced load:

   In the next case, when ultimate failure occurs by compression, no cracking was observed, as expected. However, (EI) was found to vary with moment. An increase in the moment results in a corresponding increase in the stress over the cross-section and because of the nonlinear stress-strain relationship, modulus of elasticity reduces with increase in the stress. Hence EI varies as moment increases.

Following a study of the characteristic features of (EI) plots, a simplified method was proposed which calculates EI values very similar to those developed using the load moment-curvature-relationships.

6.4 Simplified Method to Calculate Flexural rigidity

In order to arrive at rational EI values critical co-ordinates were identified in the two cases of: load less than balanced load and load greater than the balanced load. Then a procedure to calculate these these co-ordinates was presented. A variation of EI between them was then proposed using simple equations such that the resulting variations in EI resemble the variations observed using load-moment-curvature relationships.

Case 1. Load less than Balanced Load:

There are three key points to be identified in this case. They are initial flexural rigidity, flexural rigidity at cracking and flexural rigidity at ultimate.

i) Initial Flexural rigidity: The Initial Flexural rigidity corresponds to zero moment. The whole cross section is uniformly stressed due to axial load. Corresponding strain and Modulus of elasticity are determined using the nonlinear stress strain relationship. The moment of Inertia at this stage is equal to the gross moment of inertia (I_o). Therefore, initial Flexural rigidity is given by

$$(EI)_i = E_i I_o \qquad (6.7)$$

$$(e)_i = \frac{E_i I_o}{E_o I_o} \qquad (6.8)$$

where E_i is the modulus of elasticity corresponding to a uniform stress due to the axial load only.

ii) Flexural rigidity at Cracking: As the moment increases, strain over the cross section increases resulting in a change in the Modulus of Elasticity. Therefore, as moment approaches cracking moment, Modulus of Elasticity reduces slightly because of the nonlinear stress-strain behaviour of masonry. The cracking moment can be evaluated by assuming a linear strain of zero on the tension face and a strain of $2\varepsilon_a$ on the compression face. Where, ε_a is the uniform strain over the cross section due to axial load alone. Stress distribution is calculated using the stress-strain relationship. Stresses are integrated to get moments over the cross section. The ratio of Cracking Moment (M_c) to Ultimate Moment (M_u) is defined as α. At this stage, i.e. when $m = \alpha$, no cracking has occurred. But some reduction in (EI) was observed as M approached M_c for all types of walls studied. This can be associated with increase in the stress over the cross-section with increase in the moment. This change was found to depend on the axial load over the cross-section. After studying several variations, the reduction in EI at cracking was approximated with reasonable accuracy through the use of a factor of $(1 - P/3P_o)$ i.e. Flexural rigidity at cracking $(EI)_c$ is given by

$$(EI)_c = (EI)_i\left(1 - \frac{P}{3P_o}\right) \qquad (6.9)$$

$$(e)_c = \frac{(EI)_c}{E_o I_o} = e_i \left(1 - \frac{P}{3P_o} \right) \qquad (6.10)$$

Where P is the axial load on the wall and Po is the pure axial capacity of the cross-section.

iii) Flexural rigidity at Ultimate Moment:

Immediately after cracking flexural rigidity reduces sharply and by the time moment reaches ultimate the cross section is heavily cracked. At this point flexural rigidity is calculated based on two assumptions.

a) uncracked depth (x) of cross section:

The uncracked depth of the cross-section is required to determine the effective moment of inertia at ultimate moment. This is obtained by assuming a compressive edge strain of ε_o and determining the neutral axis depth by integrating stresses over the cross section and equating it to applied load.

$$x = \left(\frac{3P}{2P_o} \right) t \qquad (6.11)$$

This equation is true for a solid rectangular cross section. Therefore the ratio of moment of inertia at ultimate to gross moment of inertia is given by

$$\frac{I_u}{I_o} = \left(\frac{3P}{2P_o} \right)^3 \qquad (6.12)$$

b) Modulus of Elasticity is assumed as 50 percent of E_i. High stresses over the cross section justify the use of low E at ultimate load. Hence flexural rigidity at ultimate load is given by

$$(EI)_u = \left(\frac{3P}{2P_o} \right)^3 I_o \frac{E_i}{2} \qquad (6.13)$$

$$e_u = \frac{(EI)_u}{E_o I_o} = \left(\frac{3P}{2P_o} \right)^3 \frac{e_i}{2} \qquad (6.14)$$

A linear variation of EI is assumed between e_i and e_c and a parabolic variation is assumed between e_c and e_u due to sharp reduction in (EI) after cracking. Hence normalized flexural rigidity (e) is given by the following equations.

$$e = e_i - \left(\frac{e_i - e_c}{\alpha} \right) m \qquad \text{for } m < \alpha \qquad (6.15)$$

$$e = \left(\frac{1 - m}{1 - \alpha} \right)^2 (e_c - e_u) + e_u \qquad \text{for } m > \alpha \qquad (6.16)$$

Case 2. Load greater than Balanced Load: There are two key points to be identified in this case

i) Initial Flexural rigidity: initial flexural rigidity is calculated as in case 1..

$$(EI)_i = E_i I_o \qquad (6.17)$$

$$(e)_i = \frac{E_i I_o}{E_o I_o} \qquad (6.18)$$

ii) Flexural rigidity at Ultimate: As moment increases no cracking takes place in this case. However, E continuously changes due to the change in the stress over the cross section. This variation is observed to be parabolic. At ultimate load the modulus of elasticity is again assumed as $E_i/2$.

$$(EI)_u = \frac{E_i}{2} I_o \qquad (6.19)$$

$$(e)_u = \frac{e_i}{2} \qquad (6.20)$$

A parabolic variation of flexural rigidity is assumed in this case.

$$e = (1 - m^2 / 2)\, e_i \qquad (6.21)$$

6.5 Assessment of Accuracy of EI Values

In order to assess the accuracy of the simplified procedure to calculate EI a comparison is made between the EI values calculated using simplified procedure and those obtained using load-moment-curvature relationships. Forty different cases were studied. They include fully-bedded plain-walls, face-shell bedded plain walls and reinforced walls with reinforcement equal to balanced reinforcement, fifty percent of balanced reinforcement and minimum reinforcement, Axial load was varied in steps of 10% from 10% to 80% of axial capacity to cover several cases of load being less or greater than the balanced load. Comparison of EI values is made in Figures 6.6 to 6.45. If the axial load is greater than the balanced load EI is given by Equation 6.21 and if the axial load is less than the balanced load, EI can be determined using Equation 6.15 or 6.16. This simple approach to estimate EI is termed as Equation SA1 in Figures 6.6 to 6.45.

The simple procedure was found to predict EI values very similar to those obtained using load-moment-curvature relationships. The trend as well as magnitude was found to be very similar in the two cases for different types of cross sections and at different levels of axial loads. For a few cases the simplified procedure is found to give conservative estimates of EI, which is acceptable in a design procedure. Fairly good agreement between EI values confirms the adequacy of the assumptions made in the development of a simplified procedure to calculate flexural rigidity.

These EI values will now be used in the Moment Magnifier method and a parametric study will be carried out to assess the accuracy of this approximate method.

6.6 Parametric Study

A parametric study is carried out to determine the accuracy of the Moment Magnifier method in which the newly developed equations of EI were used. Three different cross sections representative of typical masonry construction are chosen. They include fully-bedded plain masonry walls, face-shell bedded plain masonry walls and reinforced walls with 50% of balanced reinforcement. Slenderness effects are evaluated for each of these cross sections for slenderness ratios (H/t) of 15, 20, 25 and 30.

By using the equations developed in the previous section, EI values can be calculated if the moment is known. In a slender member the primary moments are magnified and the true EI values correspond to the magnified moment. Because of the non-linear nature of the problem, the magnified moment at a given axial load is determined using an iterative procedure. To start the iterative procedure, EI is determined using the primary moment. This EI is used to calculate the initial magnified moment. The actual EI value in the member corresponds to this magnified moment and not the primary moment. Following this a new magnified moment is calculated. This process is repeated until convergence is achieved. For most of the cases the convergence was achieved in only 3 or 4 iterations. Therefore, the procedure remains to be fairly simple. After having determined the magnified moment, it is used assess failure of the slender member. If the magnified moment is found to be greater than or equal to the moment capacity of the cross-section, then failure occurs.

6.6.1 Summary of Approximate Method for Slender Walls

The Approximate Method developed in this chapter is summarized in the following steps.

1. Calculate the Strength Interaction Diagram including the Balanced Load (P_b) and the Pure Axial Capacity (P_o) for the wall cross section.
2. Determine the axial load (P) acting on the wall. Using the strength interaction diagram find the corresponding moment (M_u) the cross section can resist. Some interpolation may be required.
3. From the primary moment distribution determine moments at the ends of the member.
4. Determine Effective Rigidity (EI) corresponding to the higher end moment using one of the following three equations whichever is applicable.

(a) If P is less than or equal to the Balanced Load (P_b)

$$EI = \left(e_i - \left(\frac{e_i - e_c}{\alpha} \right) m \right) E_o I_o \qquad \text{for } m < \alpha \qquad (6.22)$$

$$EI = \left(\left(\frac{1 - m}{1 - \alpha} \right)^2 (e_c - e_u) + e_u \right) E_o I_o \quad \text{for } m > \alpha \quad (6.23)$$

I_o = Gross Moment of inertia

E_o = Initial Modulus of Elasticity at zero strain

m = Normalized Moment = M/M_u

α = Ratio of cracking moment (M_c) to ultimate moment (M_u)

$$M_c = P_o \left(R - \frac{R^2}{3} \right) \frac{d}{4} \left(\frac{8 - 3R}{3 - R} - 2 \right)$$

R = Compressive Edge Strain / Ultimate Strain

$= 2\, \varepsilon_a / \varepsilon_o$

$= 2 (1 - \sqrt{1 - \theta})$

ε_a = Uniform strain due to axial load P only

$\theta = P/P_o$

e_i = Normalized Initial Flexural rigidity = $E_i I_o / E_o I_o$

E_i = Modulus of Elasticity corresponding to uniform strain due to axial load only

e_c = Normalized Flexural rigidity at Cracking

$$= e_i \left(1 - \frac{P}{3 P_o} \right)$$

e_u = Normalized Flexural rigidity at Ultimate

$$= \left(1.5 \frac{P}{P_o} \right)^3 \frac{e_i}{2}$$

(b) If P is greater than the Balanced Load (P_b)

$$EI = (1 - 3 m^2 / 2) E_o I_o \qquad (6.24)$$

5. Calculate the Magnified moment as

$$M_{mag.} = \frac{C_m \; M_2}{\left(1 - \dfrac{P(kL)^2}{\pi^2 (EI)_{eff.}} \right)}$$

where

C_m is a factor to account for unequal end moments $= 0.6 + 0.4 M_1 / M_2 > 0.4$

M_2 = Larger End Moment

M_1 = Smaller End Moment

L = Height of the Wall

k = Effective Length factor

6. This magnified moment calculated in step 5 is used to recalculate EI using step 4. Again new magnified moment is calculated using step 5. This is repeated until the magnified moment converges. For the cases studied, convergence was achieved in only 3 to 4 iterations
7. If the converged magnified moment is greater than or equal to moment capacity of the cross section (M_u), then failure occurs.

In order to assess the validity of this approximate method, reduced capacity due to slenderness effects is calculated by the Moment Magnifier method for various cross sections and for different slenderness ratios and a comparison is made with the results of a computer based load-moment-curvature analysis method. The results are plotted in Figures 6.46 to 6.81. It was found that the new Moment Magnifier method predicts results that are close to those obtained from a load-moment-curvature based analysis method for most of the cases.

6.7 Comparisons with Tests

In this section the two analytical methods developed in this study were compared with the tests carried out at the

University of Alberta by Hatzinikolas (1978). The first three cases correspond to plain walls and the remaining seven correspond to reinforced walls.

Fig.6.82 is for plain walls in symmetric single curvature bending. The wall height is 105 in. which correspond to a H/t ratio of 13.77. The experimental results are reasonably well predicted by the two analysis methods.

In Fig.6.83 comparison is made for the case of unequal end eccentricities with eccentricity ratio of 0.0, i.e load at one of the ends is concentric. Comparing this with the previous case of symmetric single curvature bending, the wall is stronger in this form of loading because the primary and secondary moments do not occur at the same point along the height. In this case also analysis methods predicted experimental results very well.

In Fig.6.84 the case of double curvature bending with an eccentricity ratio of -1 was studied. Experimental studies have indicated that the ultimate failure occurs by unwinding from a double to a single curvature mode. At higher axial loads Newmark's numerical method indeed exhibited unwinding phenomenon. However for this case the experimental results were found to be higher than the analytical predictions. For some of the cases the experimental points were found to lie outside the strength interaction curve.

In Fig.6.85 to Fig6.90 reinforced walls under single curvature bending were studied. For all of these cases predictions by the analysis method were conservative. Fairly good agreement between experimental and analytical results was found for lower reinforcement ratios as shown in Fig 6.89 and Fig. 6.90.

In Fig.6.91 reinforced walls in double curvature bending were studied. Again, as for plain walls in double curvature bending, unwinding occurred at higher axial loads. Experimental results were found to be higher than analytical results.

6.8 Assessment of Approximate Methods

The superiority of this approximate method over the current code procedures is demonstrated by numerical comparisons. Four cases are studied and the reduction in capacity due to slenderness effects is calculated by Code Moment Magnifier method, Coefficient method, the New proposed Moment Magnifier method and load-moment-curvature based analysis method. The results are compared in figures 6.92 to 6.95. Such a comparison concludes that this approximate method is a significant improvement over the current approximate methods available for design of slender masonry walls.

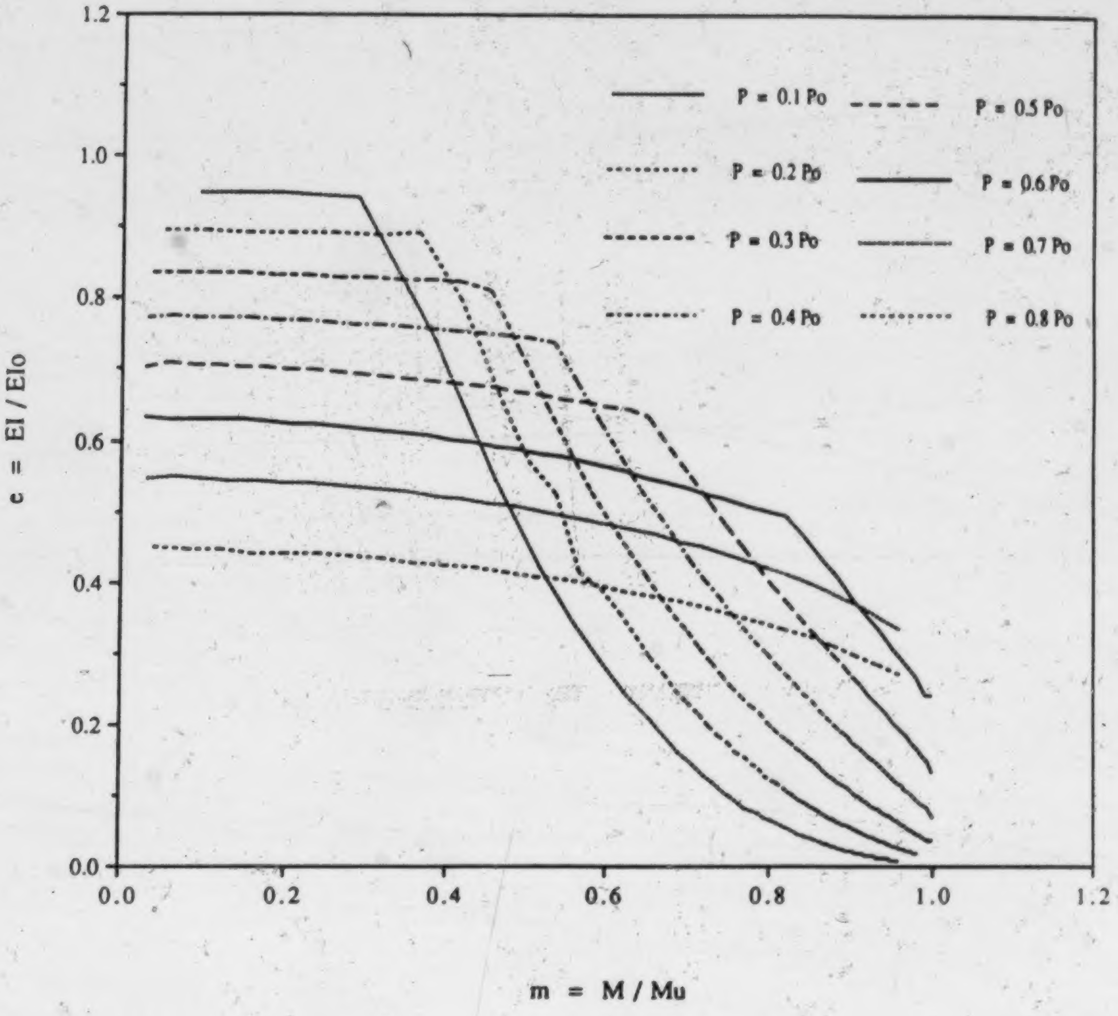

Fig.6.1 Variation of Stiffness for Fully bedded Plain Masonry Walls

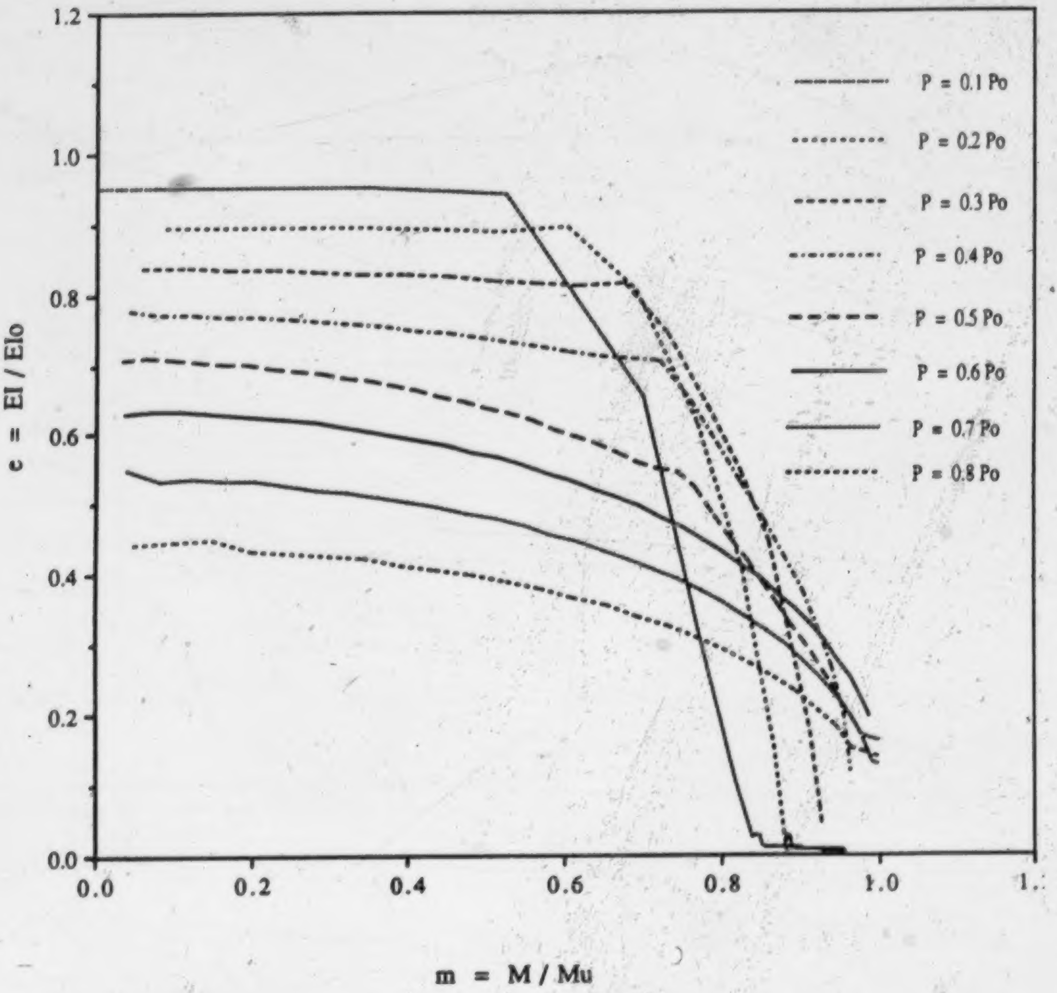

Fig.6.2 Variation of Stiffness for faceshell bedded Plain masonry Walls

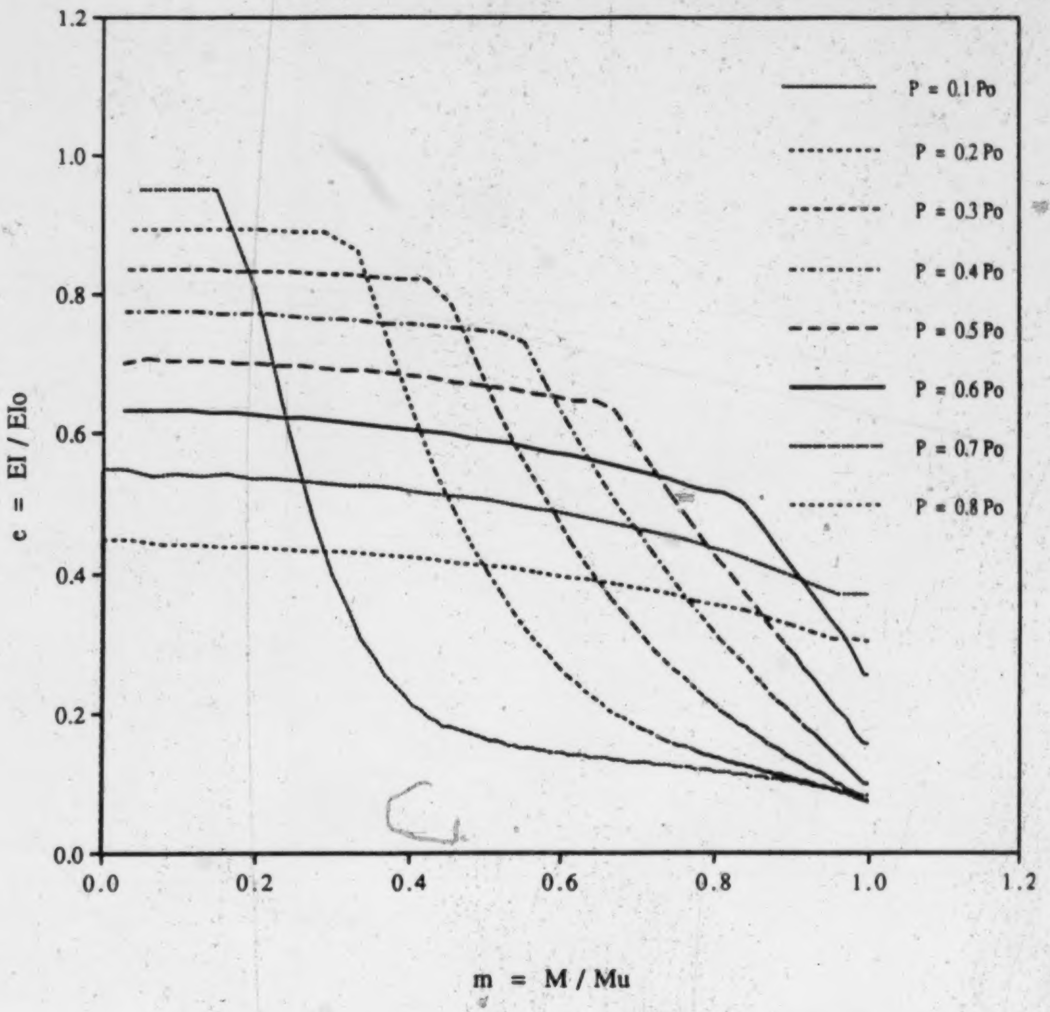

Fig.6.3 Variation of Stiffness for Reinforced Walls
As = Balanced Reinforcement

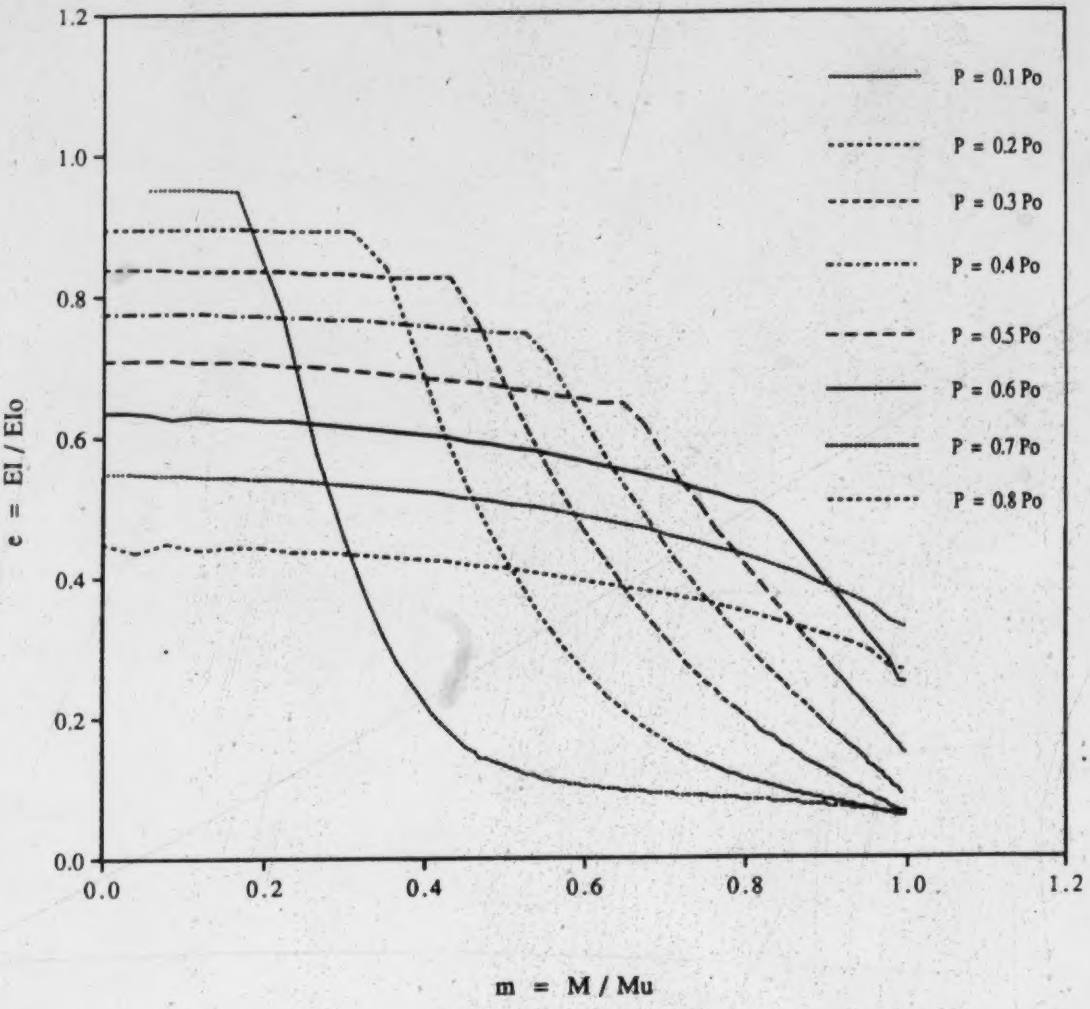

Fig.6.4 Variation of Stiffness for Reinforced Walls
As = 0.5 * Balanced Reinforcement

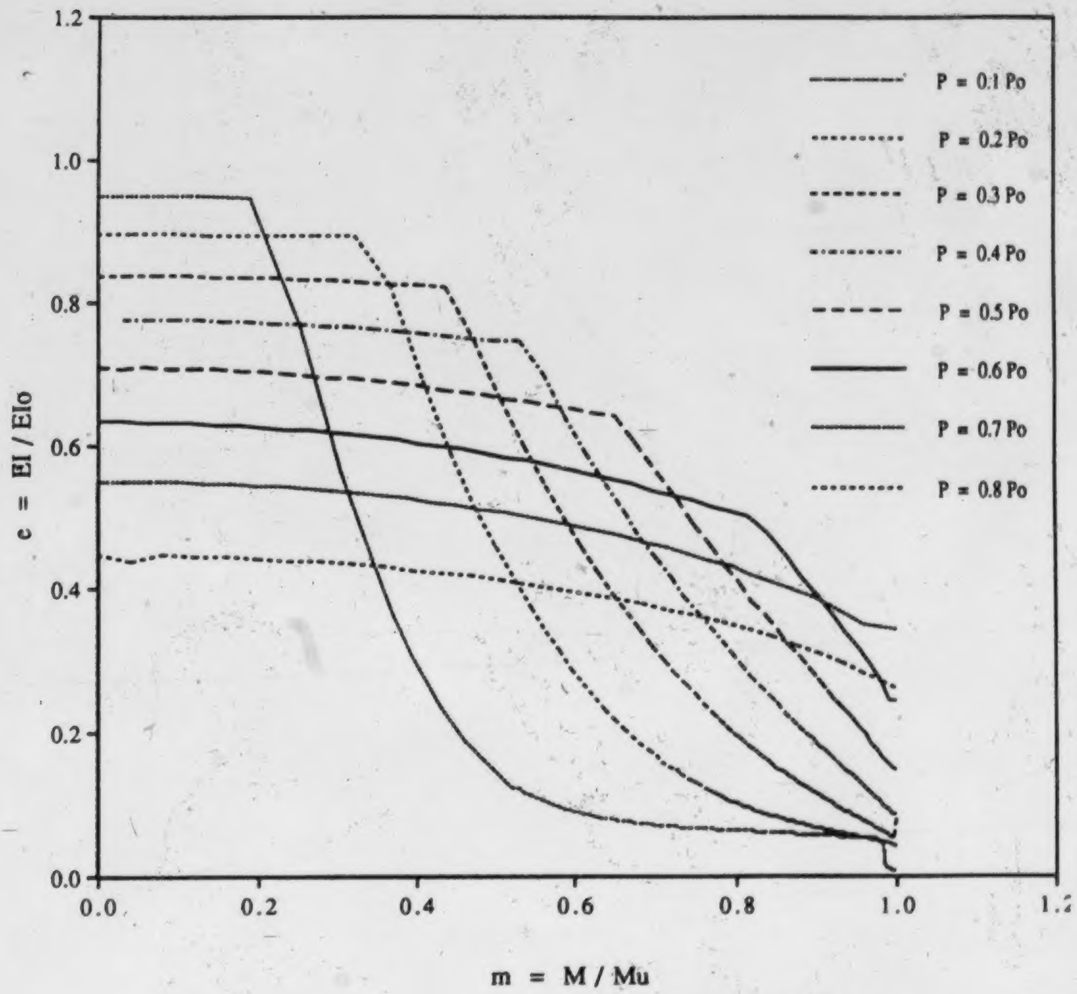

Fig.6.5 Variation of Stiffness for Reinforced Walls
As = Minimum Reinforcement

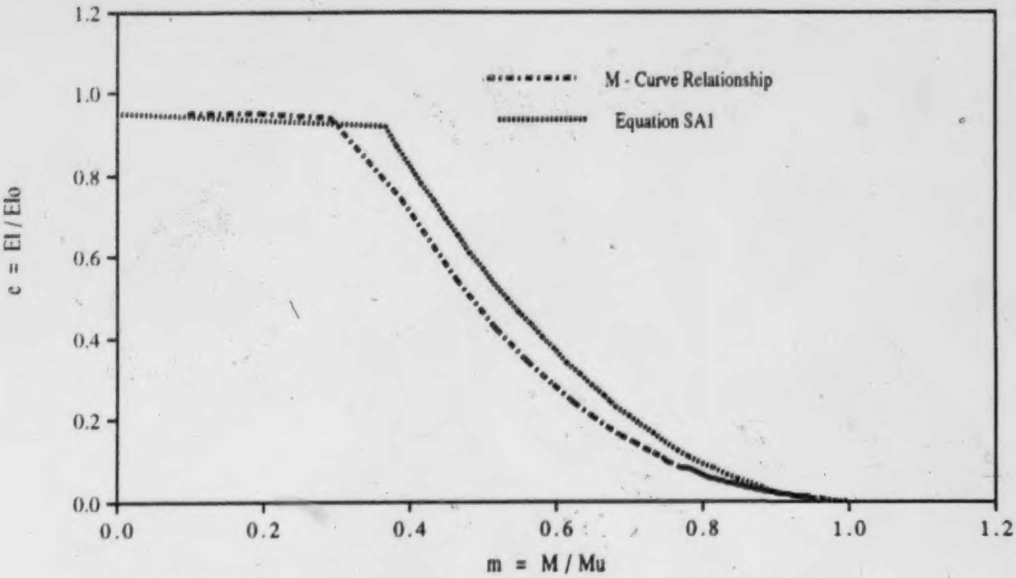

Fig. 6.6 Evaluation of Flexural Rigidity for Fully Bedded Plain Masonry, P/Po = 0.1

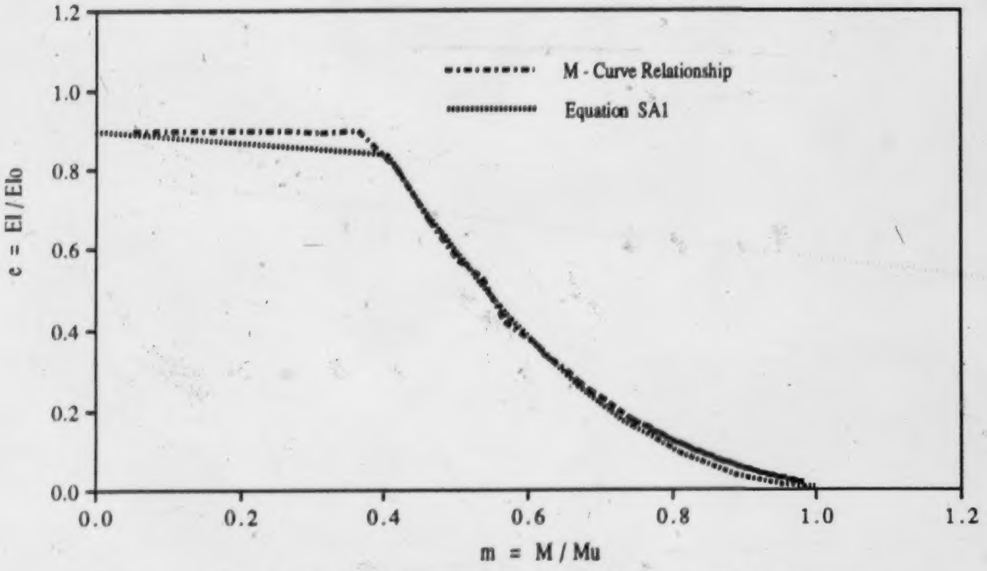

Fig. 6.7 Evaluation of Flexural Rigidity for Fully Bedded Plain Masonry Walls, P/Po = 0.2

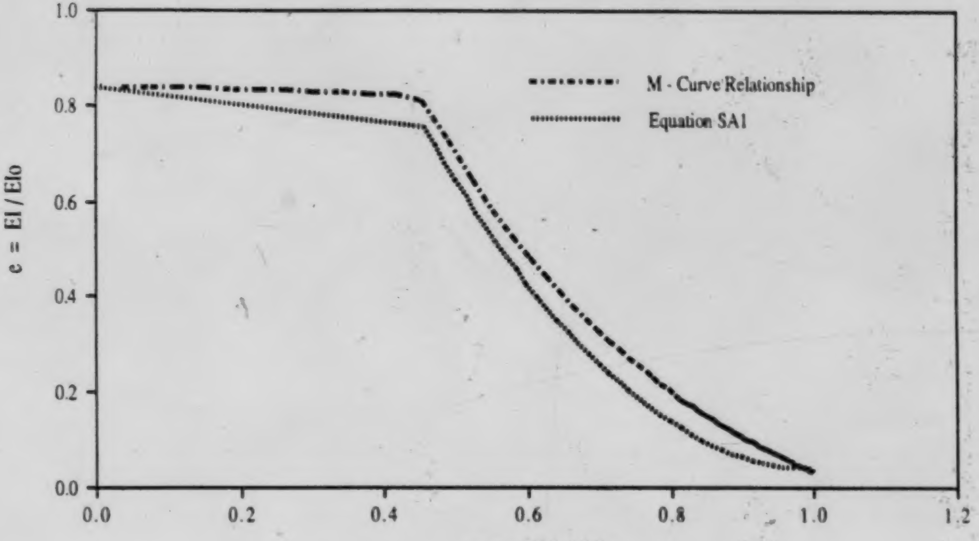

Fig. 6.8 Evaluation of Flexural Rigidity for Fully Bedded Plain Masonry Walls, P/Po = 0.3

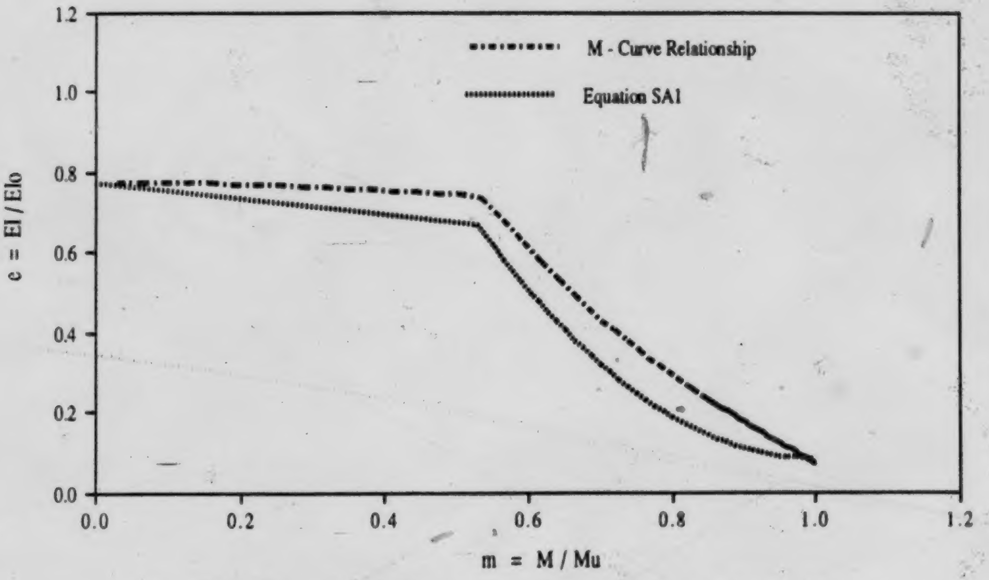

Fig. 6.9 Evaluation of Flexural Rigidity for Fully Bedded Plain Masonry Walls, P/Po = 0.4

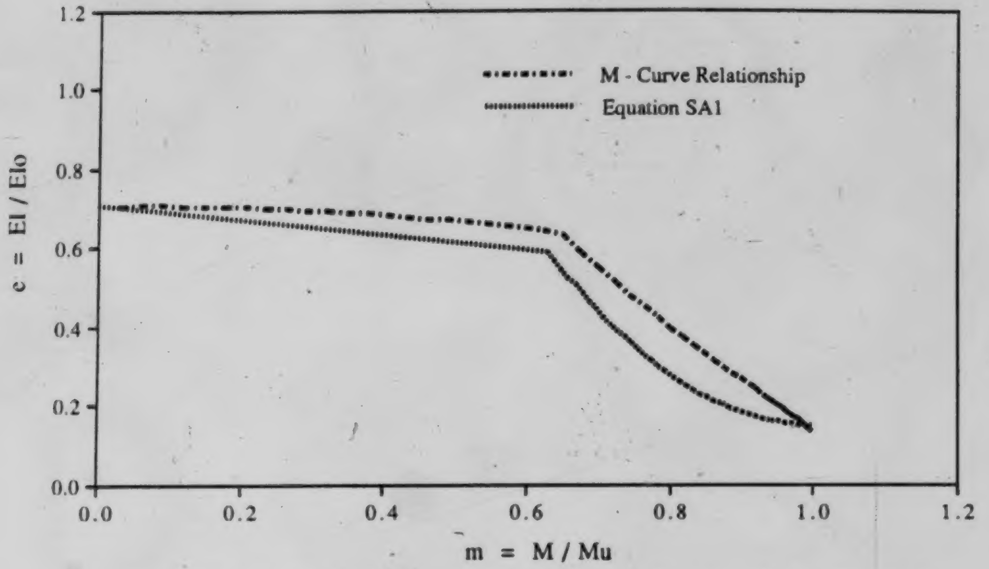

Fig. 6.10 Evaluation of Flexural Rigidity for Fully Bedded Plain Masonry Walls, P/Po = 0.5

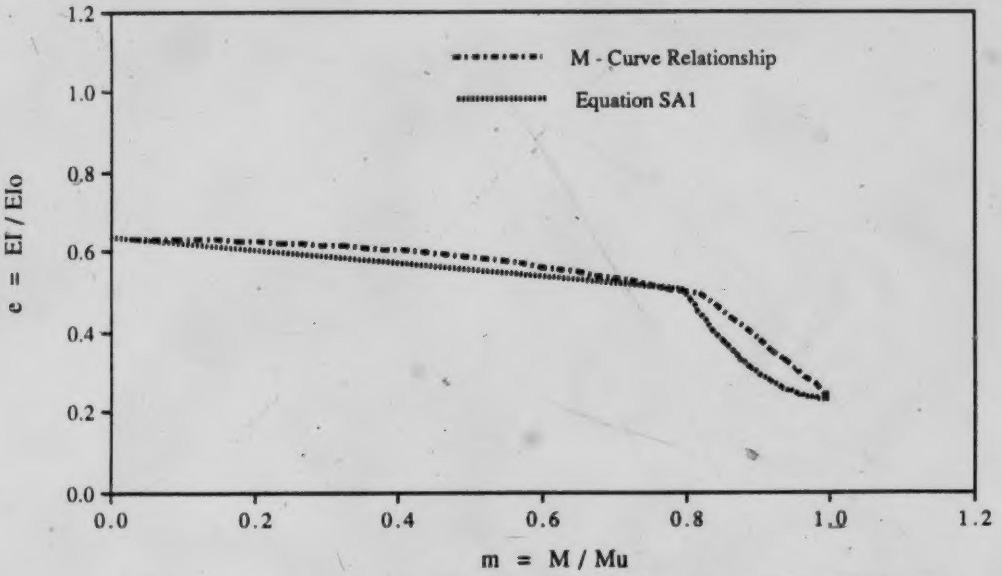

Fig. 6.11 Evaluation of Flexural Rigidity for Fully Bedded Plain Masonry Walls, P/Po = 0.6

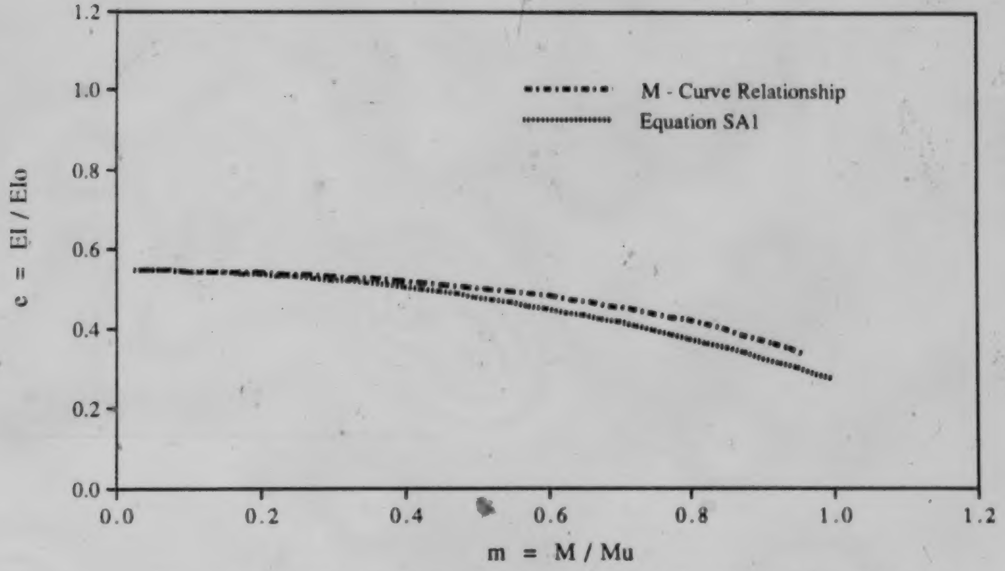

Fig. 6.12 Evaluation of Flexural Rigidity for Fully Bedded Plain Masonry Walls, P/Po = 0.7

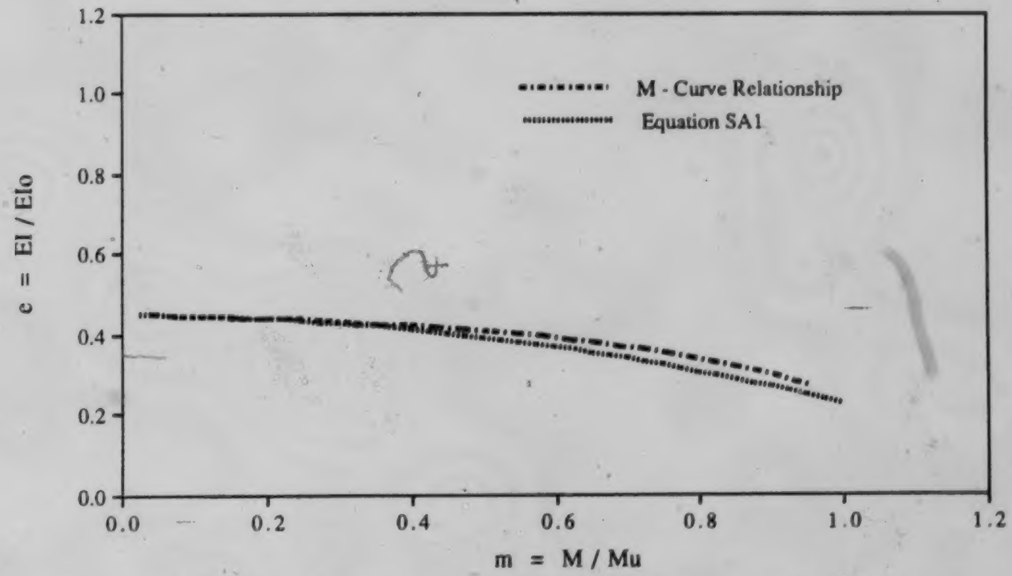

Fig. 6.13 Evaluation of Flexural Rigidity for Fully Bedded Plain Masonry Walls, P/Po = 0.8

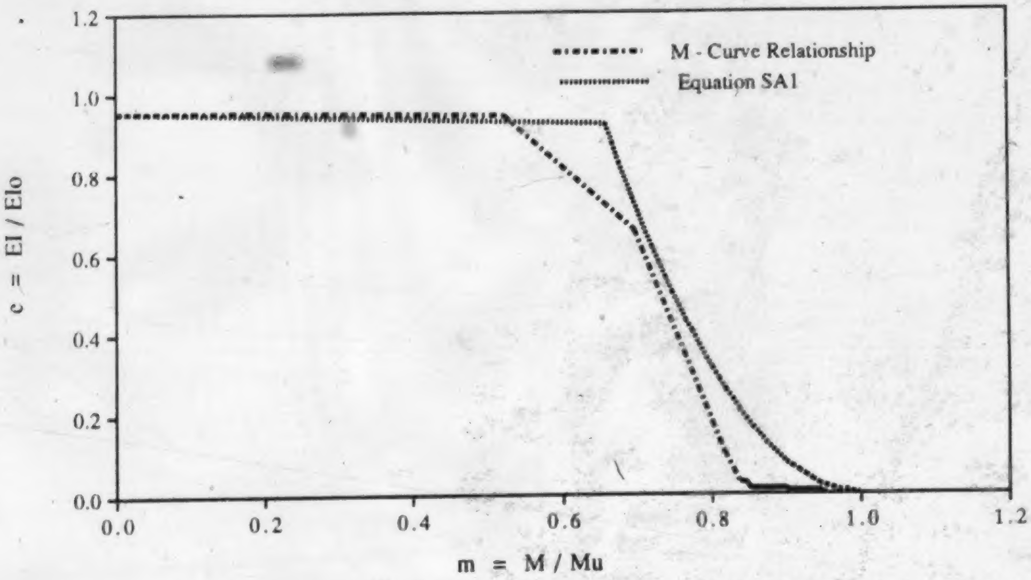

Fig. 6.14 Evaluation of Flexural Rigidity for Faceshell Bedded Plain Masonry, P/Po = 0.1

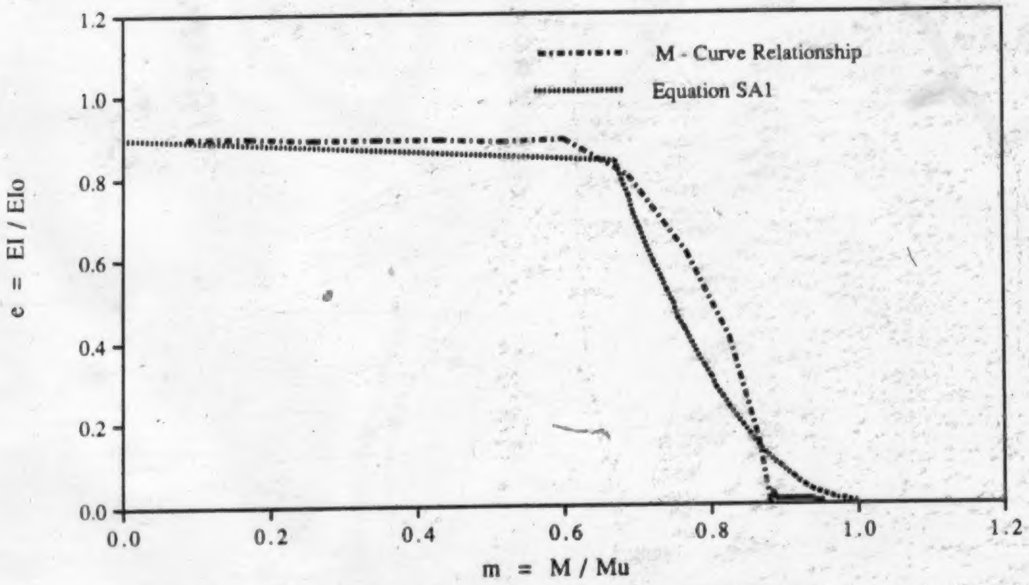

Fig. 6.15 Evaluation of Flexural Rigidity for Faceshell Bedded Plain Masonry, P/Po = 0.2

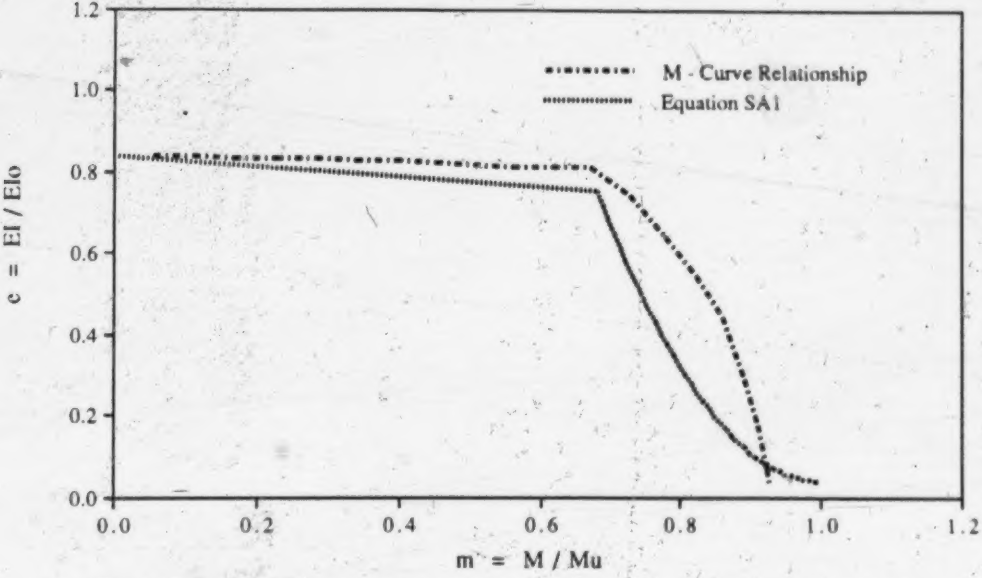

Fig. 6.16 Evaluation of Flexural Rigidity for Faceshell Bedded Plain Masonry, P/Po = 0.3

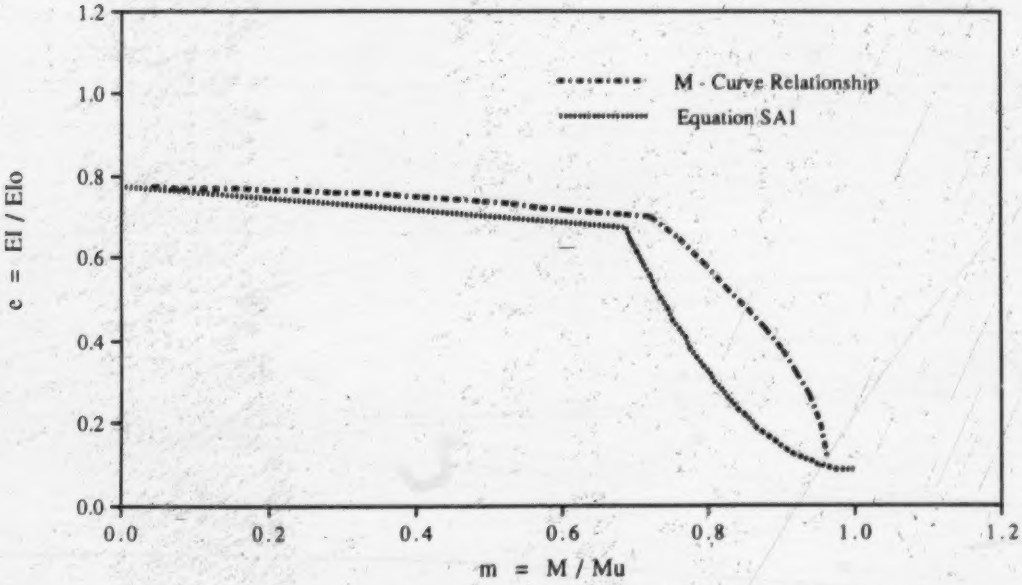

Fig. 6.17 Evaluation of Flexural Rigidity for Faceshell Bedded Plain Masonry, P/Po = 0.4

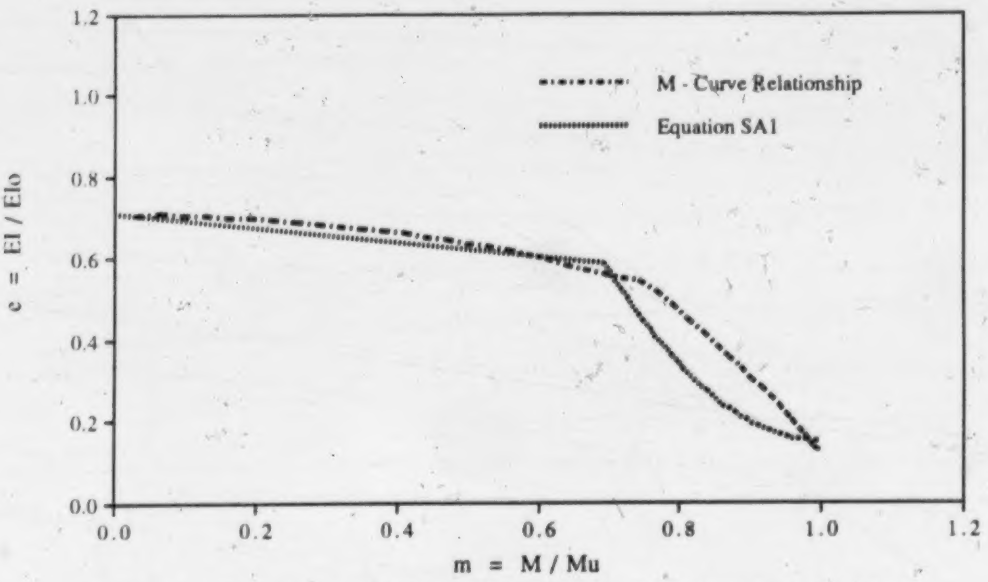

Fig. 6.18 Evaluation of Flexural Rigidity for Faceshell Bedded Plain Masonry, P/Po = 0.5

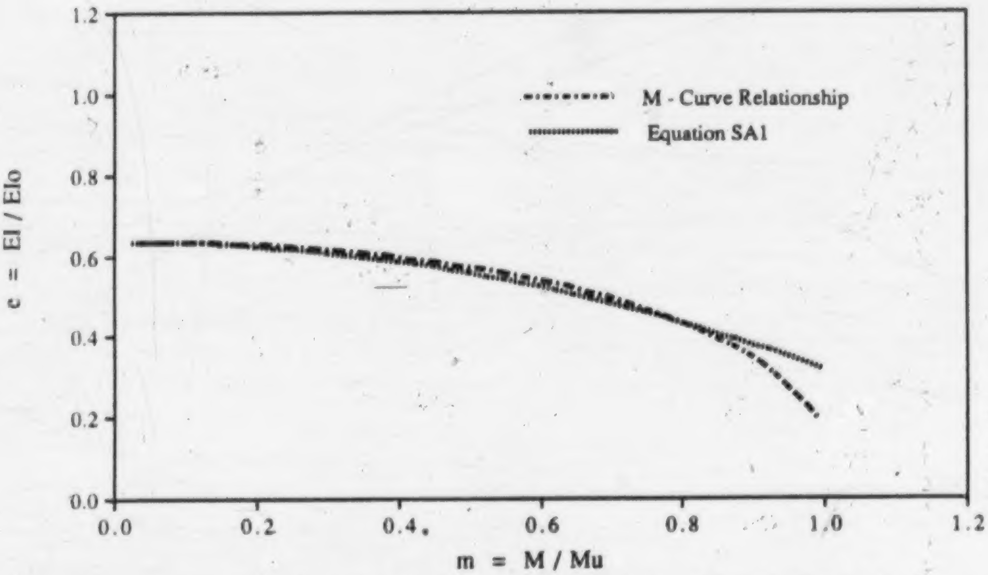

Fig. 6.19 Evaluation of Flexural Rigidity for Faceshell Bedded Plain Masonry, P/Po = 0.6

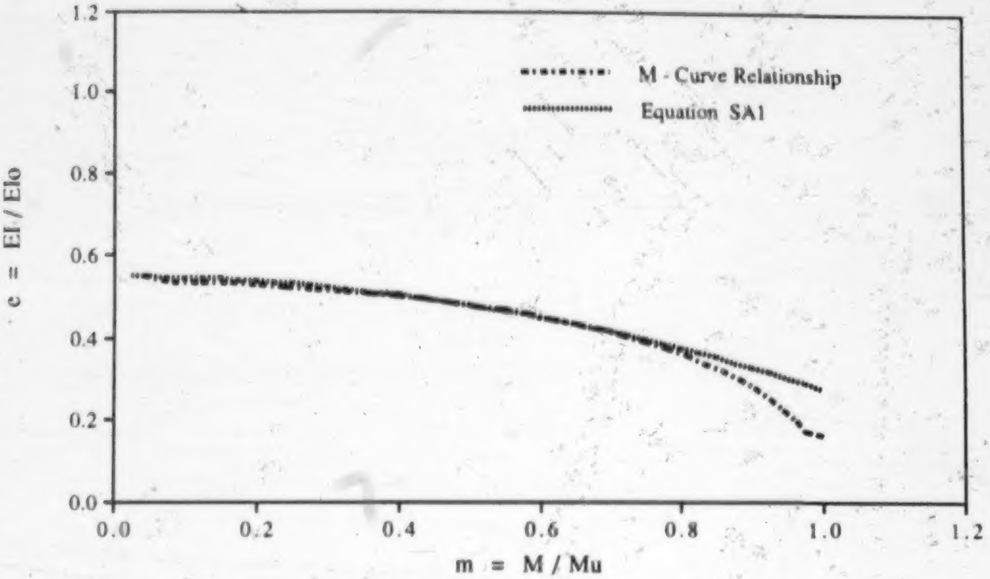

Fig. 6.20 Evaluation of Flexural Rigidity for Faceshell Bedded Plain Masonry, P/Po = 0.7

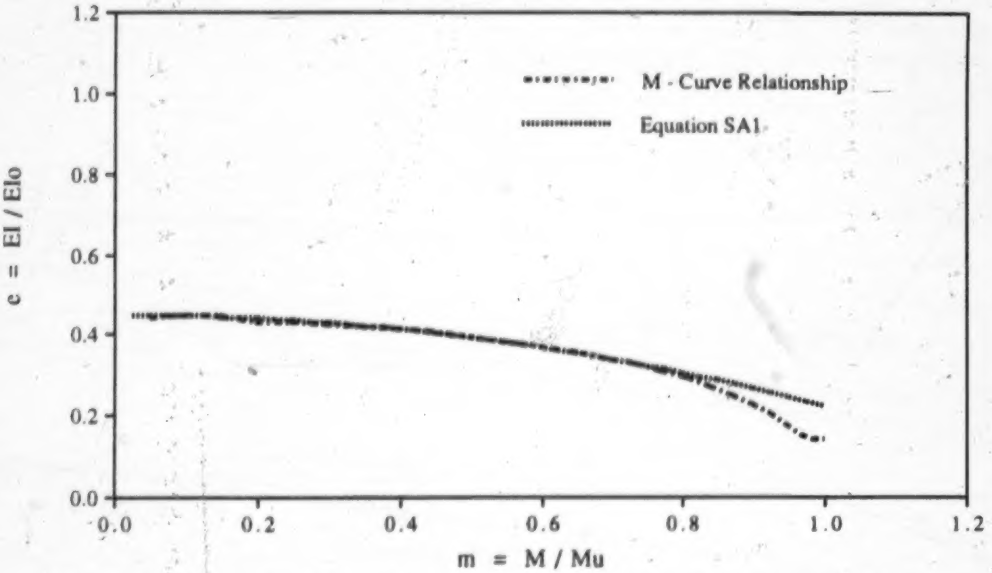

Fig. 6.21 Evaluation of Flexural Rigidity for Faceshell Bedded Plain Masonry, P/Po = 0.8

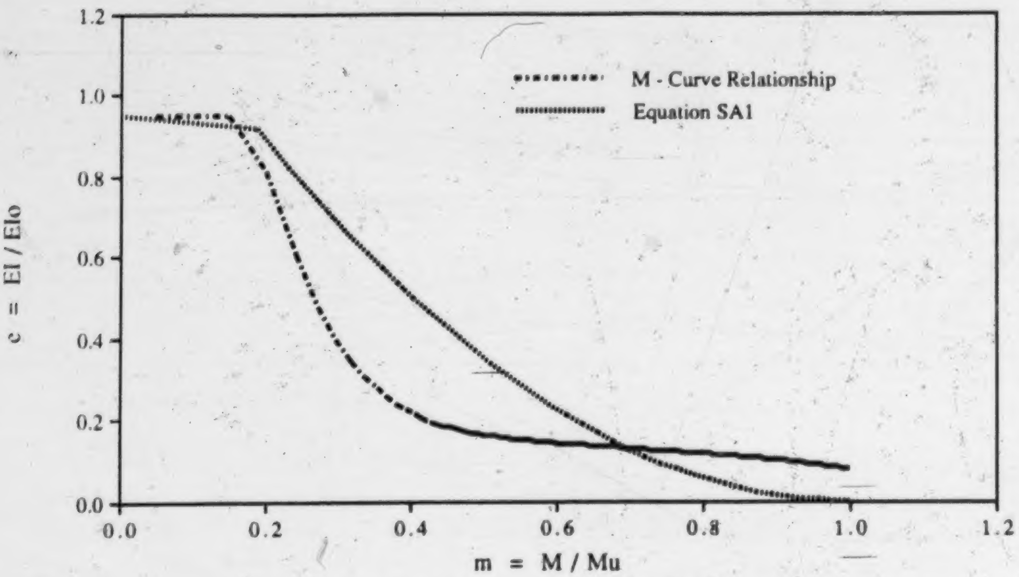

Fig. 6.22 Evaluation of Flexural Rigidity for Reinforced Masonry
As = Balanced Reinforcement, P/Po = 0.1

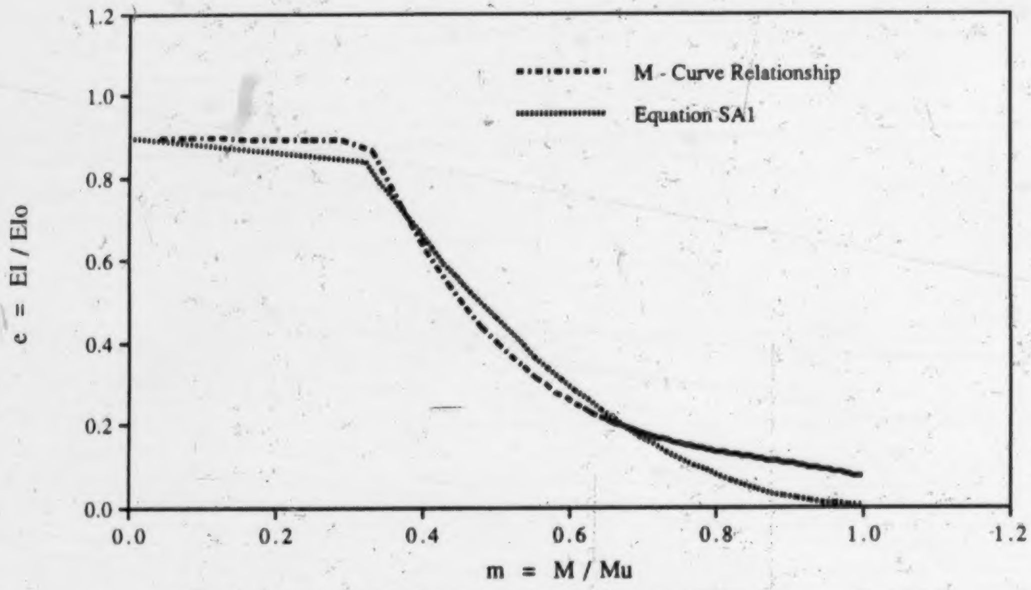

Fig. 6.23 Evaluation of Flexural Rigidity for Reinforced Masonry
As = Balanced Reinforcement, P/Po = 0.2

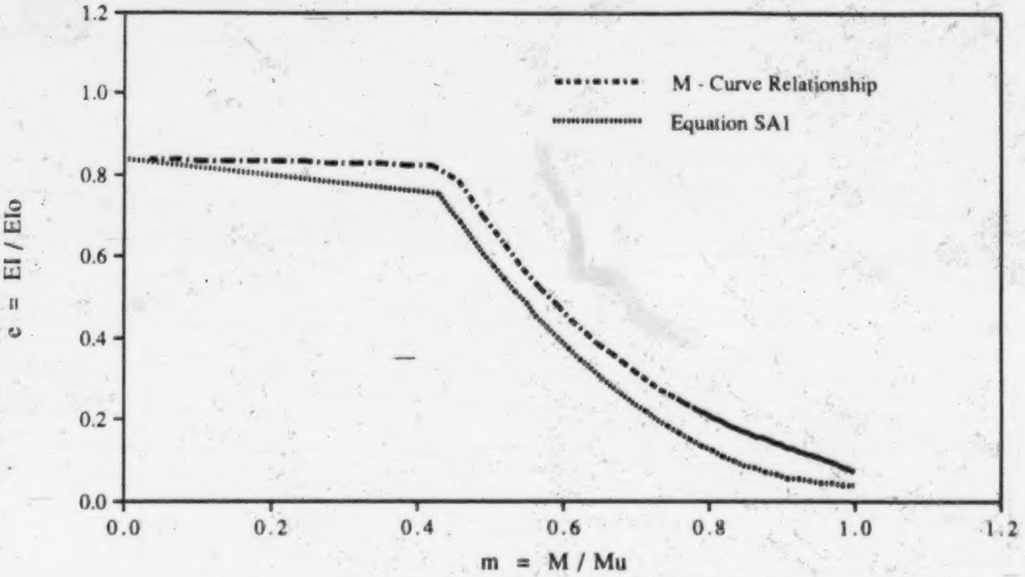

Fig. 6.24 Evaluation of Flexural Rigidity for Reinforced Masonry
As = Balanced Reinforcement, P/Po = 0.3

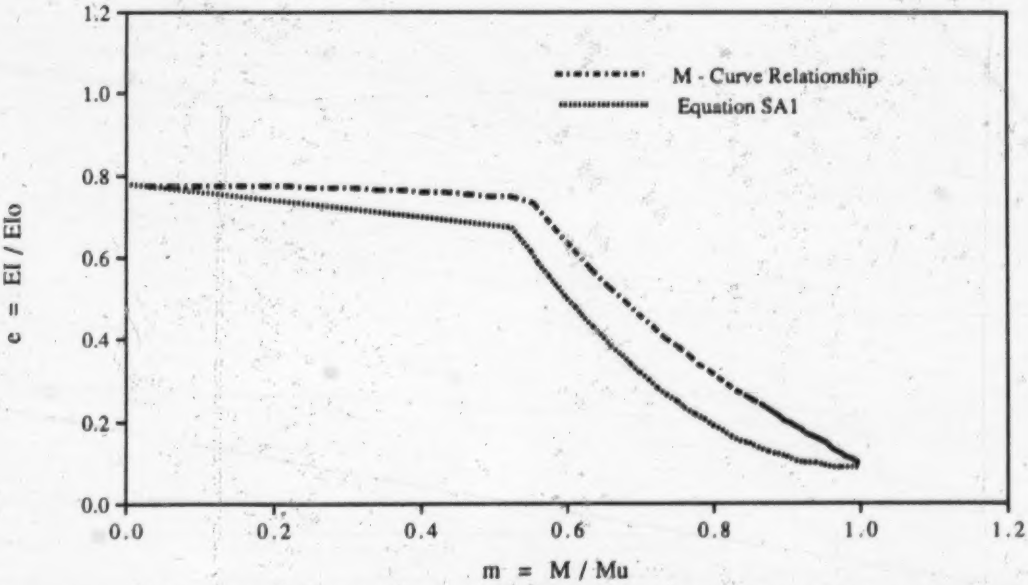

Fig. 6.25 Evaluation of Flexural Rigidity for Reinforced Masonry
As = Balanced Reinforcement, P/Po = 0.4

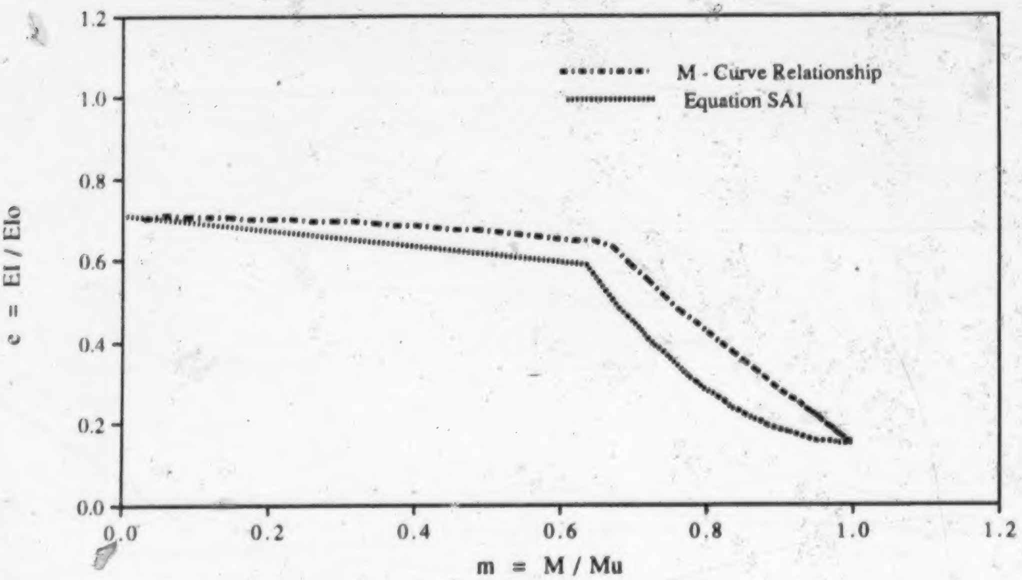

Fig. 6.26 Evaluation of Flexural Rigidity for Reinforced Masonry
As = Balanced Reinforcement, P/Po = 0.5

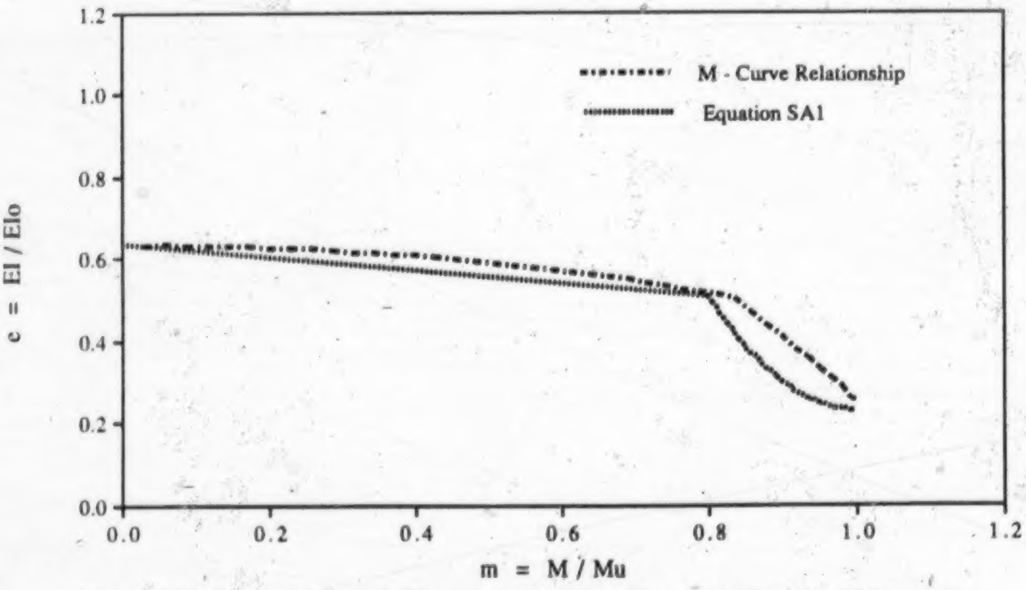

Fig. 6.27 Evaluation of Flexural Rigidity for Reinforced Masonry
As = Balanced Reinforcement, P/Po = 0.6

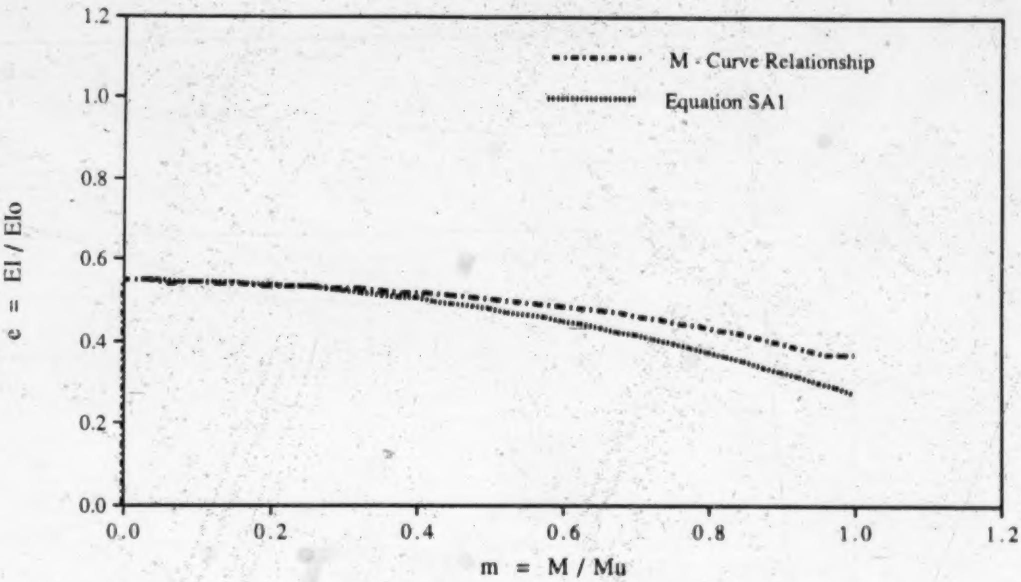

Fig. 6.28 Evaluation of Flexural Rigidity for Reinforced Masonry As = Balanced Reinforcement, P/Po = 0.7

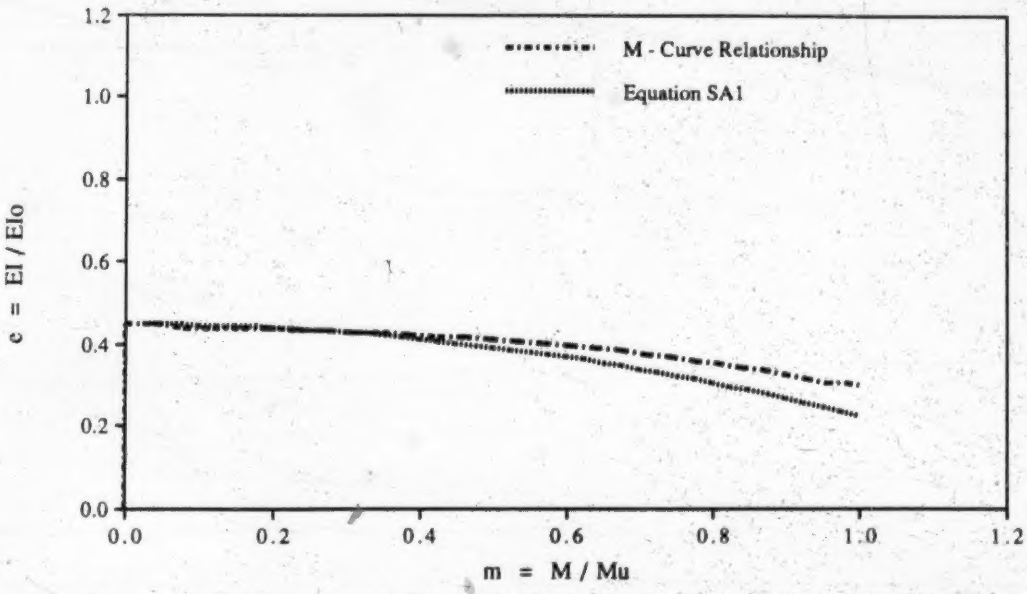

Fig. 6.29 Evaluation of Flexural Rigidity for Reinforced Masonry As = Balanced Reinforcement, P/Po = 0.8

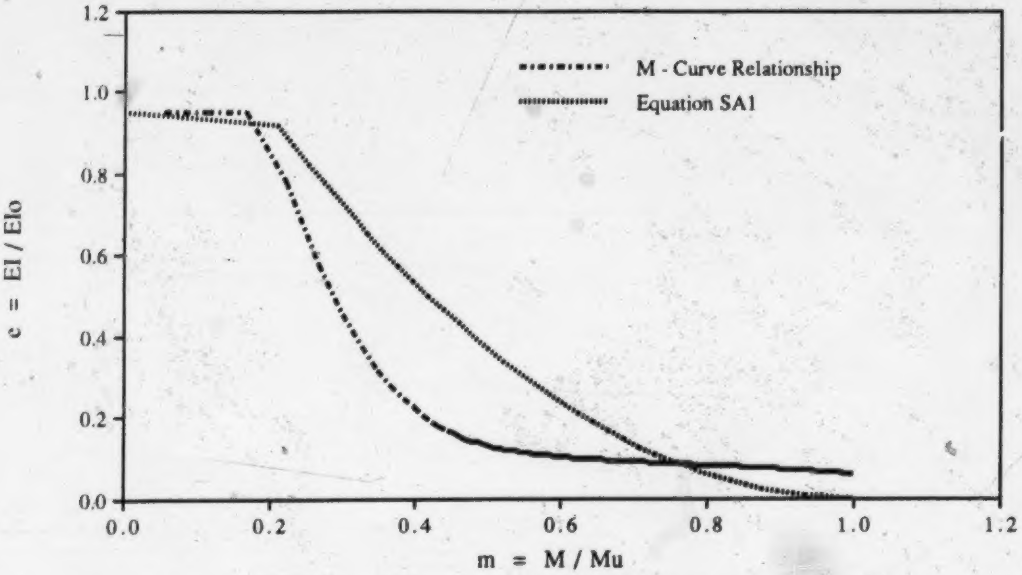

Fig. 6.30 Evaluation of Flexural Rigidity for Reinforced Masonry
As = 0.5 * Balanced Reinforcement, P/Po = 0.1

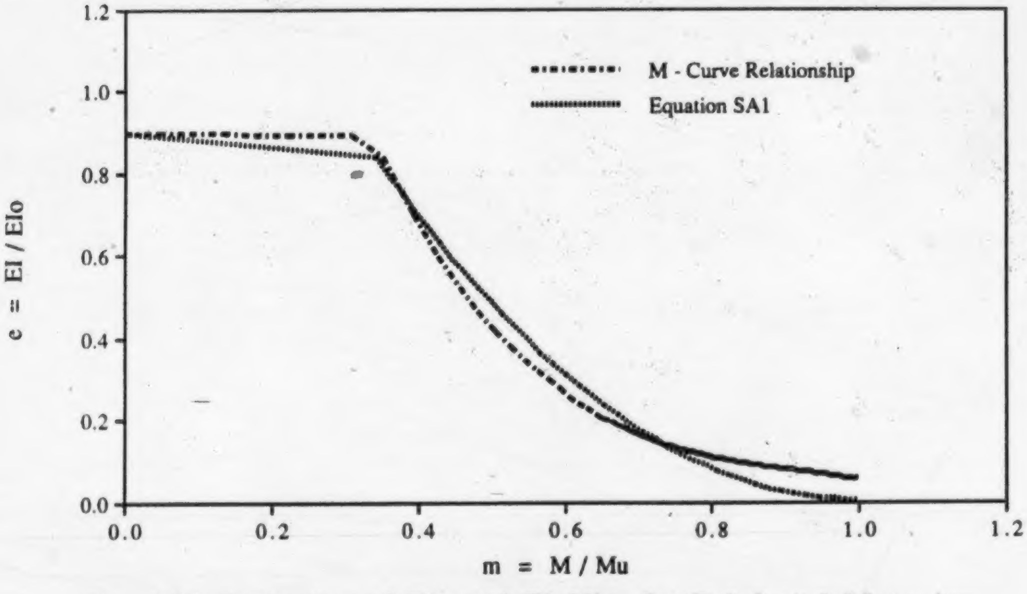

Fig. 6.31 Evaluation of Flexural Rigidity for Reinforced Masonry
As = 0.5 * Balanced Reinforcement, P/Po = 0.2

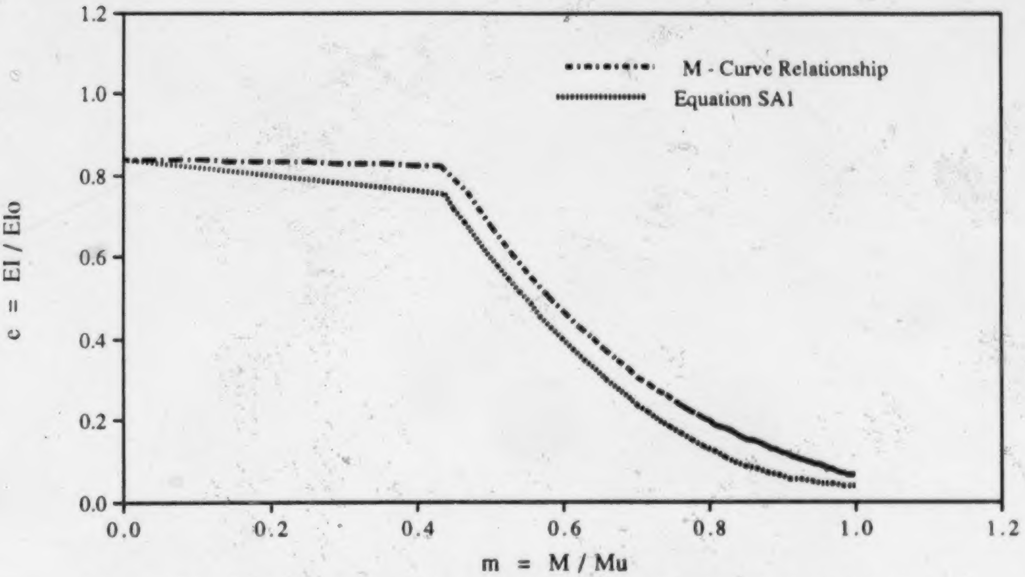

Fig. 6.32 Evaluation of Flexural Rigidity for Reinforced Masonry
As = 0.5 * Balanced Reinforcement, P/Po = 0.3

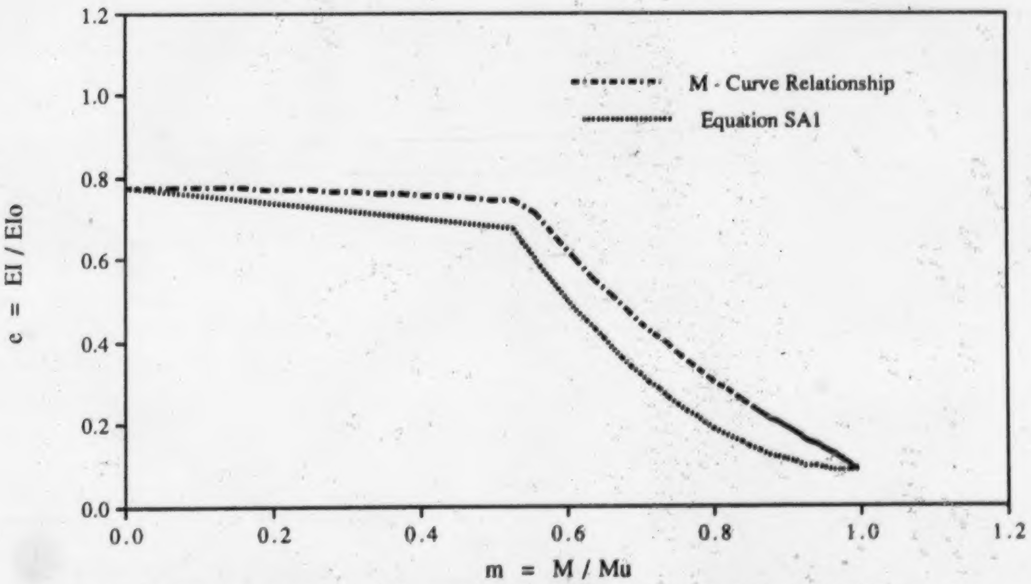

Fig. 6.33 Evaluation of Flexural Rigidity for Reinforced Masonry
As = 0.5 * Balanced Reinforcement, P/Po = 0.4

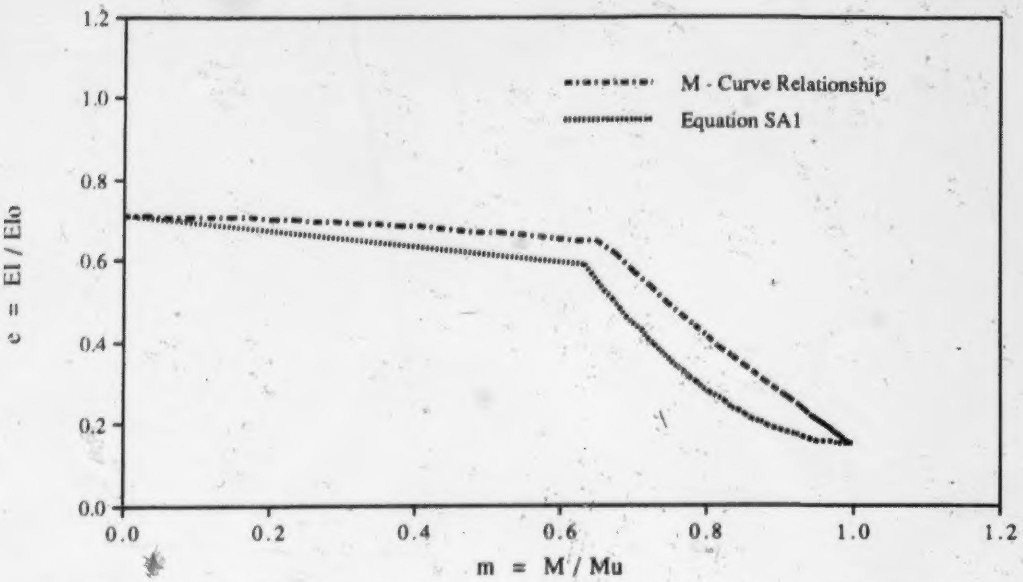

Fig. 6.34 Evaluation of Flexural Rigidity for Reinforced Masonry
As = 0.5 * Balanced Reinforcement, P/Po = 0.5

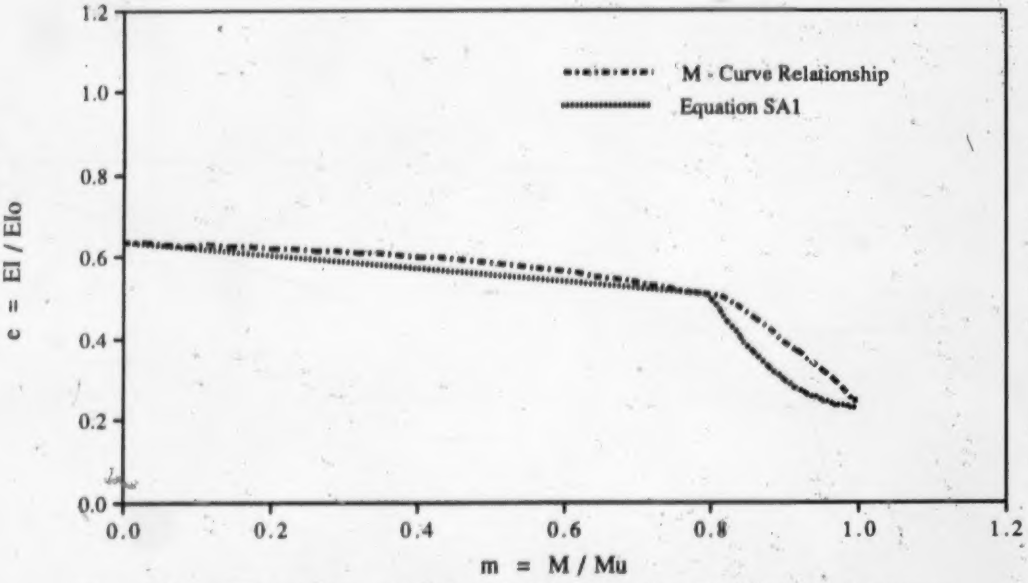

Fig. 6.35 Evaluation of Flexural Rigidity for Reinforced Masonry
As = 0.5 * Balanced Reinforcement, P/Po = 0.6

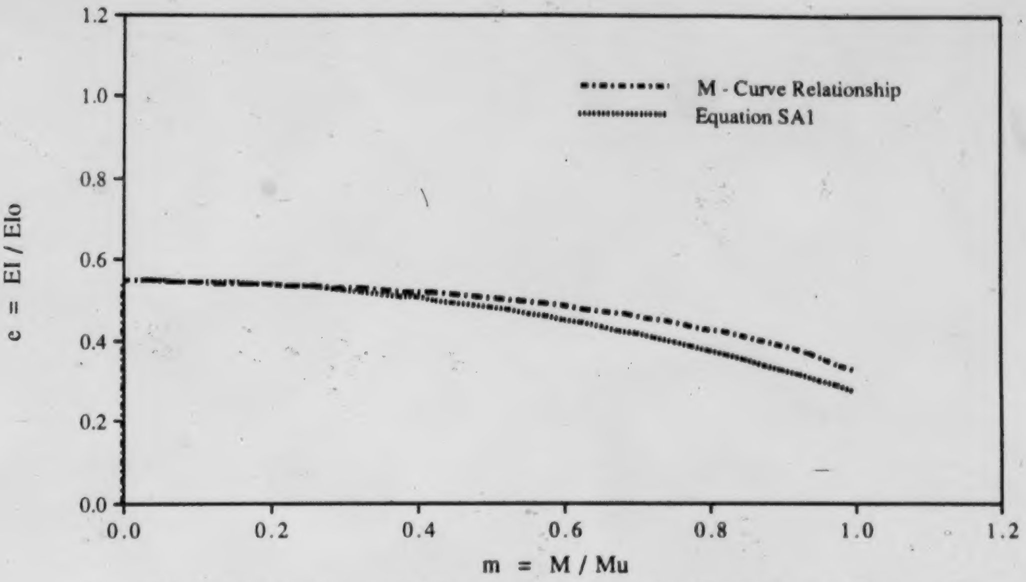

Fig. 6.36 Evaluation of Flexural Rigidity for Reinforced Masonry
As = 0.5 * Balanced Reinforcement, P/Po = 0.7

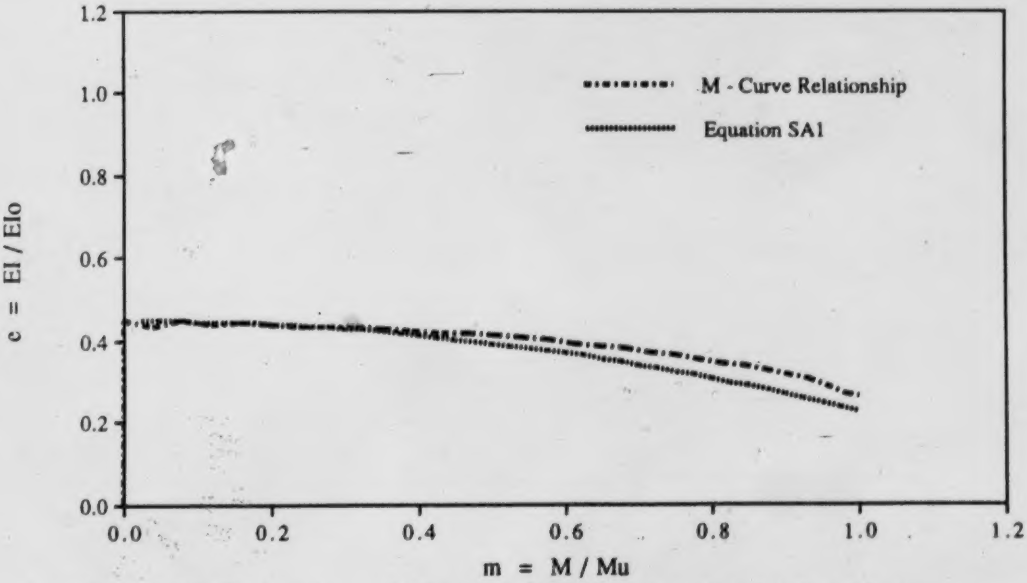

Fig. 6.37 Evaluation of Flexural Rigidity for Reinforced Masonry
As = 0.5 * Balanced Reinforcement, P/Po = 0.8

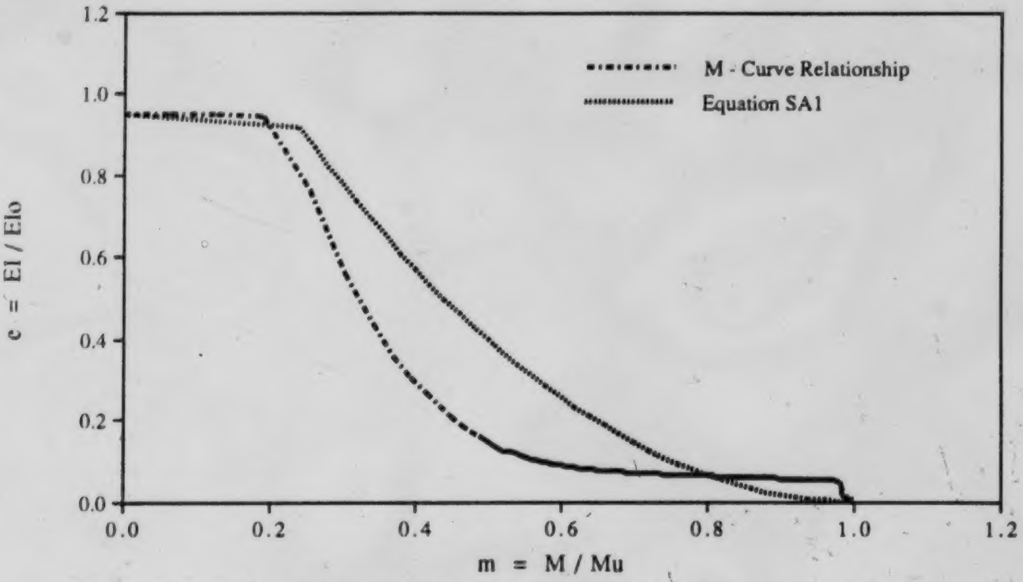

Fig. 6.38 Evaluation of Flexural Rigidity for Reinforced Masonry
As = Minimum Reinforcement, P/Po = 0.1

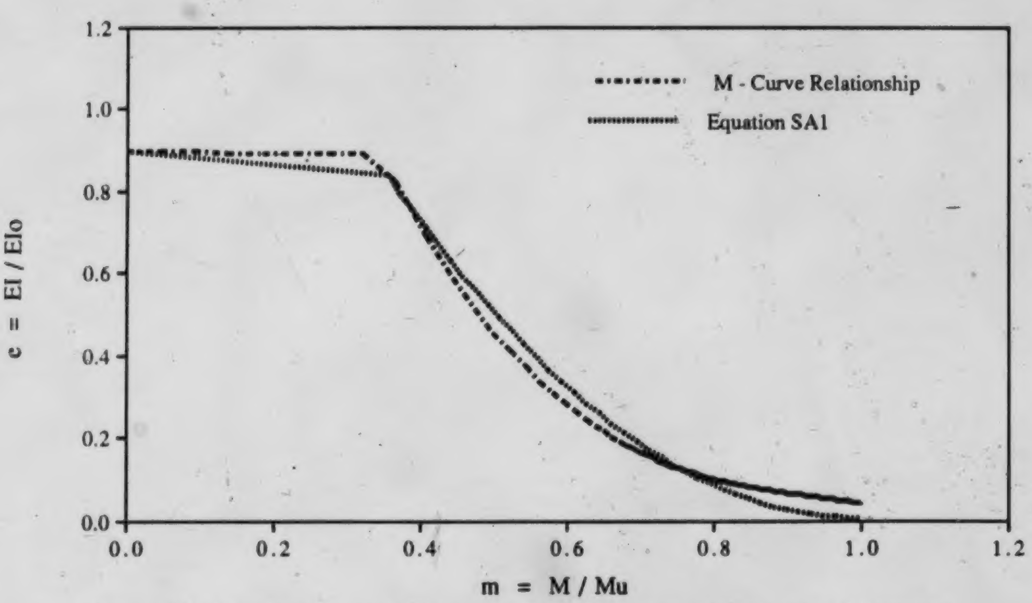

Fig. 6.39 Evaluation of Flexural Rigidity for Reinforced Masonry
As = Minimum Reinforcement, P/Po = 0.2

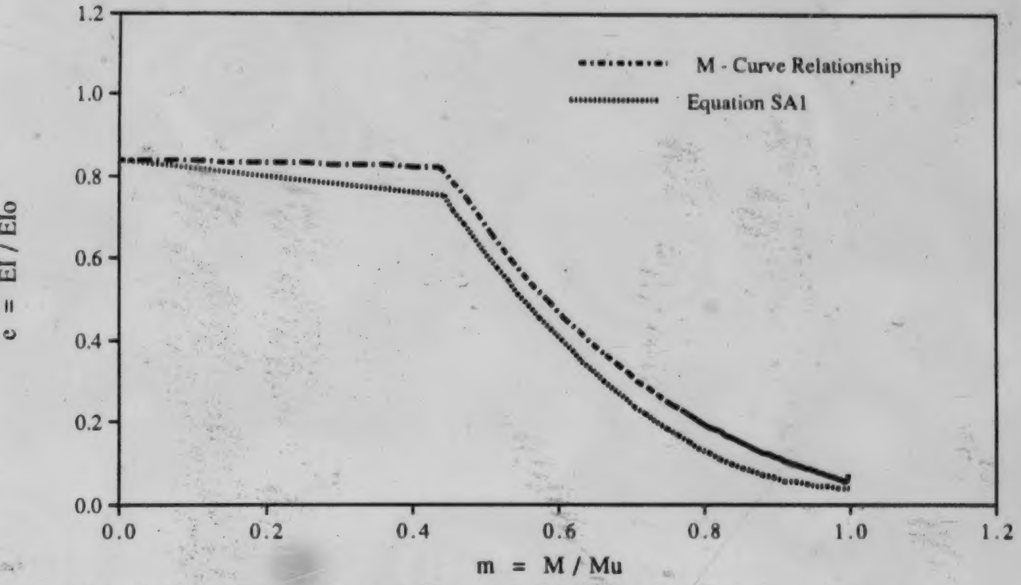

Fig. 6.40 Evaluation of Flexural Rigidity for Reinforced Masonry
As = Minimum Reinforcement, P/Po = 0.3

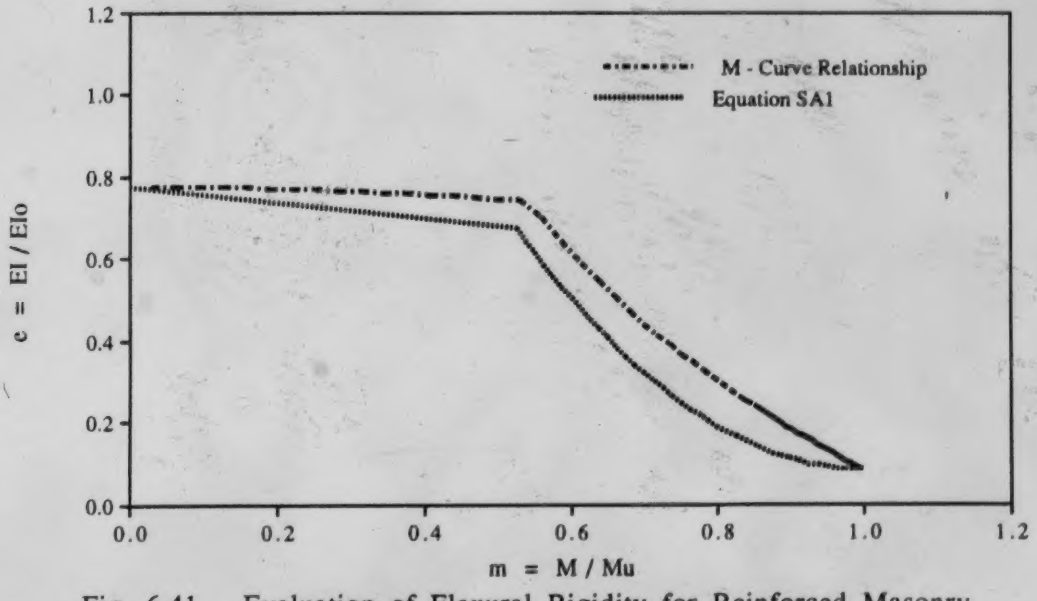

Fig. 6.41 Evaluation of Flexural Rigidity for Reinforced Masonry
As = Minimum Reinforcement, P/Po = 0.4

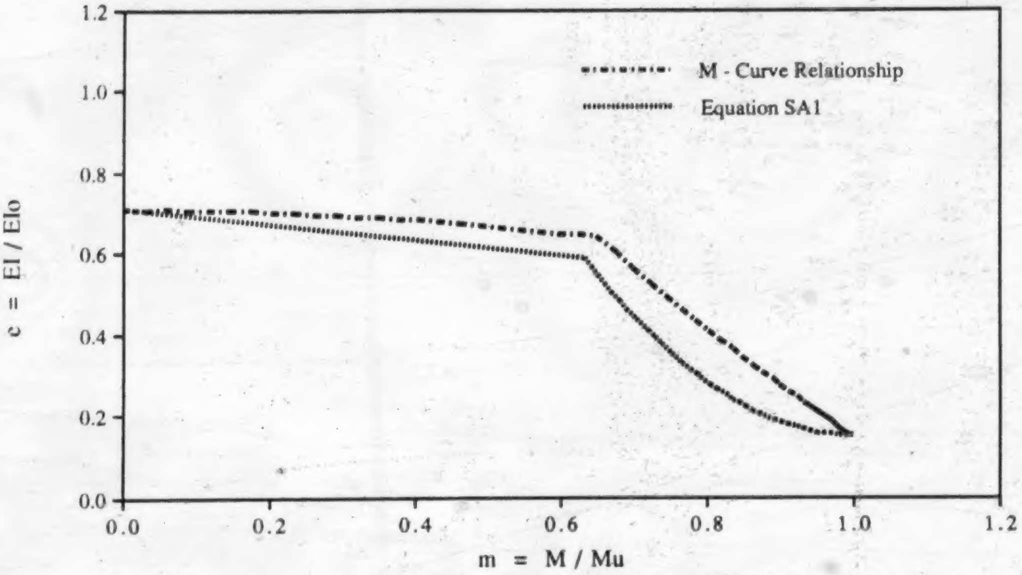

Fig. 6.42 Evaluation of Flexural Rigidity for Reinforced Masonry
As = Minimum Reinforcement, P/Po = 0.5

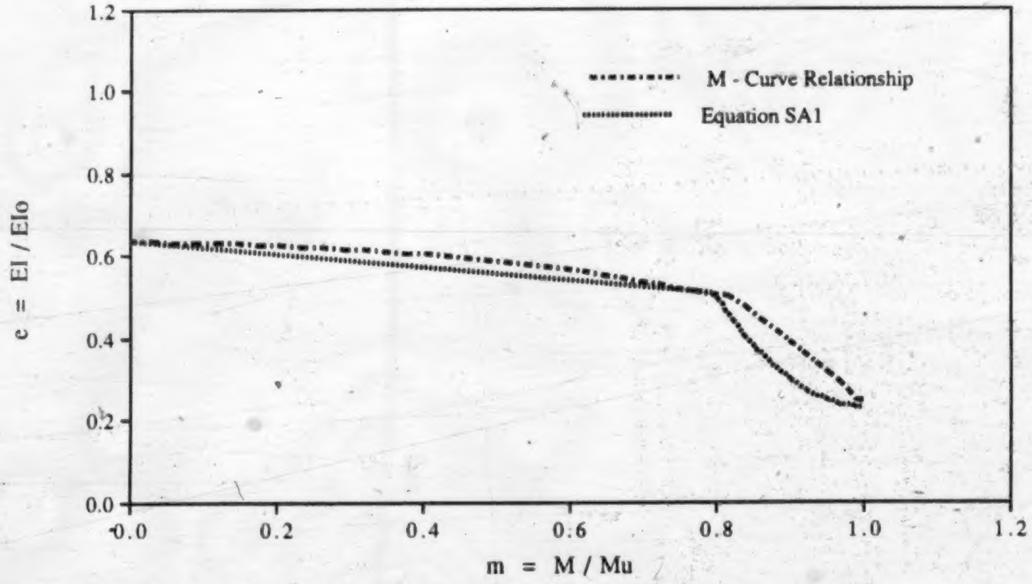

Fig. 6.43 Evaluation of Flexural Rigidity for Reinforced Masonry
As = Minimum Reinforcement, P/Po = 0.6

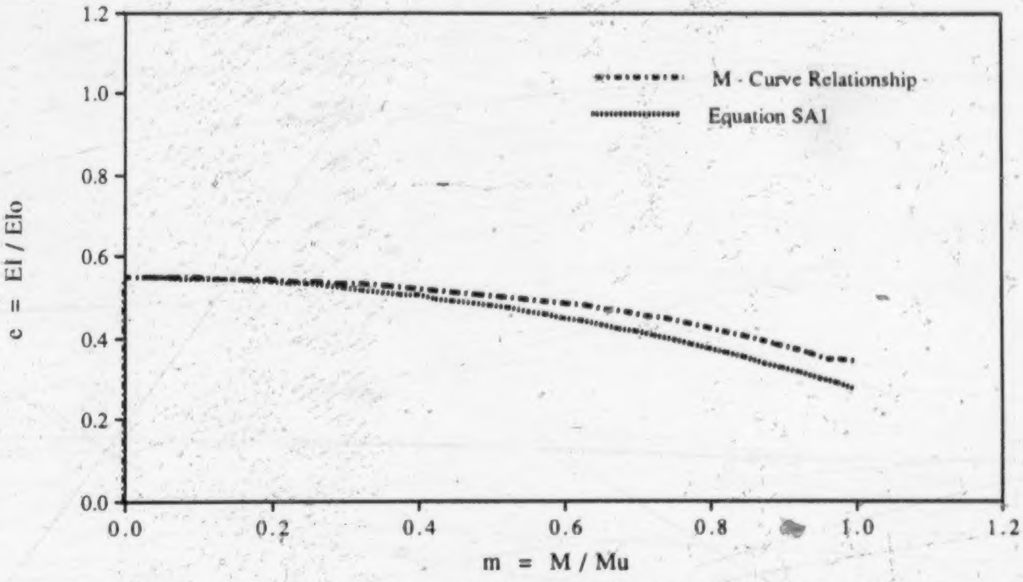

Fig. 6.44 Evaluation of Flexural Rigidity for Reinforced Masonry
As = Minimum Reinforcement, P/Po = 0.7

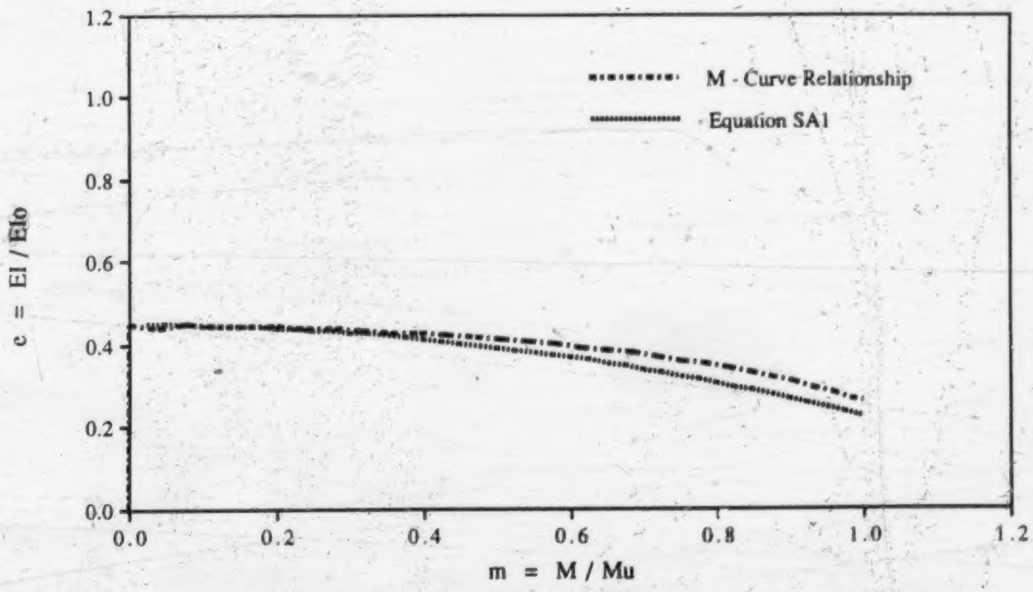

Fig. 6.45 Evaluation of Flexural Rigidity for Reinforced Masonry
As = Minimum Reinforcement, P/Po = 0.8

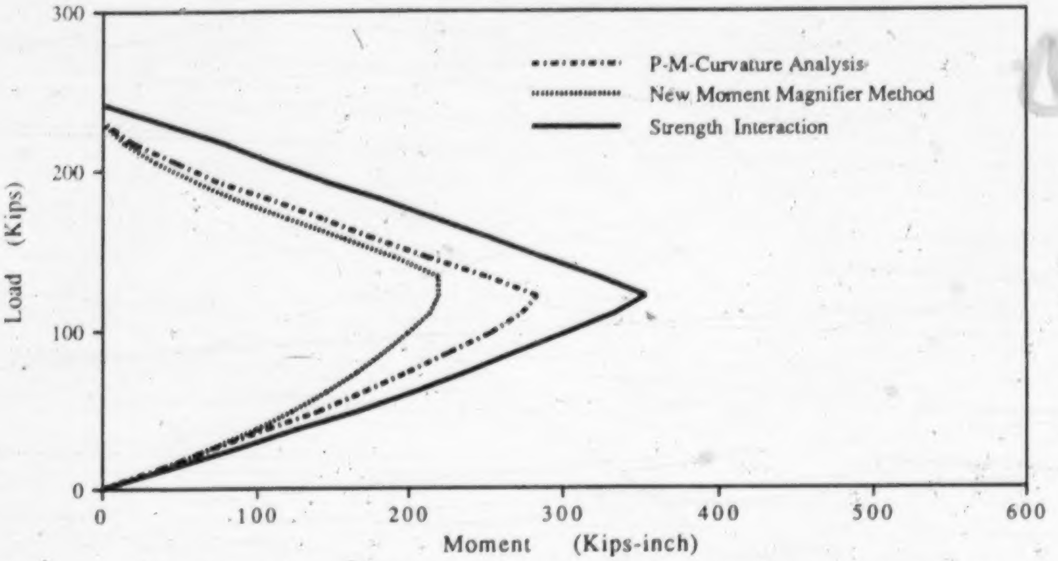

Fig. 6.46 Comparison of Analysis Methods for Face shell Bedded Plain Masonry Wall H/t = 15, e2/e1 = 1.0

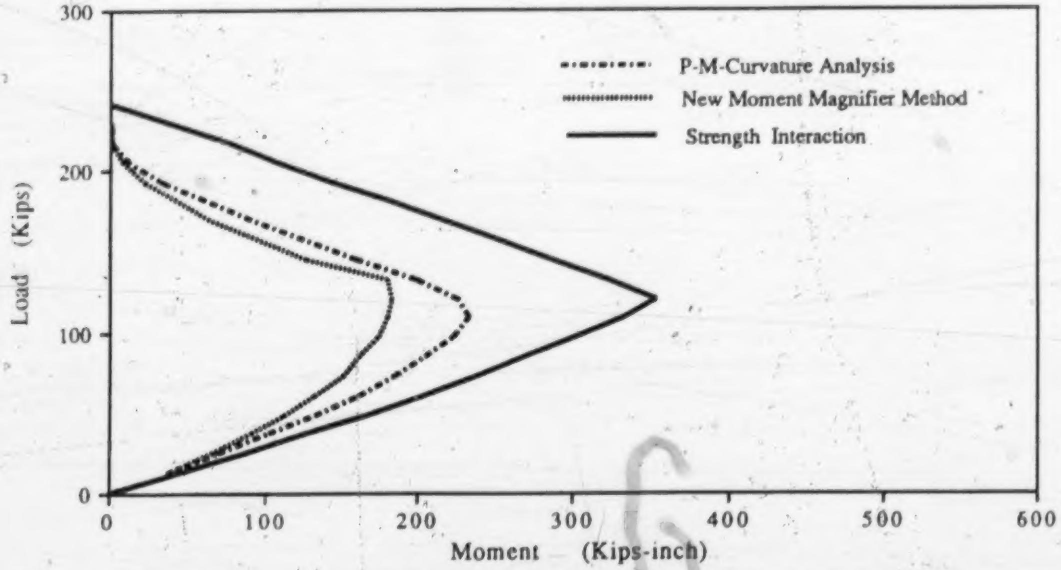

Fig. 6.47 Comparison of Analysis Methods for Face shell Bedded Plain Masonry Wall, H/t = 20, e2/e1 = 1.0

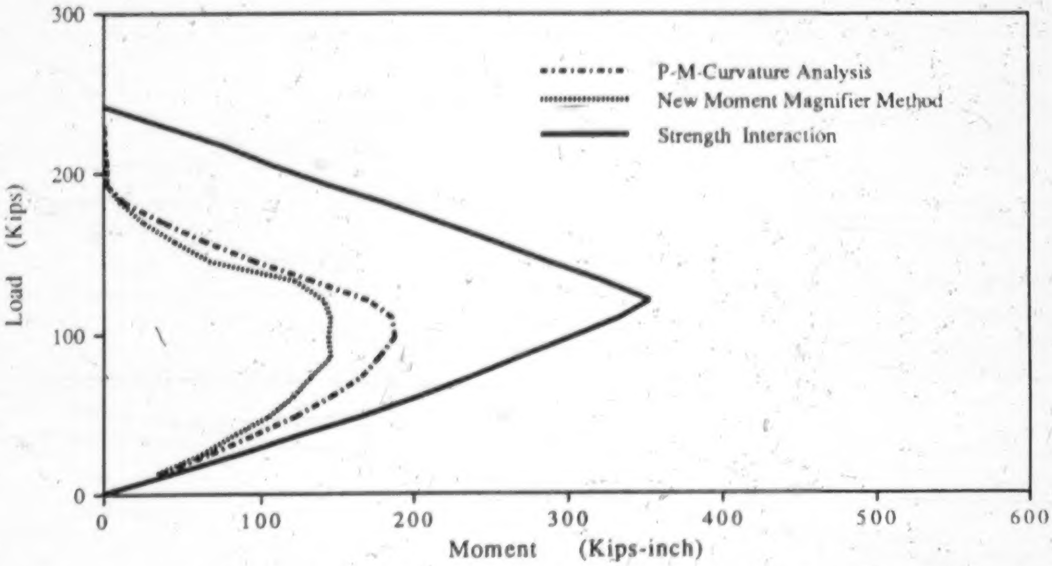

Fig. 6.48 Comparison of Analysis Methods for Face shell Bedded Plain Masonry Wall, H/t = 25, e2/e1 = 1.0

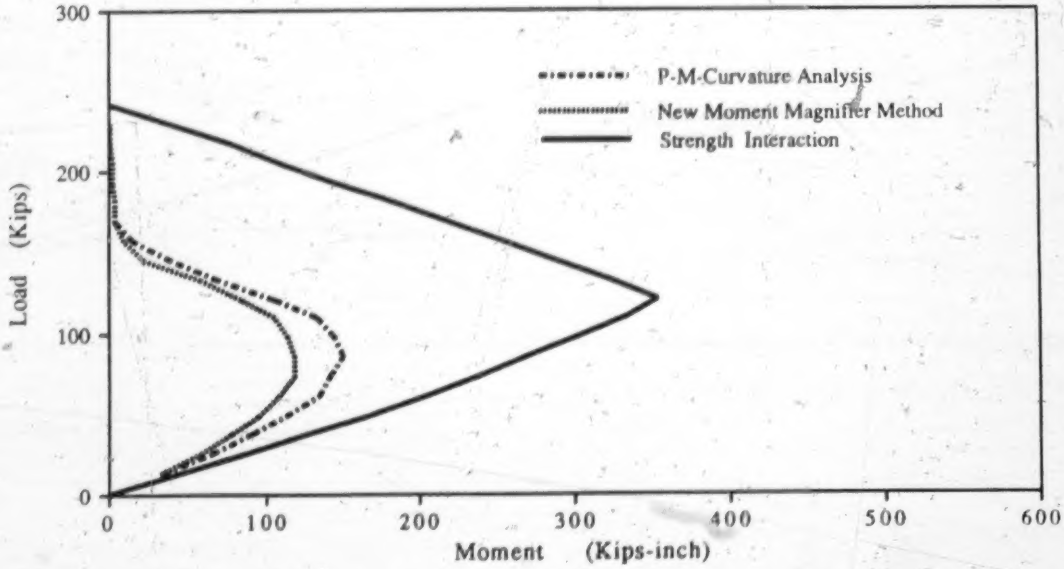

Fig. 6.49 Comparison of Analysis Methods for Face shell Bedded Plain Masonry Wall, H/t = 30, e2/e1 = 1.0

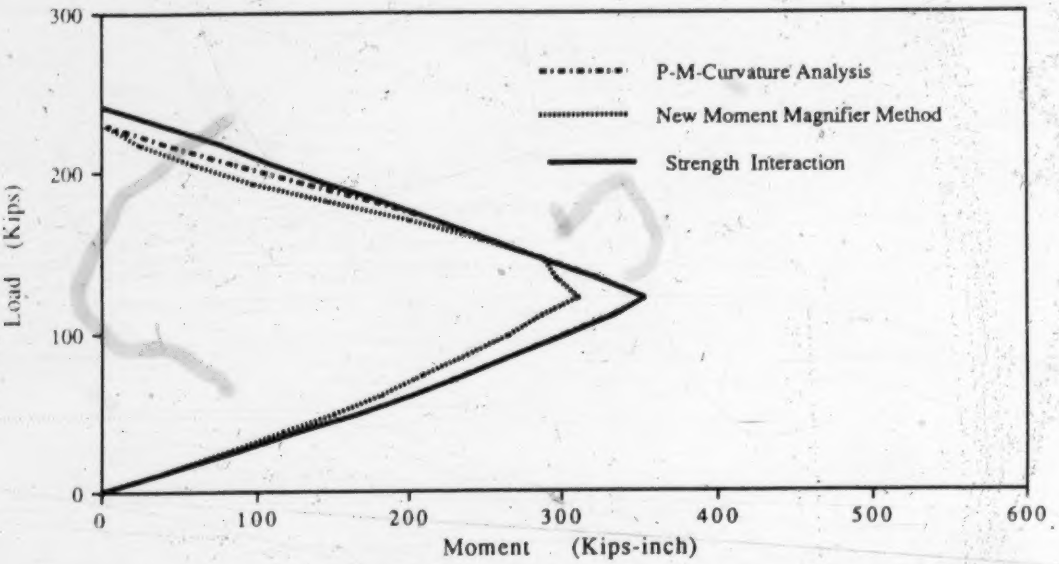

Fig. 6.50 Comparison of Analysis Methods for Face shell Bedded Plain Masonry Wall, H/t = 15, e2/e1 = 0.0

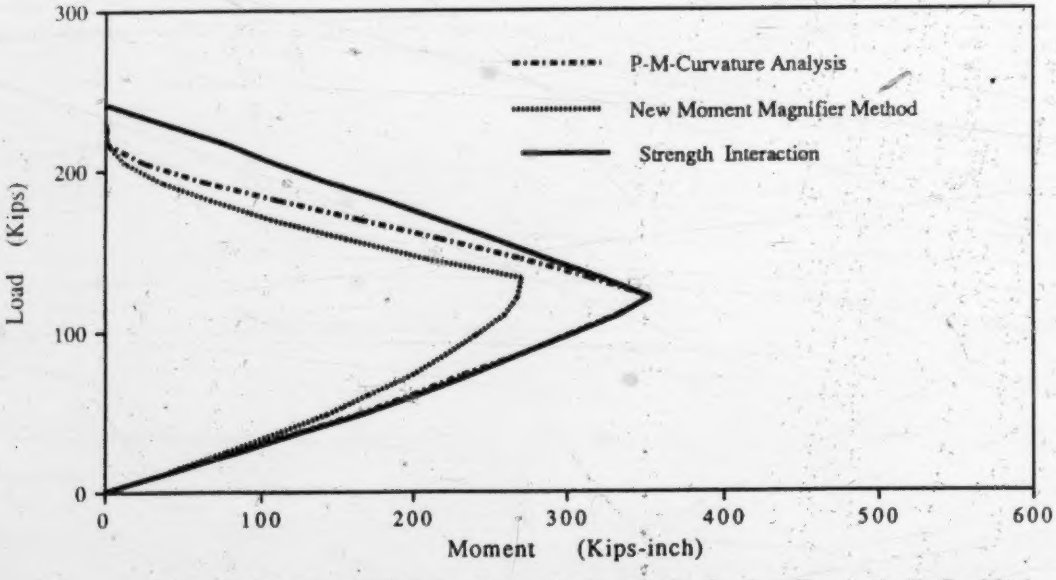

Fig. 6.51 Comparison of Analysis Methods for Face shell Bedded Plain Masonry Wall, H/t = 20, e2/e1 = 0.0

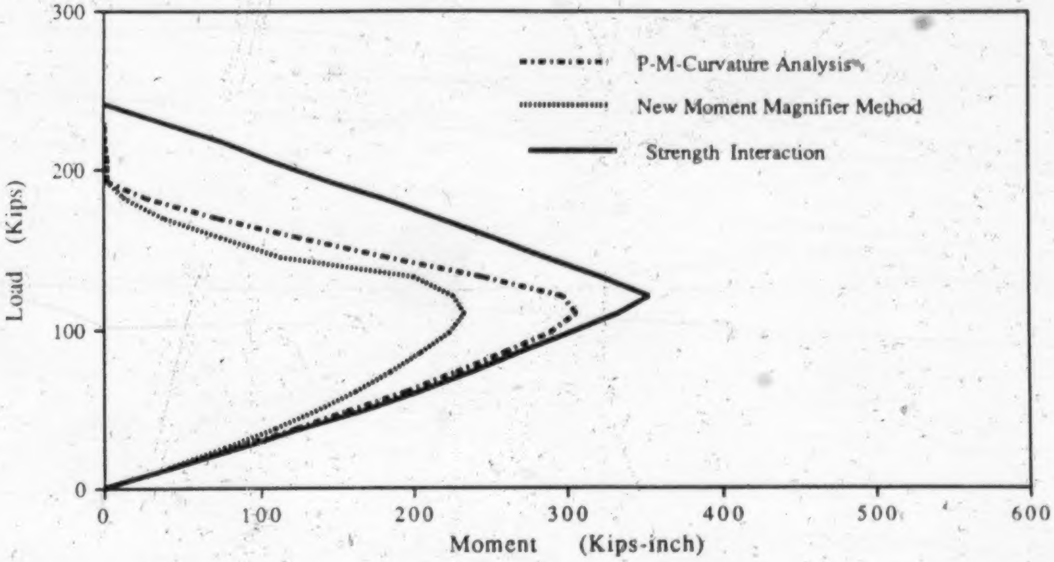

Fig. 6.52 Comparison of Analysis Methods for Face shell Bedded Plain Masonry Wall, H/t = 25, e2/e1 = 0.0

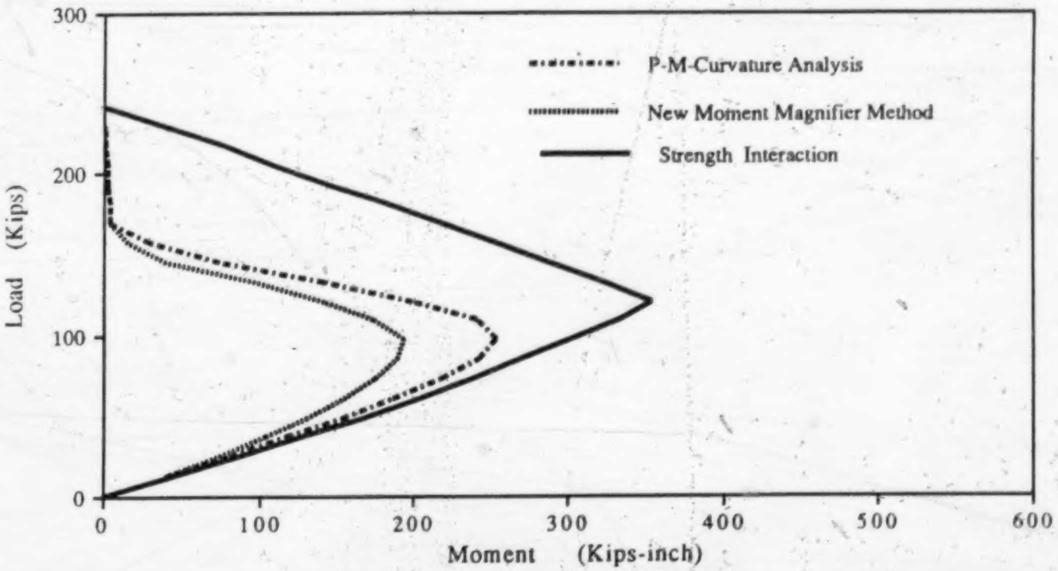

Fig. 6.53 Comparison of Analysis Methods for Face shell Bedded Plain Masonry Wall, H/t = 30, e2/e1 = 0.0

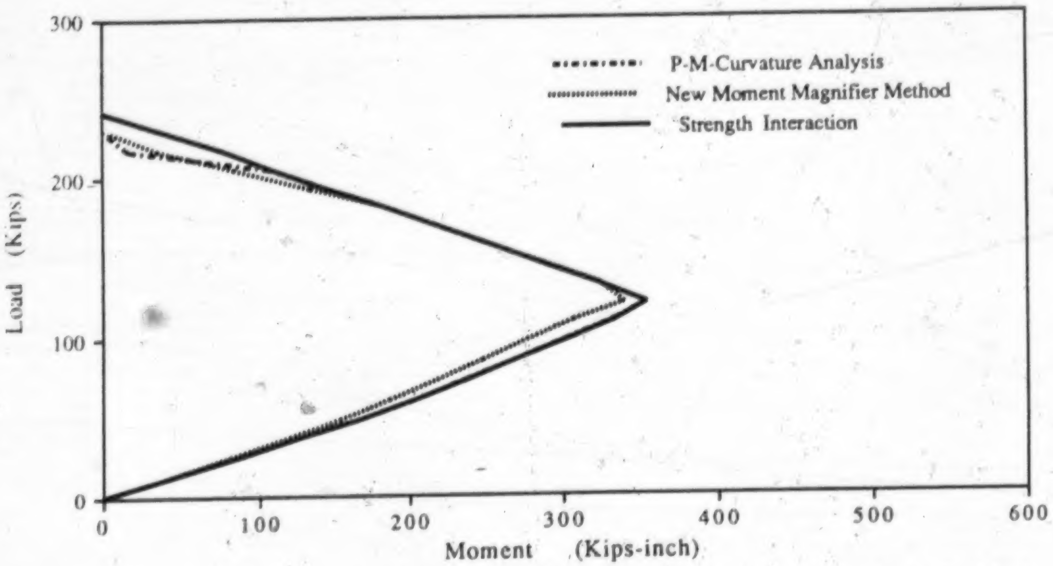

Fig. 6.54 Comparison of Analysis Methods for Face shell Bedded Plain Masonry Wall, H/t = 15, e2/e1 = -1.0

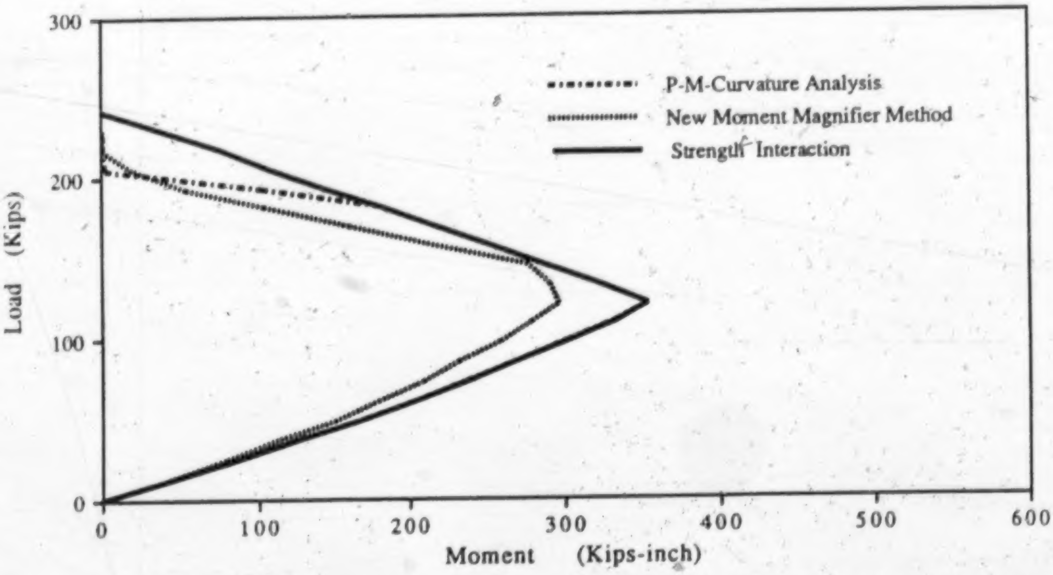

Fig. 6.55 Comparison of Analysis Methods for Face shell Bedded Plain Masonry Wall, H/t = 20, e2/e1 = -1.0

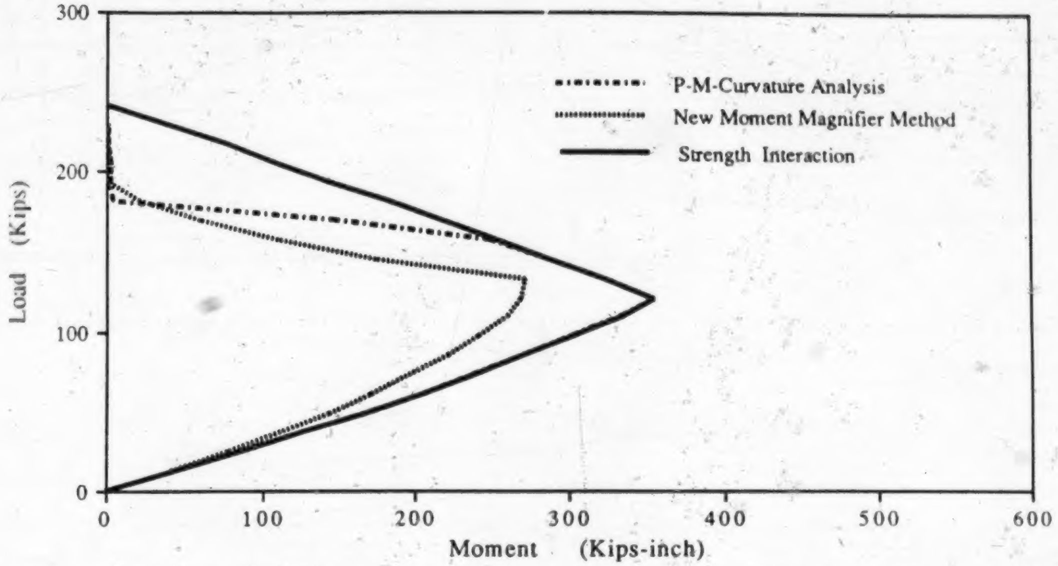

Fig. 6.56 Comparison of Analysis Methods for Face shell Bedded Plain Masonry Wall, H/t = 25, e2/e1 = -1.0

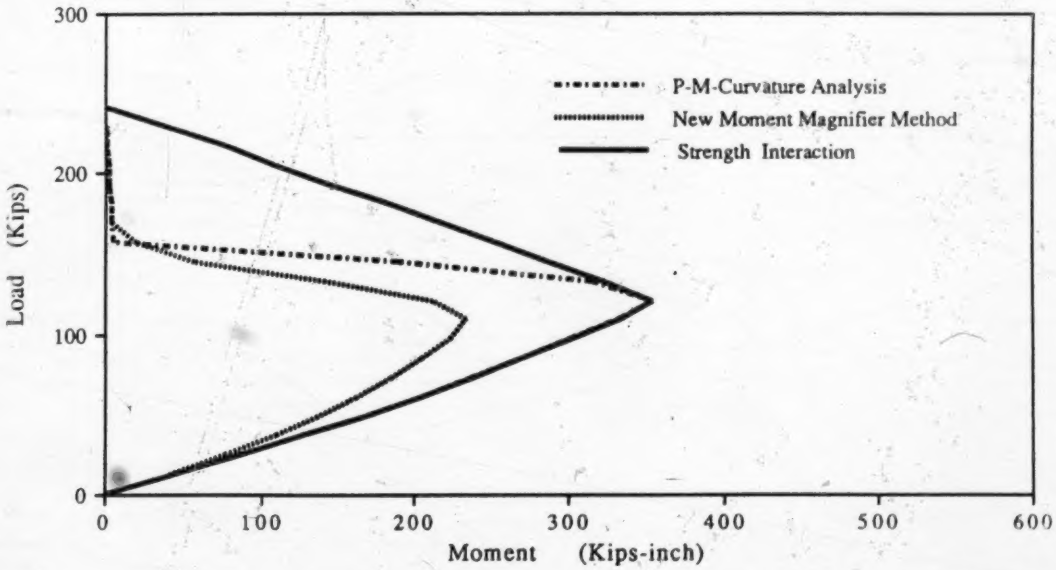

Fig. 6.57 Comparison of Analysis Methods for Face shell Bedded Plain Masonry Wall, H/t = 30, e2/e1 = -1.0

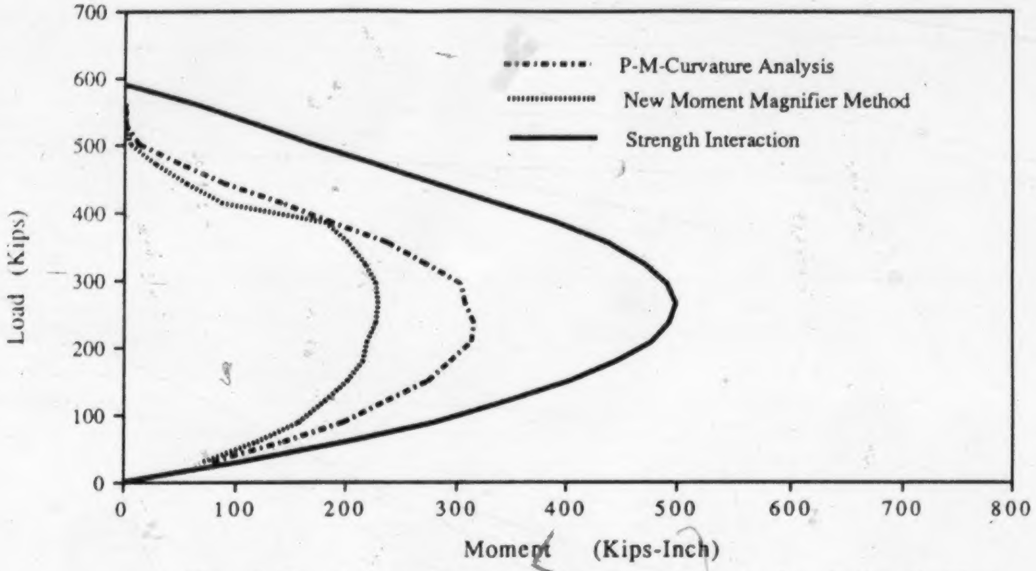

Fig. 6.58 Comparison of Analysis Methods for Fully Bedded Plain Masonry Wall, H/t = 15, e2/e1 = 1.0

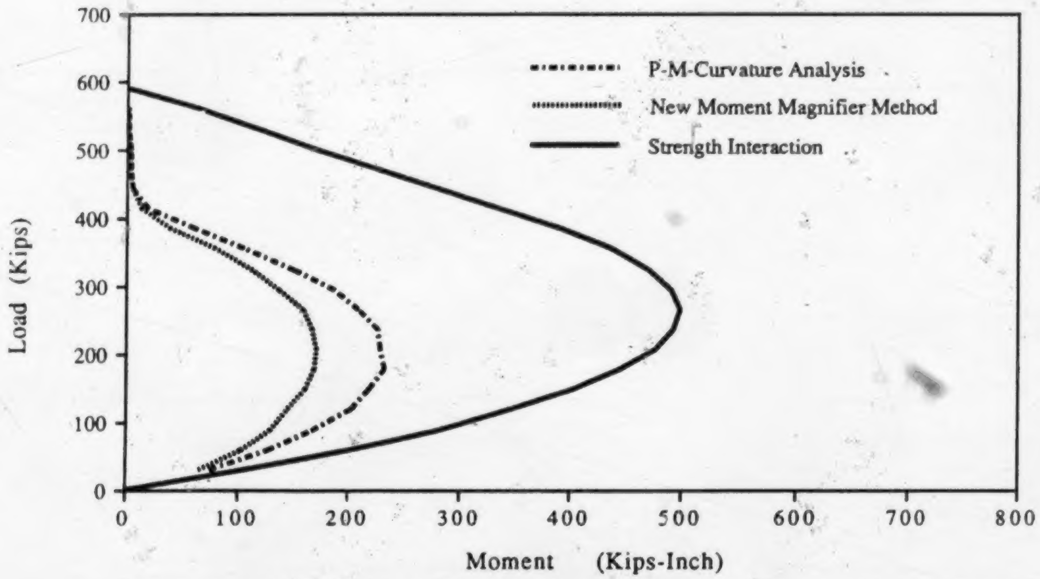

Fig. 6.59 Comparison of Analysis Methods for Fully Bedded Plain Masonry Wall, H/t = 20, e2/e1 = 1.0

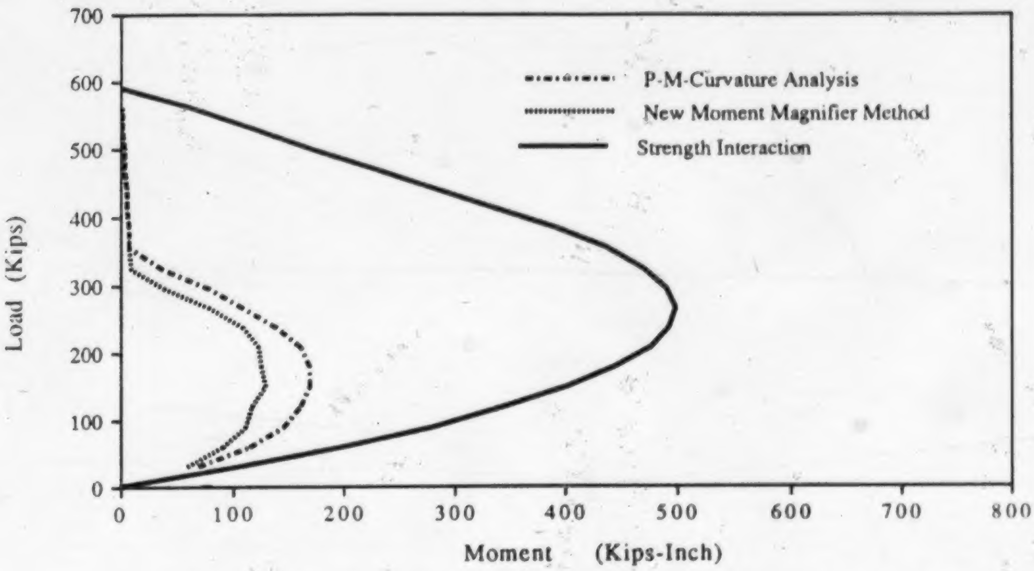

Fig. 6.60 Comparison of Analysis Methods for Fully Bedded Plain Masonry Wall, H/t = 25, e2/e1 = 1.0

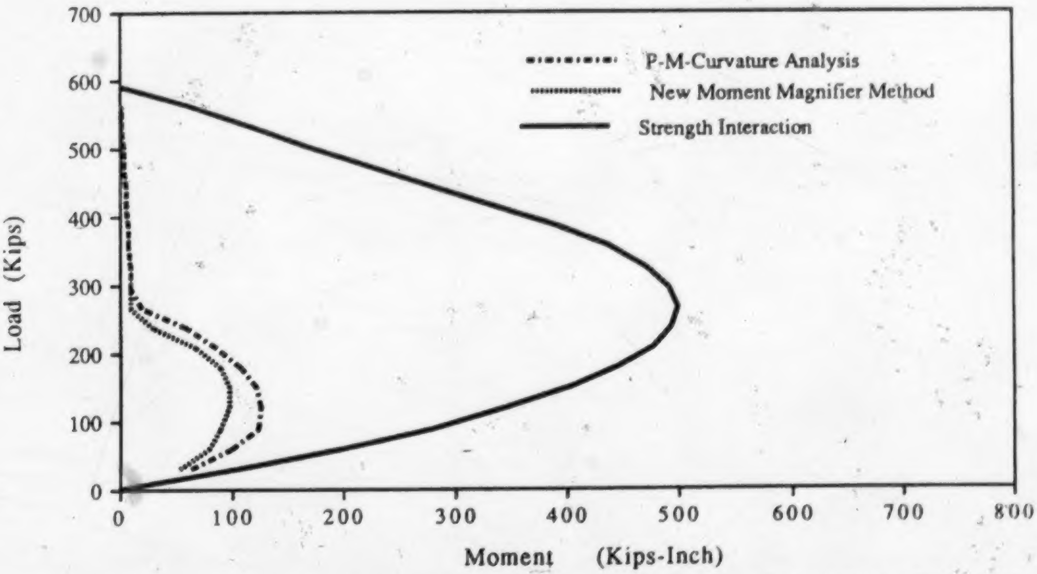

Fig. 6.61 Comparison of Analysis Methods for Fully Bedded Plain Masonry Wall, H/t = 30, e2/e1 = 1.0

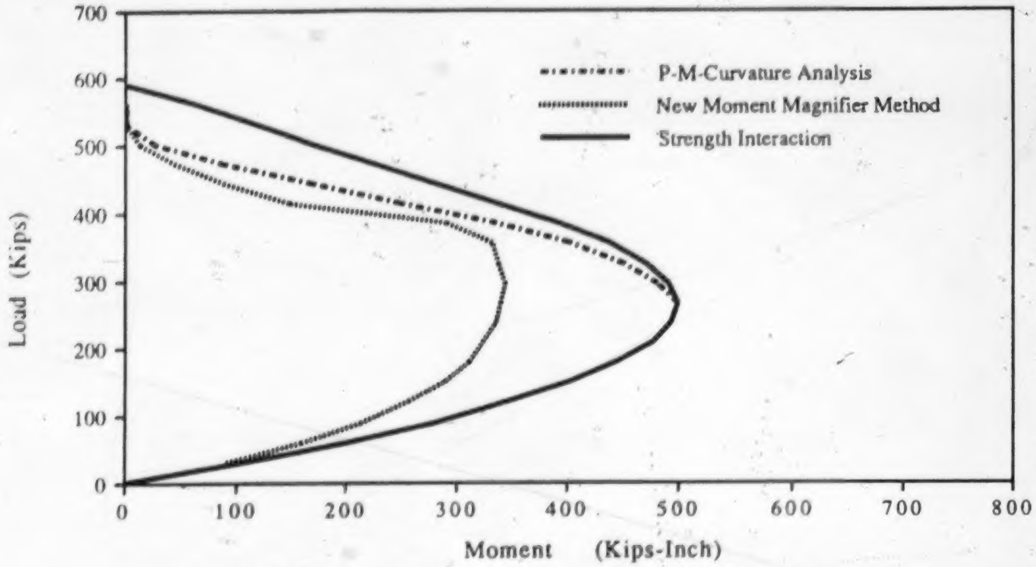

Fig. 6.62 Comparison of Analysis Methods for Fully Bedded Plain Masonry Wall, H/t = 15, e2/e1 = 0.0

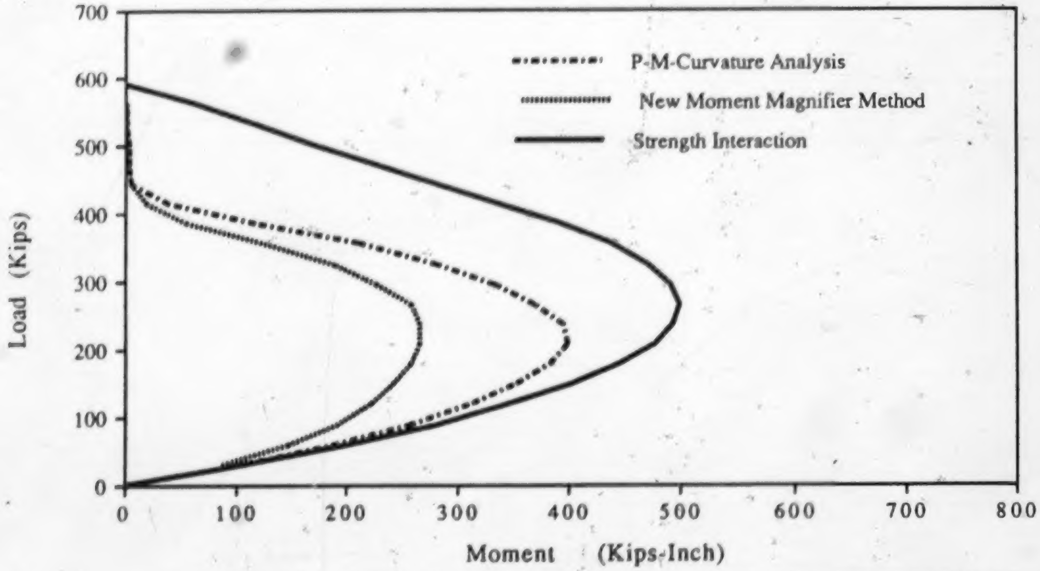

Fig. 6.63 Comparison of Analysis Methods for Fully Bedded Plain Masonry Wall, H/t = 20, e2/e1 = 0.0

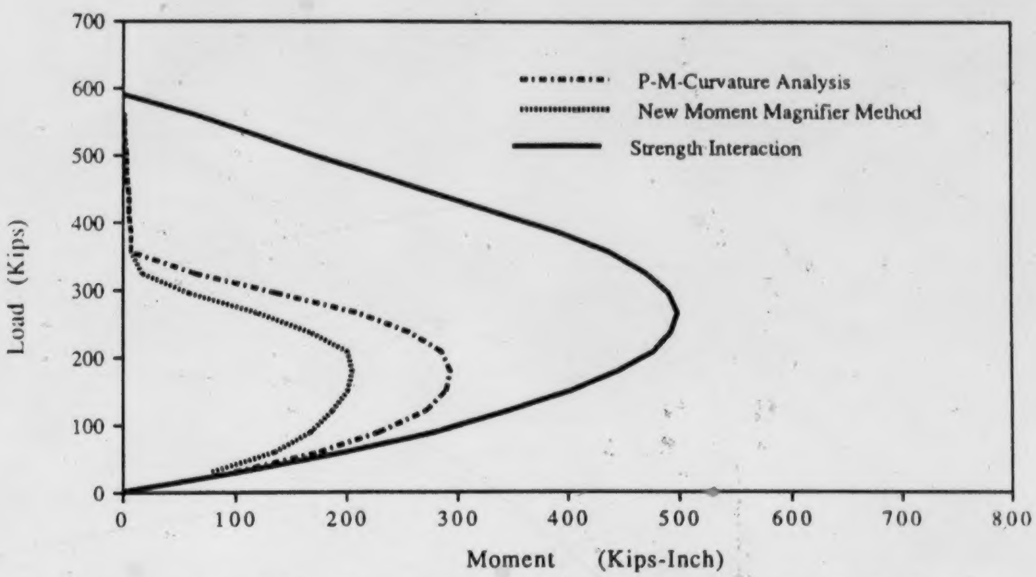

Fig. 6.64 Comparison of Analysis Methods for Fully Bedded Plain Masonry Wall, H/t = 25, e2/e1 = 0.0

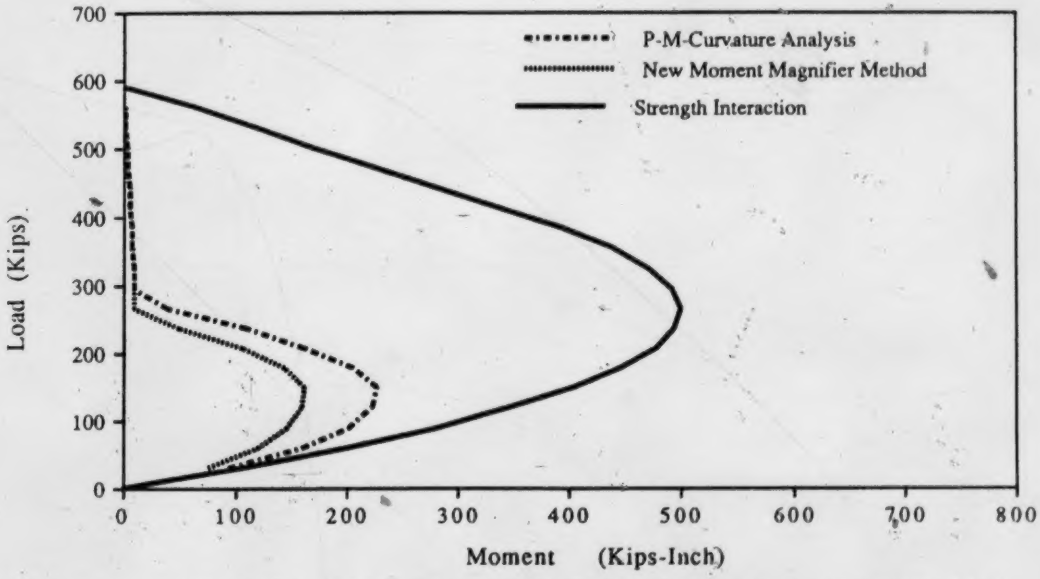

Fig. 6.65 Comparison of Analysis Methods for Fully Bedded Plain Masonry Wall, H/t = 30, e2/e1 = 0.0

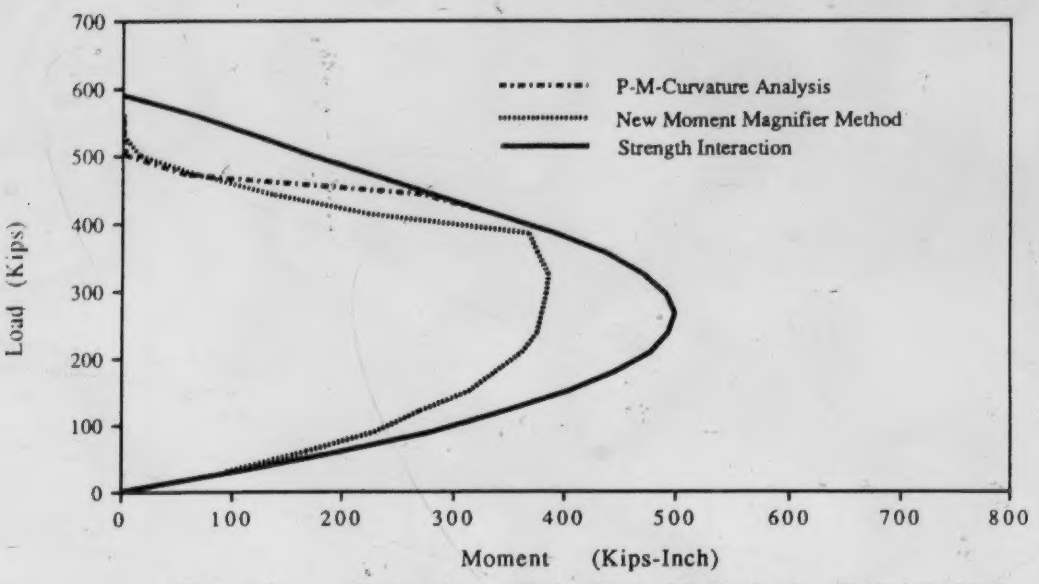

Fig. 6.66 Comparison of Analysis Methods for Fully Bedded Plain Masonry Wall, H/t = 15, e2/e1 = -1.0

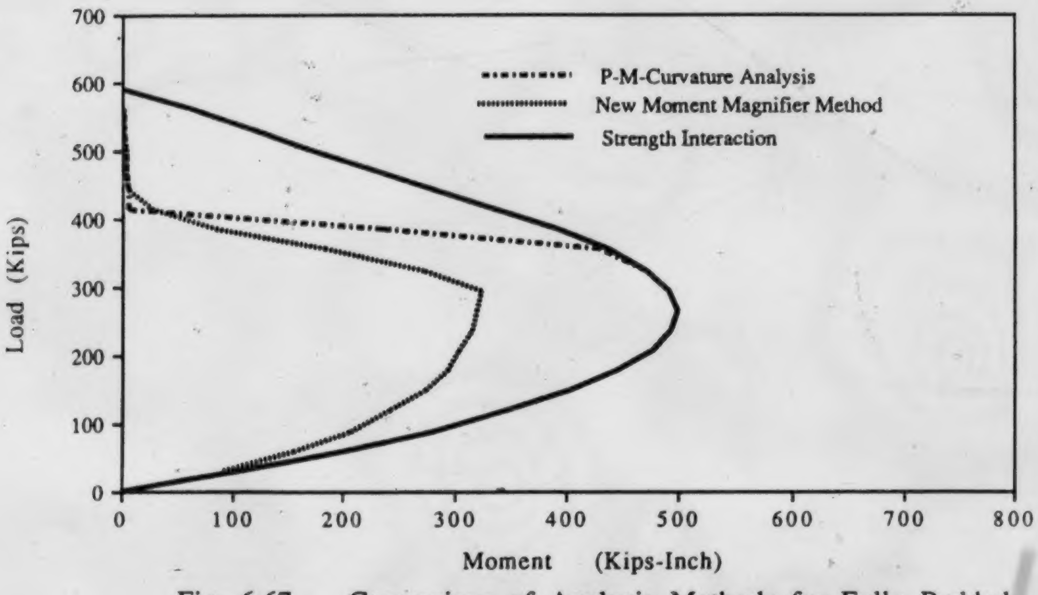

Fig. 6.67 Comparison of Analysis Methods for Fully Bedded Plain Masonry Wall, H/t = 20, e2/e1 = -1.0

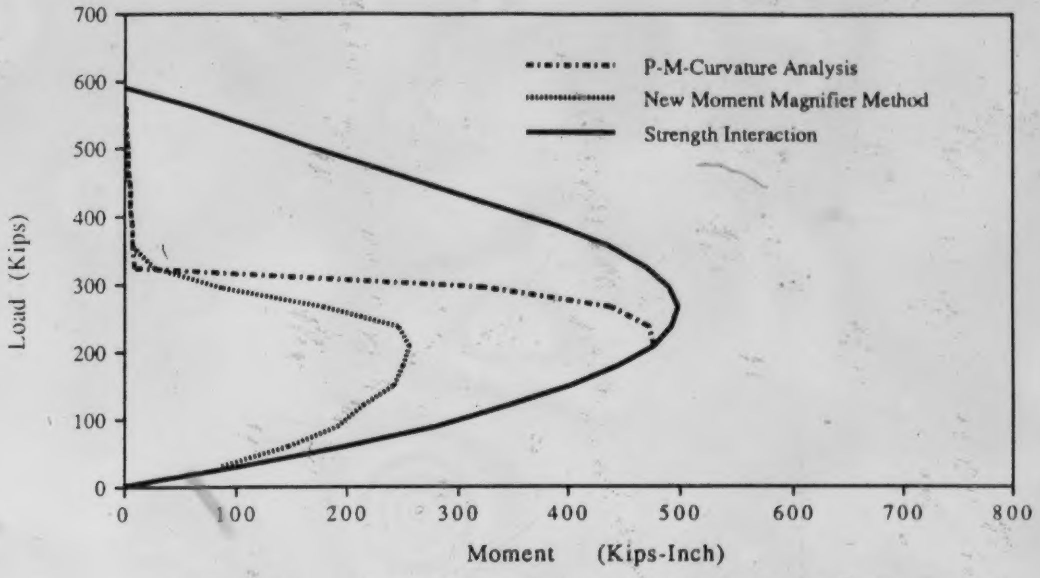

Fig. 6.68 Comparison of Analysis Methods for Fully Bedded Plain Masonry Wall, H/t = 25, e2/e1 = -1.0

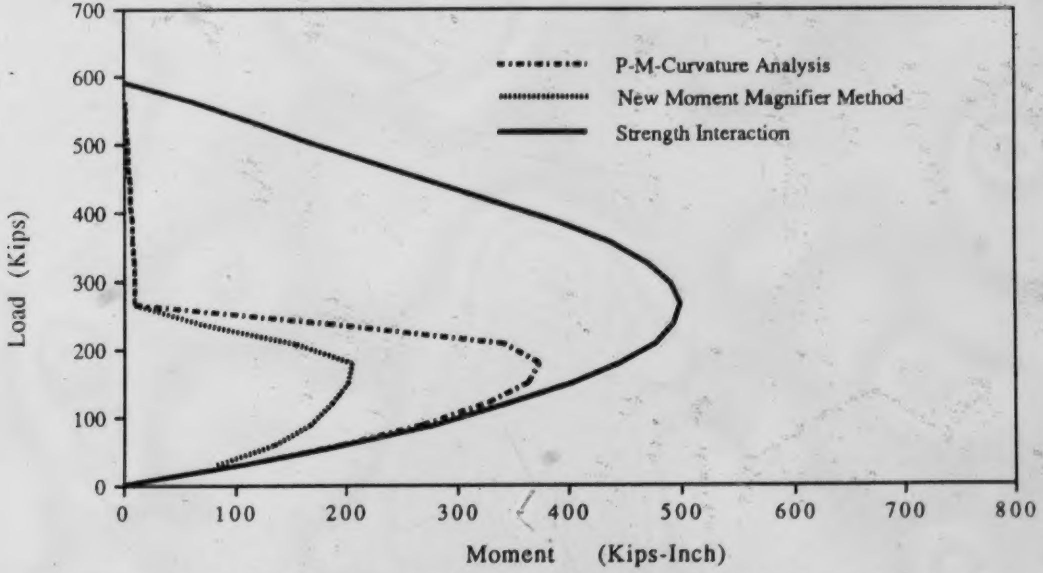

Fig. 6.69 Comparison of Analysis Methods for Fully Bedded Plain Masonry Wall, H/t = 30, e2/e1 = -1.0

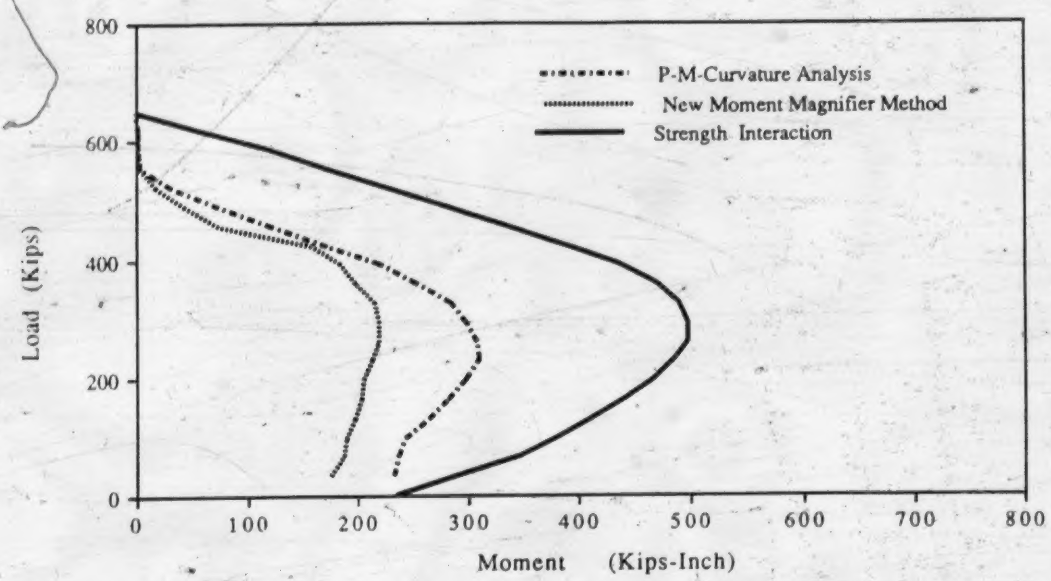

Fig. 6.70 Comparison of Analysis Methods for Fully Grouted Reinforced Masonry Wall, H/t = 15, e2/e1 = 1.0

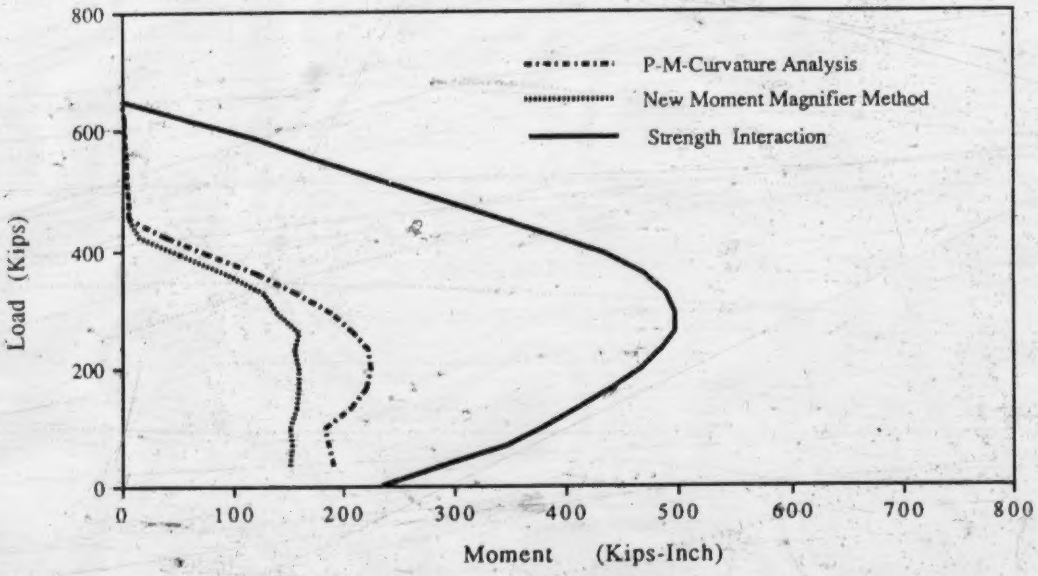

Fig. 6.71 Comparison of Analysis Methods for Fully Grouted Reinforced Masonry Wall, H/t = 20, e2/e1 = 1.0

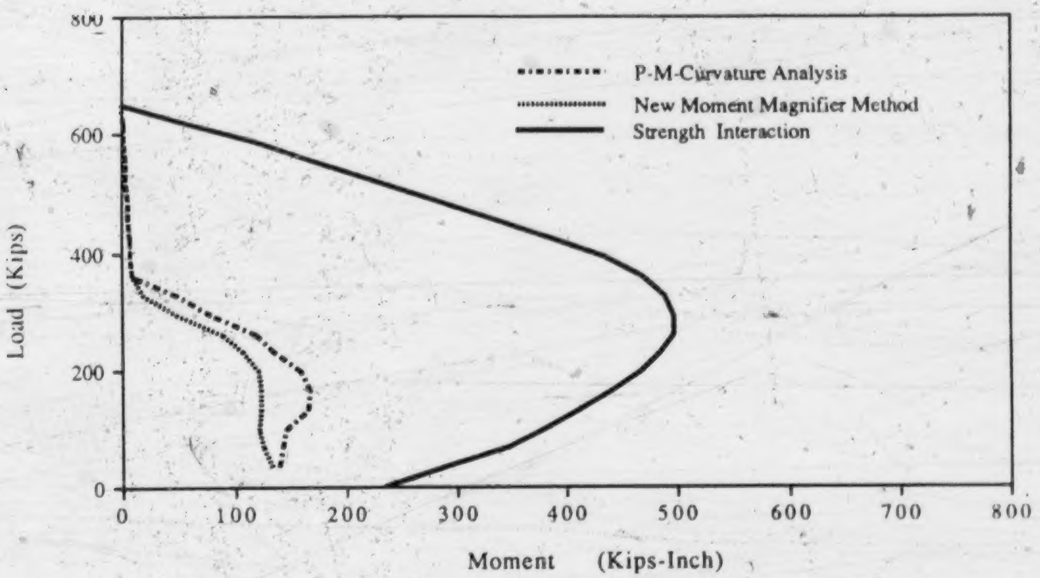

Fig. 6.72 Comparison of Analysis Methods for Fully Grouted Reinforced Masonry Wall, H/t = 25, e2/e1 = 1.0

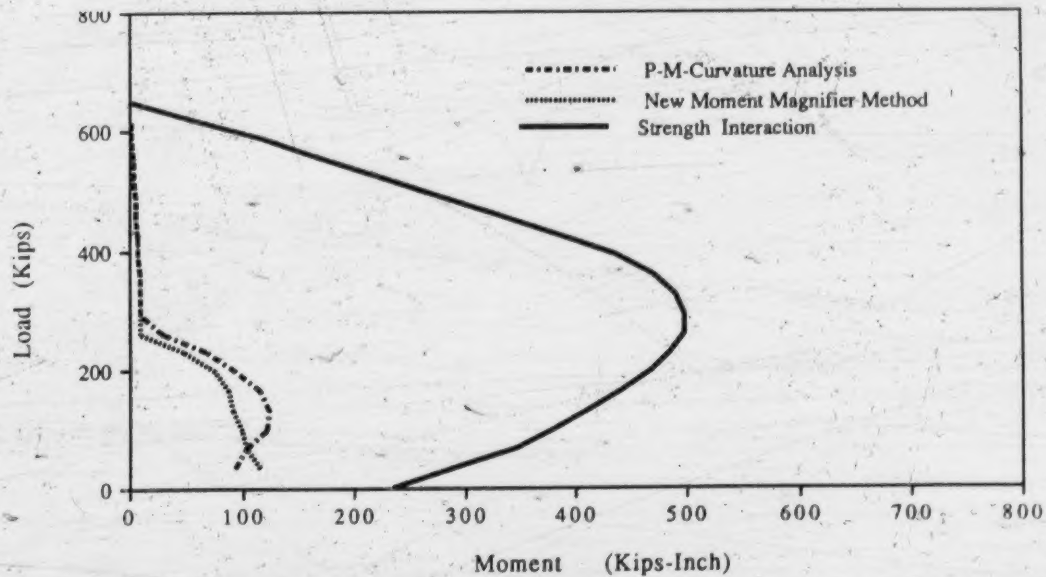

Fig. 6.73 Comparison of Analysis Method for Fully Grouted Reinforced Masonry Wall, H/t = 30, e2/e1 = 1.0

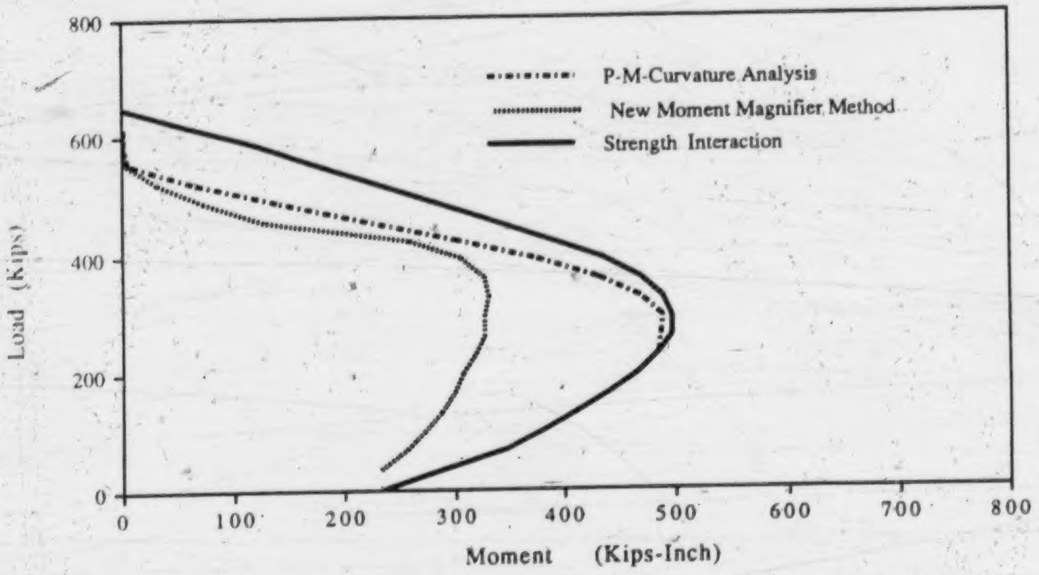

Fig. 6.74 Comparison of Analysis Methods for Fully Grouted Reinforced Masonry Wall, H/t = 15, e2/e1 = 0.0

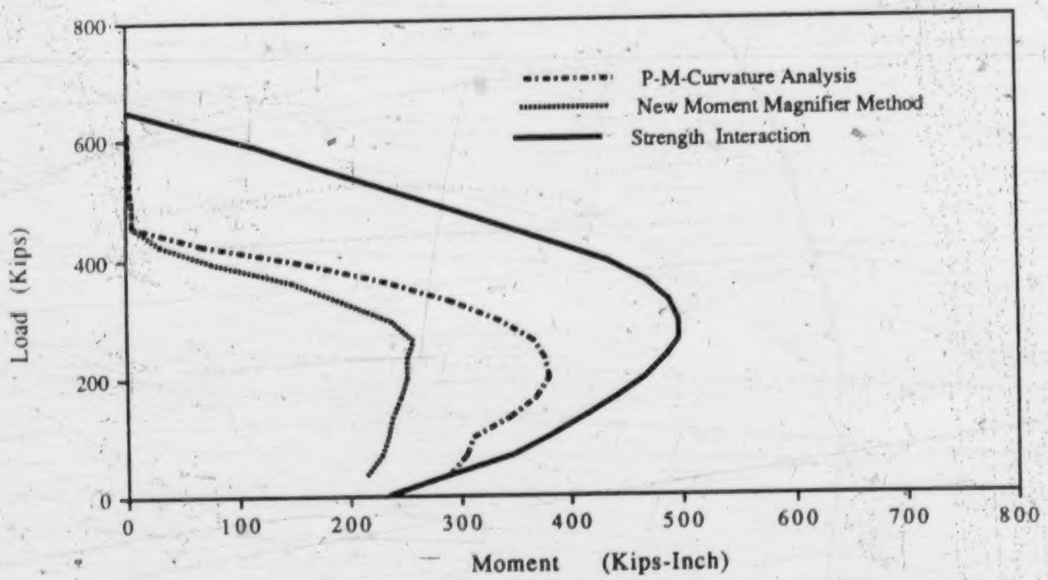

Fig. 6.75 Comparison of Analysis Methods for Fully Grouted Reinforced Masonry Wall, H/t = 20, e2/e1 = 0.0

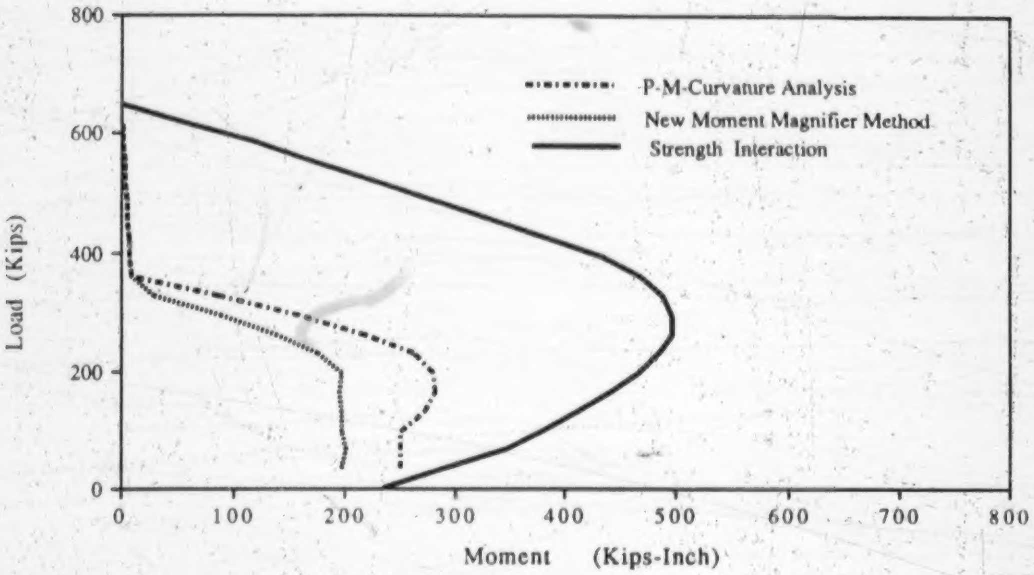

Fig. 6.76 Comparison of Analysis Methods for Fully Grouted Reinforced Masonry Wall, H/t = 25, e2/e1 = 0.0

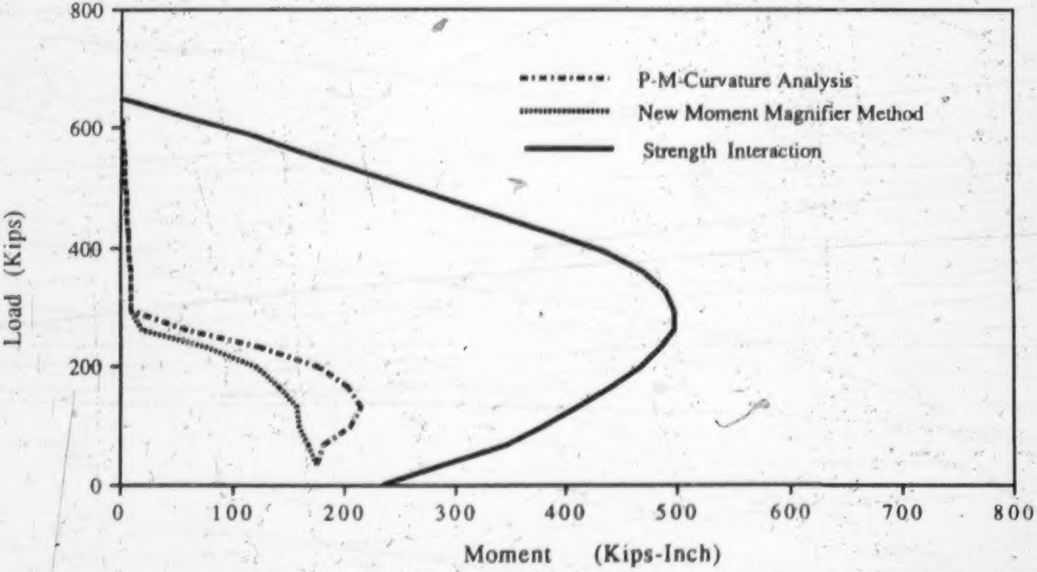

Fig. 6.77 Comparison of Analysis Methods for Fully Grouted Reinforced Masonry Wall, H/t = 30, e2/e1 = 0.0

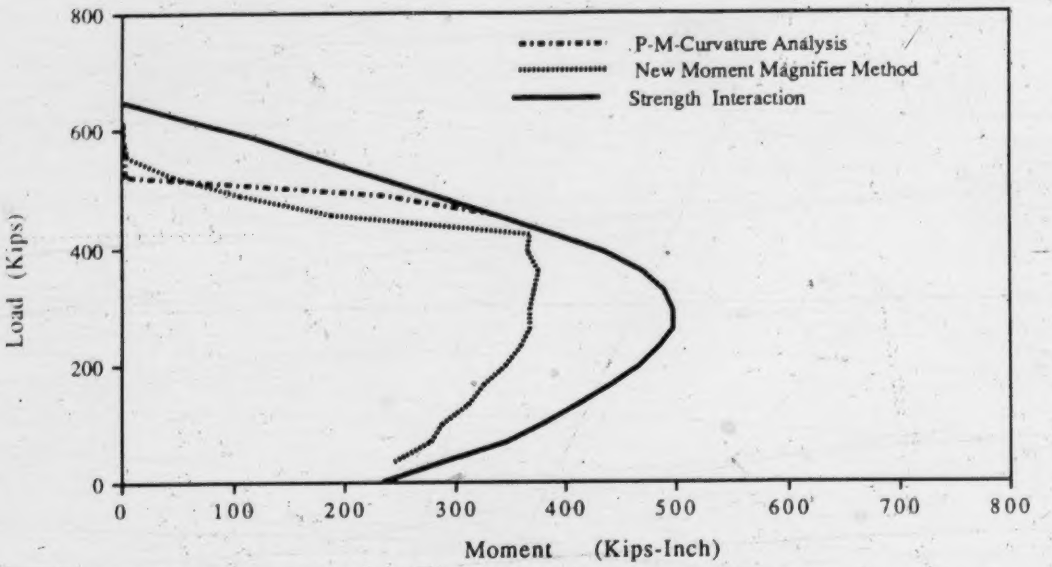

Fig. 6.78 Comparison of Analysis Methods for Fully Grouted Reinforced Masonry Wall, H/t = 15, e2/e1 = -1.0

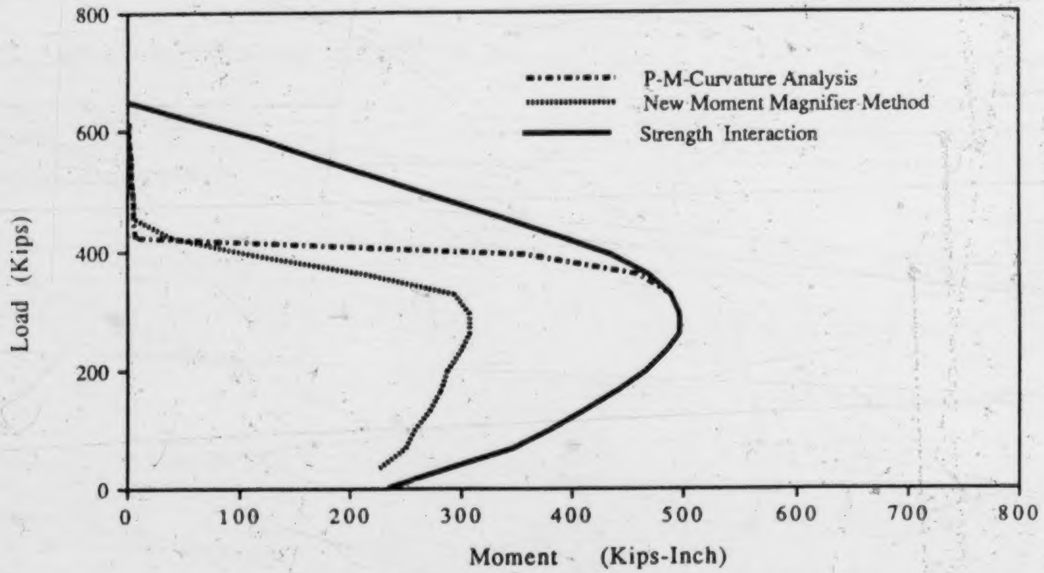

Fig. 6.79 Comparison of Analysis Methods for Fully Grouted Reinforced Masonry Wall, H/t = 20, e2/e1 = -1.0

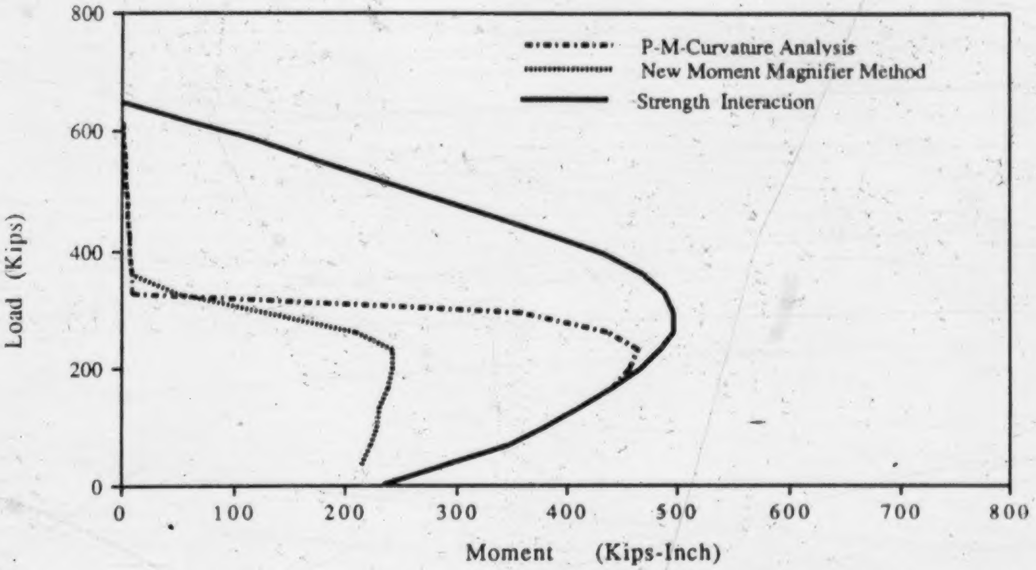

Fig. 6.80 Comparison of Analysis Methods for Fully Grouted Reinforced Masonry Wall, H/t = 25, e2/e1 = -1.0

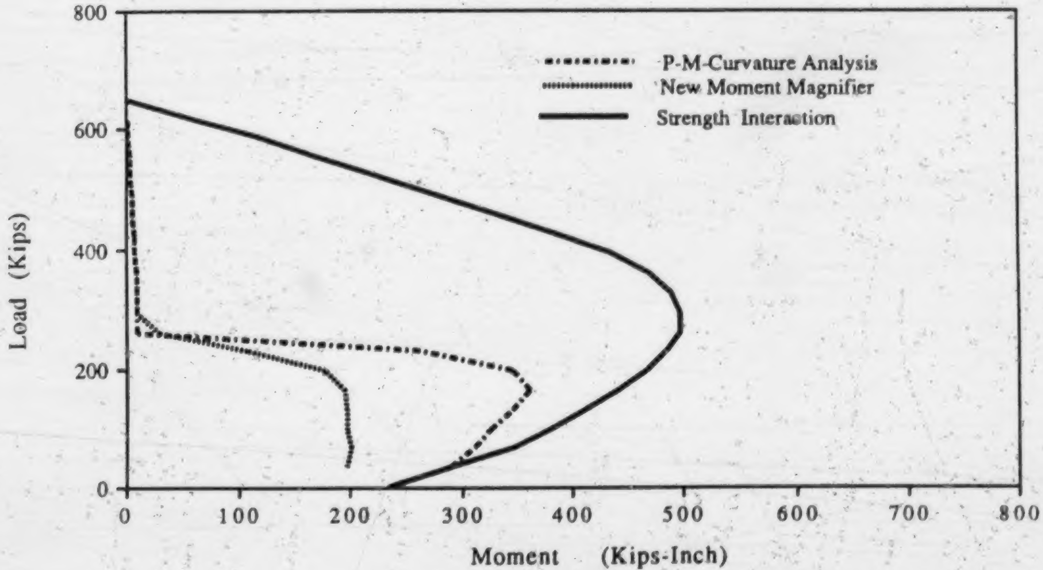

Fig. 6.81 Comparison of Analysis Methods for Fully Grouted Reinforced Masonry Wall, H/t = 30, e2/e1 = -1.0

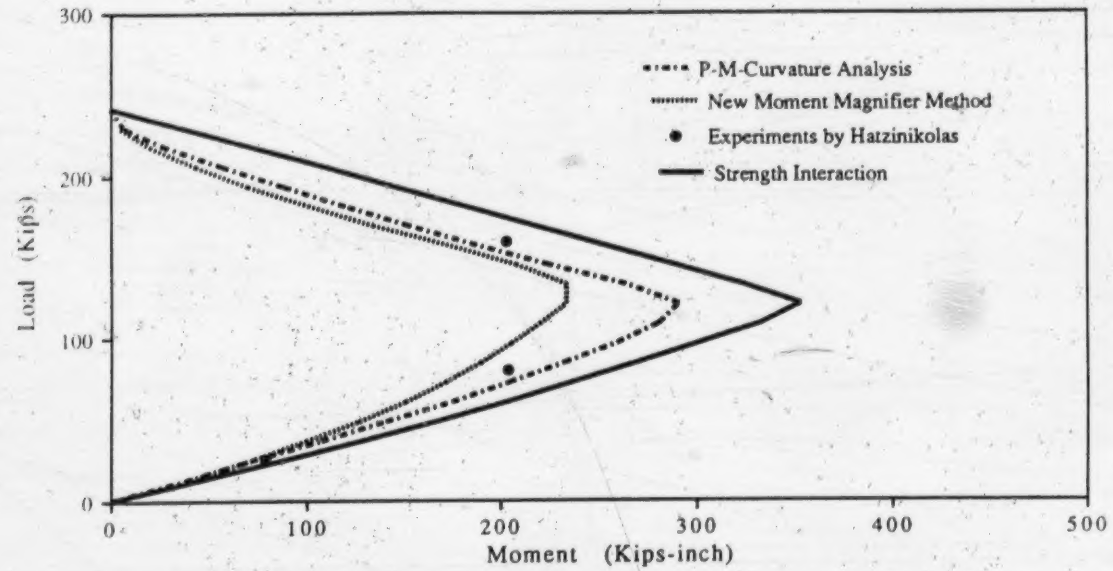

Fig.6.82 Comparison with Test Results, Plain walls
e2/e1 = 1.0, H/t = 13.77, H = 105 in.

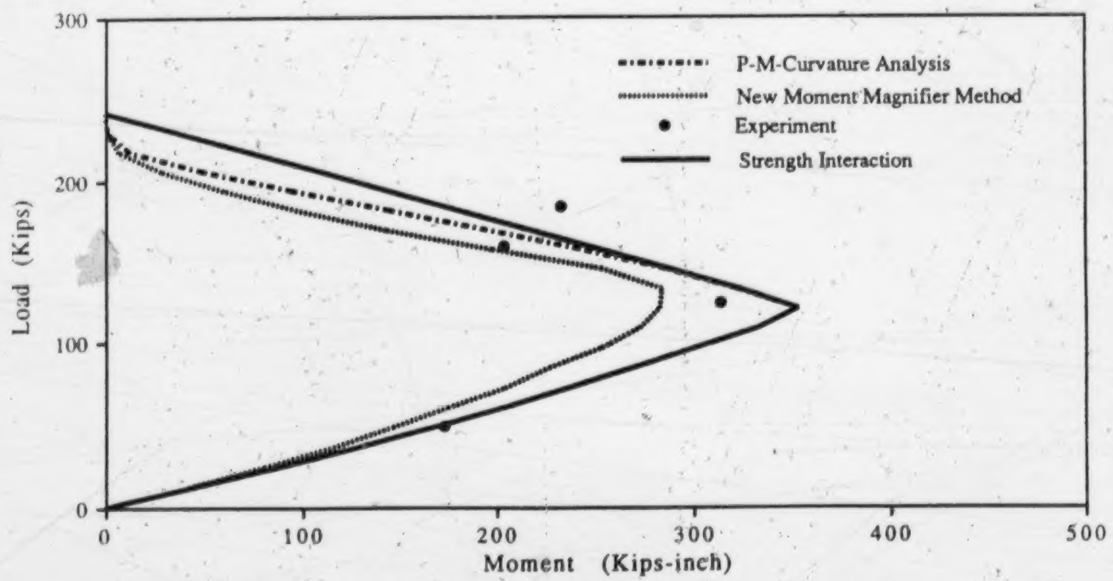

Fig.6.83 Comparison with Test Results, Plain walls
e2/e1 = 0.0, H/t = 18, H = 137 in.

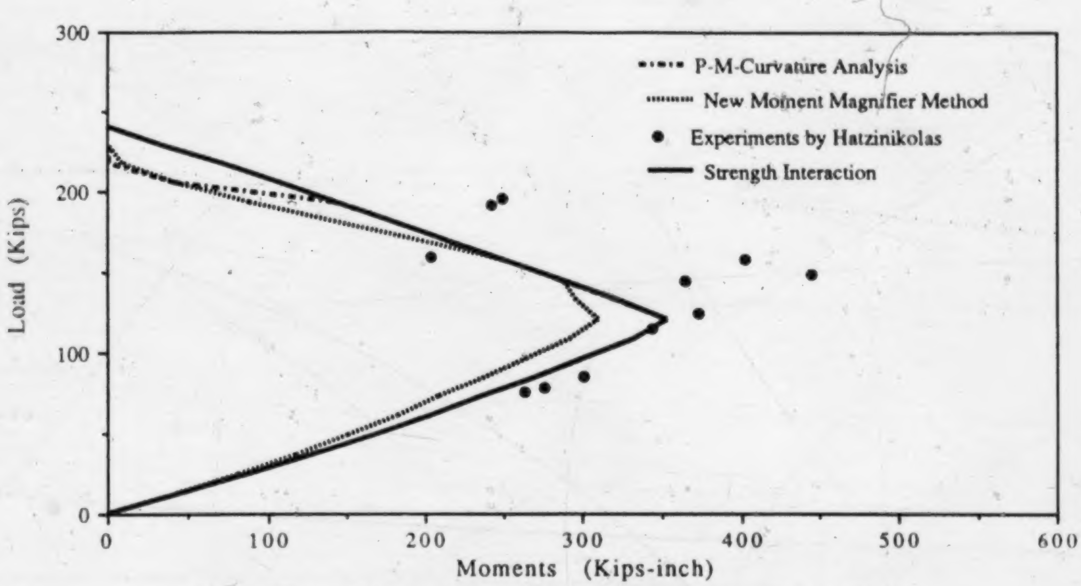

Fig. 6.84 Comparison with Tests Results, Plain Walls
e2/e1 = -1.0, H/t = 18, H = 137 in.

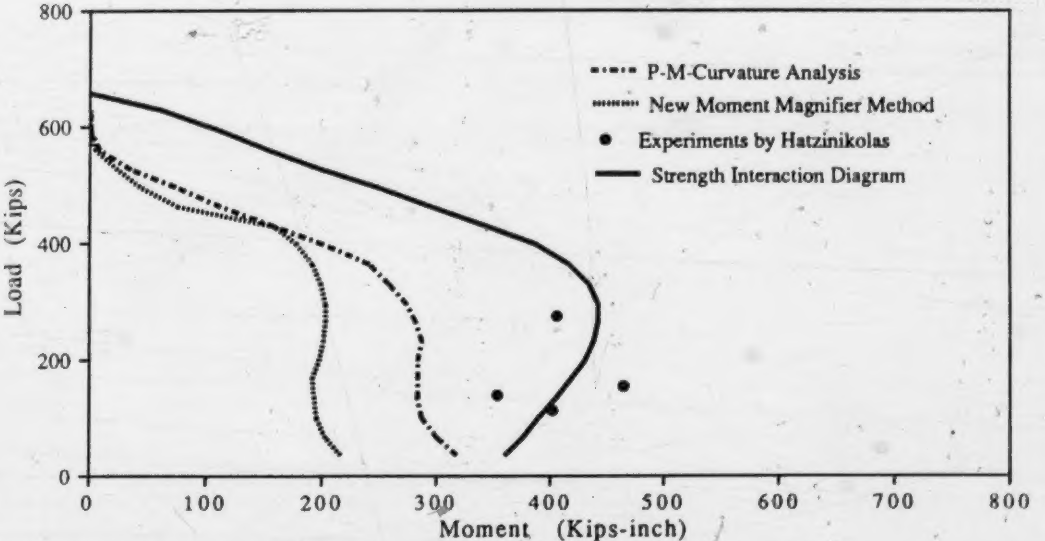

Fig.6.85 Comparison to test results, Reinforced walls
e2/e1 = 1.0, H/t = 14, H = 105 in., As = 3.0 in. sq.

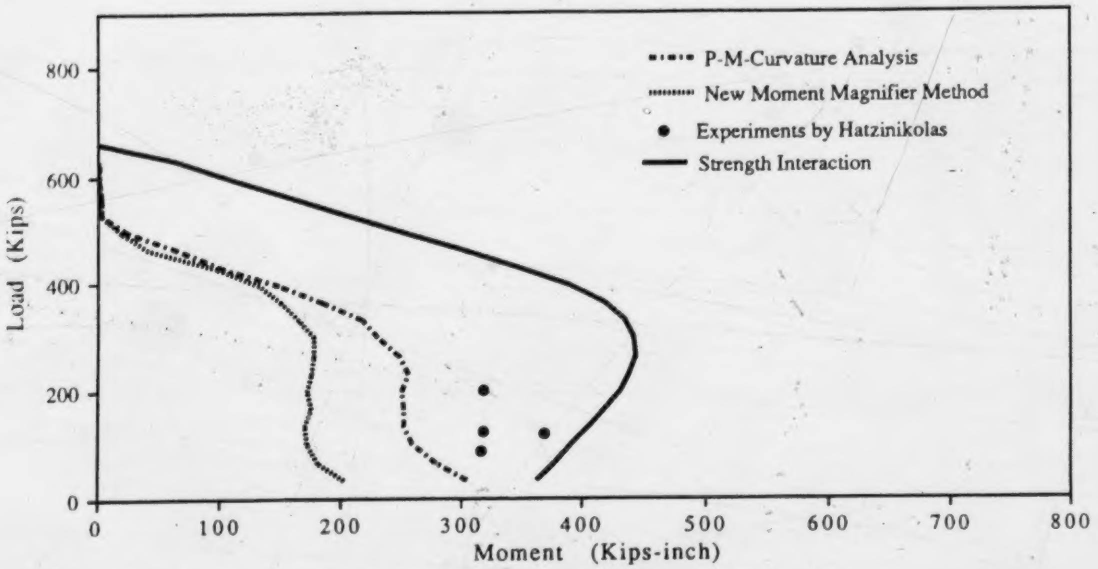

Fig.6.86 Comparison to test results, Reinforced walls
e2/e1 = 1.0, H/t = 16, H = 121 in., As = 3.0 in. sq.

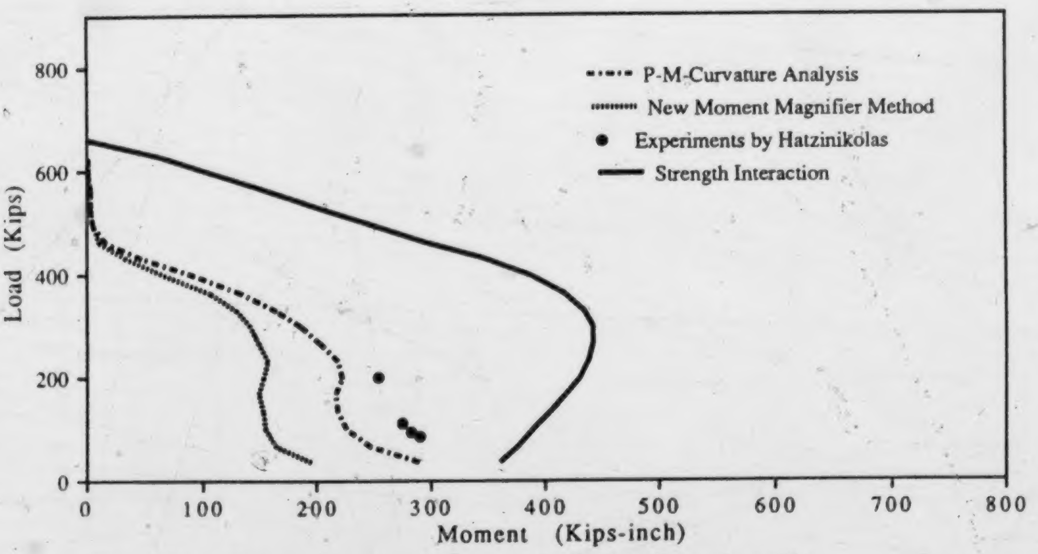

Fig.6.87 Comparison to test results, Reinforced walls
e2/e1 = 1.0, H/t = 18, H = 137 in., As = 3.0 in. sq.

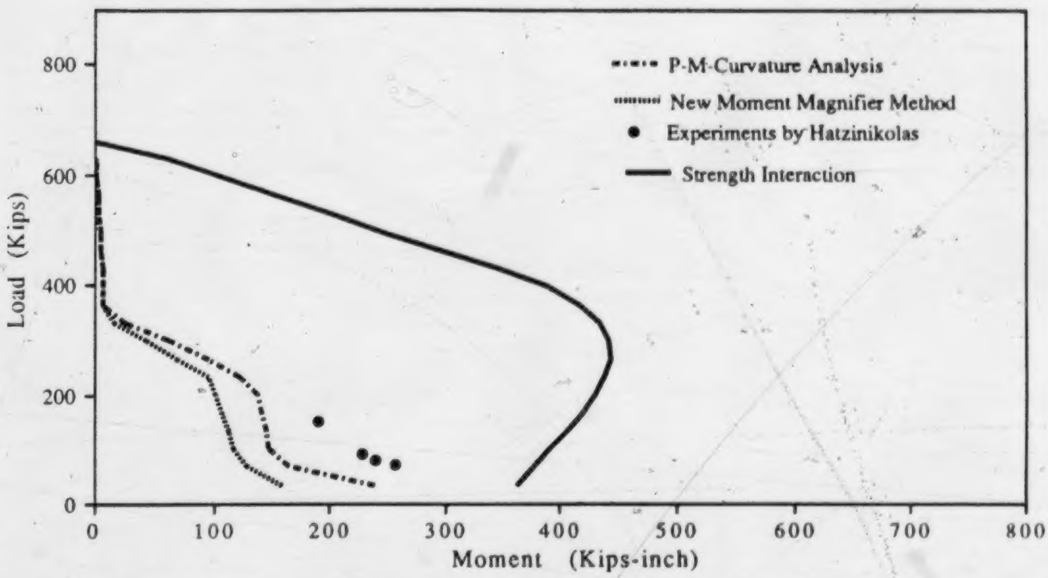

Fig.6.88 Comparison to test results, Reinforced walls
e2/e1 = 1.0, H/t = 24.26, H = 185 in., As = 3.0 in. sq.

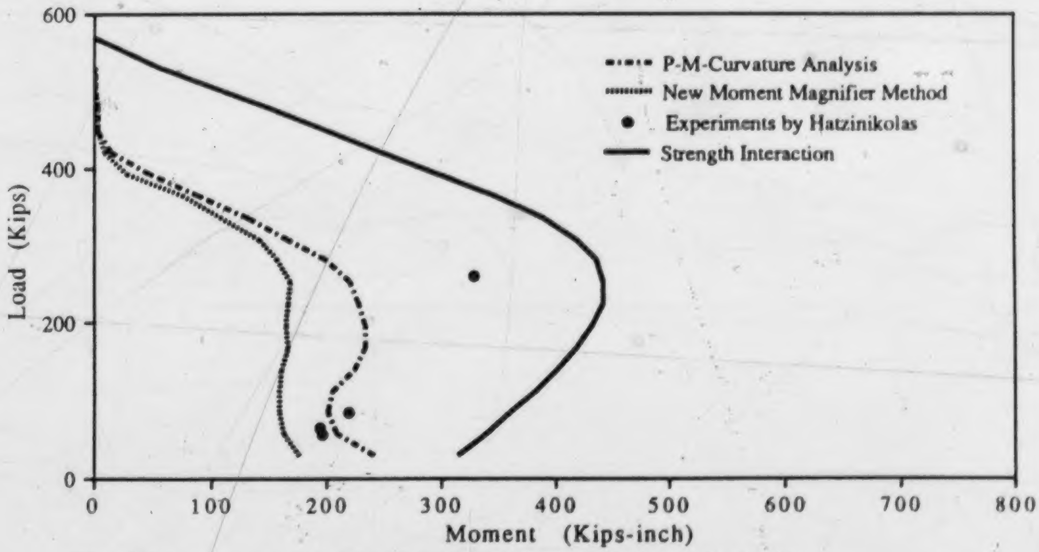

Fig.6.89 Comparison to test results, Reinforced walls
e2/e1 = 1.0, H/t = 17.97, H = 137 in., As = 1.32 in. sq.

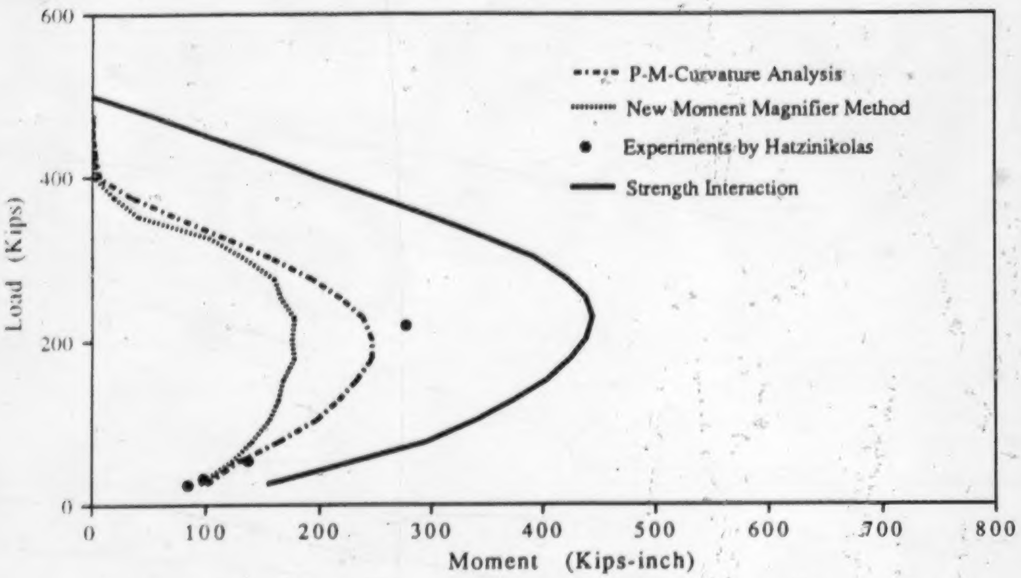

Fig.6.90 Comparison to test results, Reinforced walls
e2/e1 = 1.0, H/t = 18, H = 137 in., As = .33 in. sq.

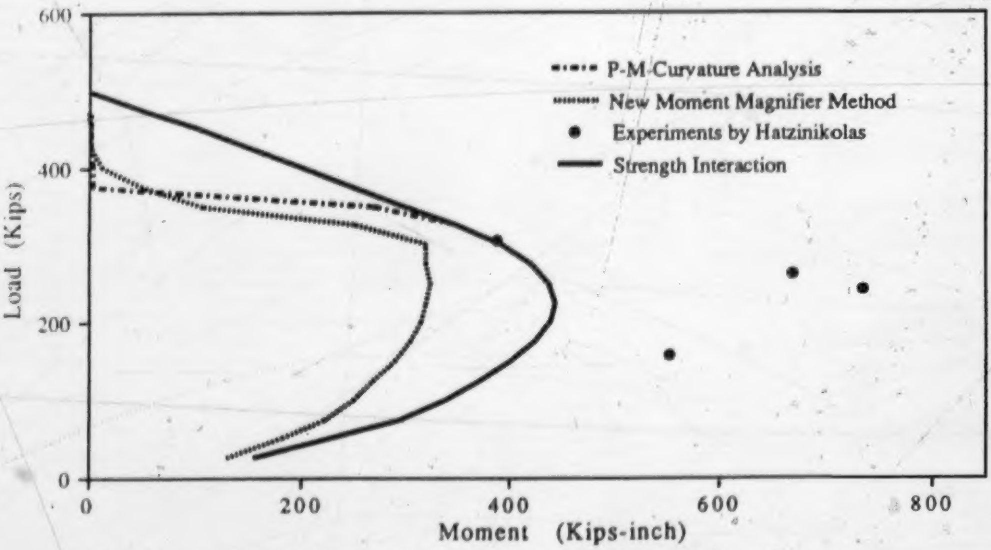

Fig.6.91 Comparison to test results, Reinforced walls
e2/e1 = -1.0, H/t = 17.97, H = 137 in., As = .33 in. sq.

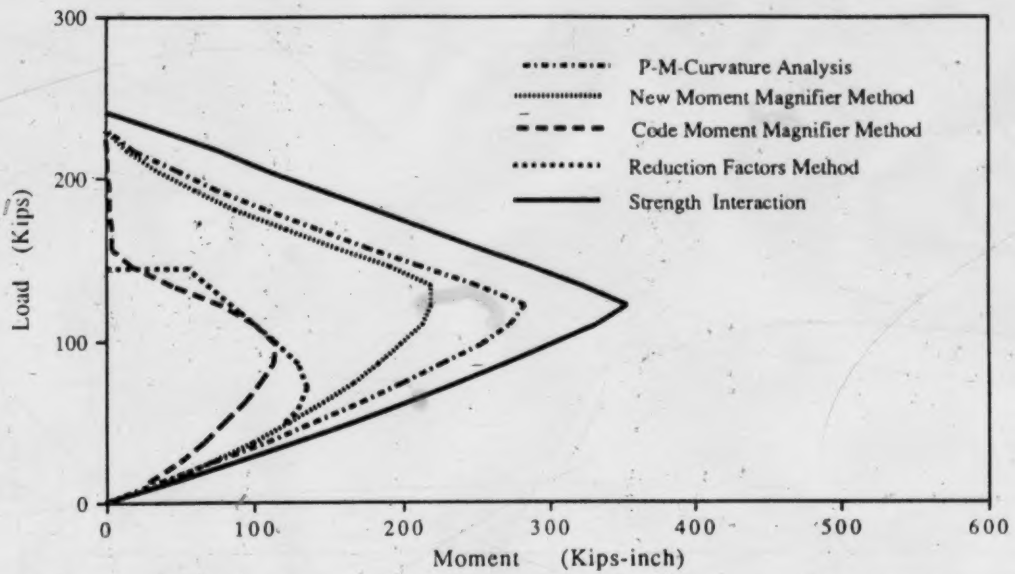

Fig. 6.92 Assessment of Code Procedures for Face shell Bedded Plain Masonry Wall H/t = 15, e2/e1 = 1.0

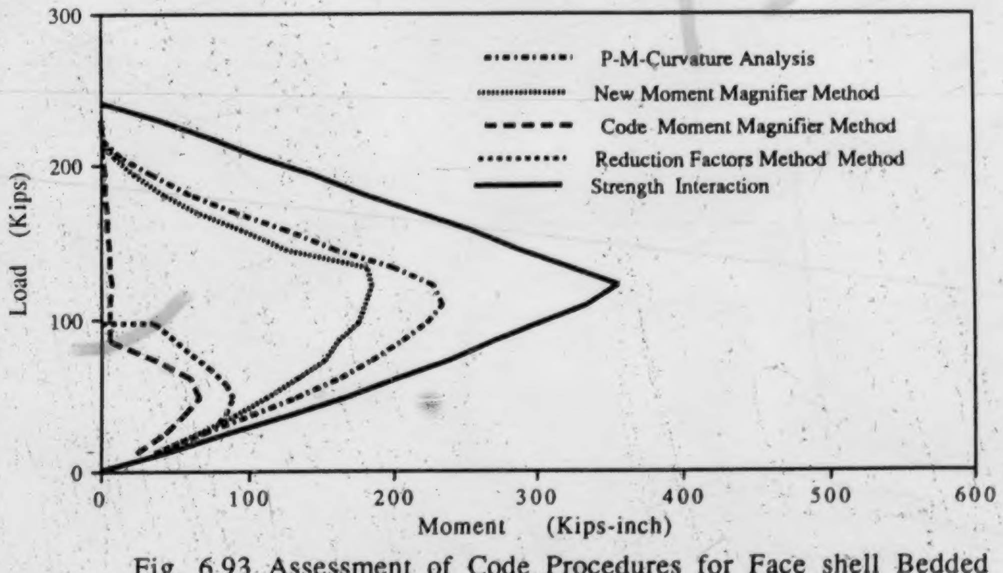

Fig. 6.93 Assessment of Code Procedures for Face shell Bedded Plain Masonry Wall, H/t = 20, e2/e1 = 1.0

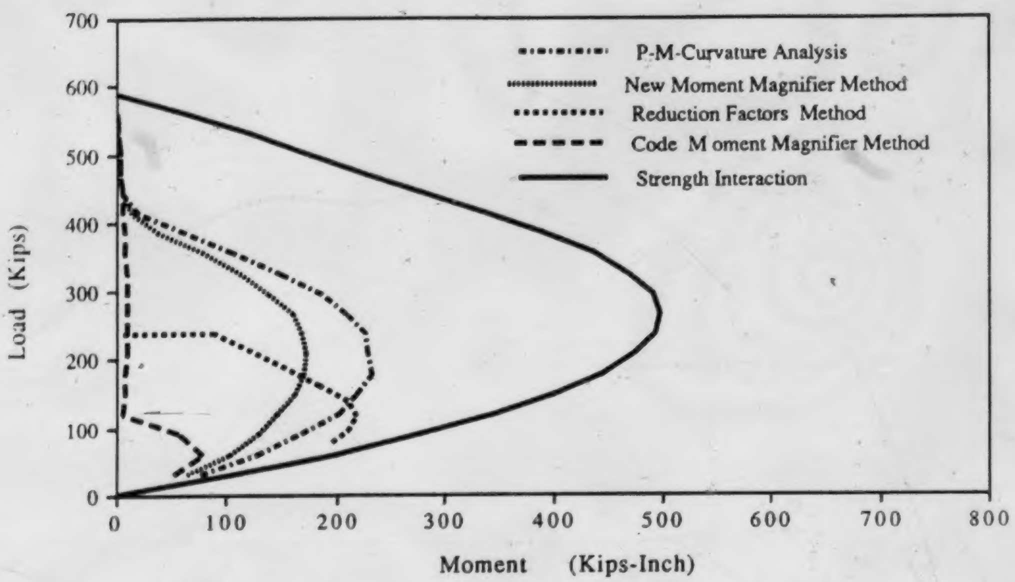

Fig. 6.94 Assessment of Code Procedures for Fully Bedded Plain Masonry Wall, H/t = 20, e2/e1 = 1.0

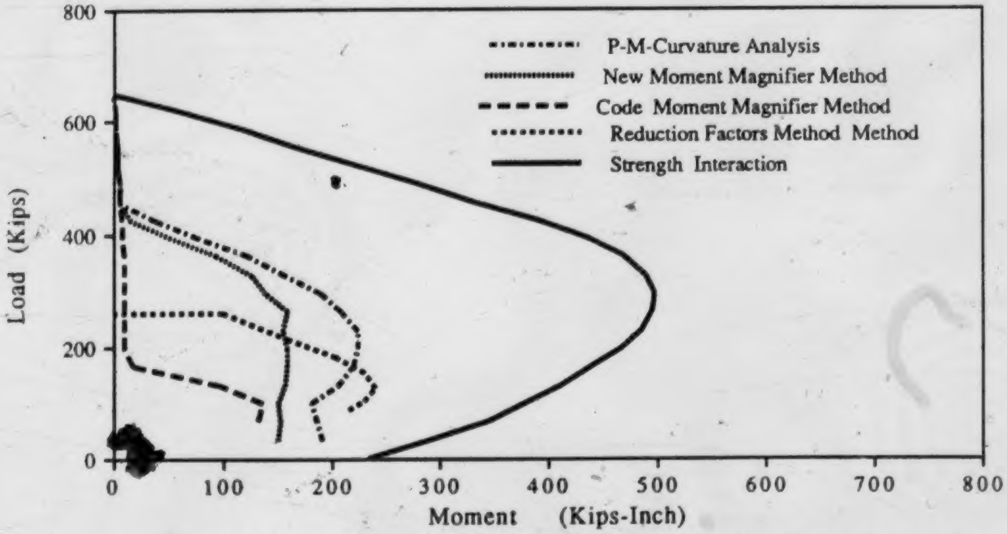

Fig. 6.95 Assessment of Code Procedures for Fully Grouted Reinforced Masonry Wall, H/t = 20, e2/e1 = 1.0

CHAPTER 7

SUMMARY, CONCLUSIONS AND RECOMMENDATIONS

7.1 Summary

Analytical studies were carried out to study the behaviour of slender concrete masonry walls under axial load and out-of-plane bending. A Load-Moment-Curvature based analysis method using Newmark's Numerical Method and Column Deflection Curve approach was used. The analytical model was verified using experimental data previously obtained at the University of Alberta. The numerical accuracy of the program was established by comparing it with a differential equation solution.

The variation of EI at different combinations of axial load and bending moments was studied using the Load-Moment-Curvature relationships. Simple equations based on rational assumptions were proposed to calculate EI values as a function of load and moment over the cross-section. A parametric study was carried out to show that the Moment Magnifier Method gives results similar to the analytical model when new EI values are used. Finally the new Moment Magnifier Method is demonstrated to be better than the current approach in the present CSA standard S304-M84.

7.2 Conclusions

The following conclusions can be derived from this study on eccentrically loaded slender masonry walls.

1. The wall capacity is reduced drastically with increase in slenderness and eccentricity but not as much as predicted using the procedures in the present CSA standard S304-M84.
2. The analytical model correctly predicts experimental results and provides accurate estimates for wall capacity for eccentrically loaded slender masonry walls. Material and stability failures can be determined using this analytical model. For walls bent in double curvature bending unwinding can also be predicted.
3. This analytical method accounts for material nonlinearity and cracking of the cross section. Therefore, in addition to ultimate strength, load deflection behaviour are well predicted for the entire history of loading.
4. The analytical model generates behavioural information for cases where no experimental data is available for slender masonry walls with different grouting and bedding conditions under a variety of bending configurations. Hence this method facilitates the development of a limit states design method for slender masonry walls.
5. The proposed EI values are based on rational assumptions and take into account the nonlinearity of the stress strain curve and cracking of the cross section. They are uniquely defined for a given axial load and bending moment.

6. The Moment Magnifier method when used along with these new EI values gives more conservative results than the load-moment-curvature based analysis method. This conclusion is based on the parametric study carried out for walls with a slenderness ratio (H/t) less than or equal to 30, bent either in single or in double curvature bending.

7.3 Recommendations for Future Research

1. Extensive experimental work should be conducted to examine the material behaviour of masonry under eccentric compression which will help to accurately calculate the strength interaction diagram.
2. Further tests on full-scale walls must be performed to obtain statistically significant data.
3. Parametric studies using analytical models similar to the one proposed in this study should be carried out to evaluate the effect of different variables. Results of such a parametric study and statistical analysis of experimental data should be used to develop a limit states design method for slender masonry walls which designers can use with confidence.

REFERENCES

1. Amrhein, J.E (1978), "Reinforced Masonry Engineering Handbook", 3rd edition, Masonry Institute of America, Los Angeles, California , 445 pages.

2. Amrhein, J.E (1981), "Slender Walls Research by California Structural Engineers" The Masonry Society Journal, Vol. 1, No.2, December 1981, pp. G9 - G16.

3. Angervo "Uber Knickung and Tragfahigkeit eins exzentrisch gedruckten Pfeilers ohne Zugfestigkeit" [On the Buckling and Bearing Capacity of an Eccentrically Compressed Pillar with no Tensile strength] Staatliche Technische Forschungsunstalt, Finnland, Publication 26, Helsinki, 1954.

4. Chapman, J.C. and Slatford, J. (1957), "The Elastic Buckling of Brittle Columns" Paper No. 6147, Proceedings of the Institute of Civil Engineers, London, Vol. 6, pp. 107-125, January 1957.

5. Chen, W.F. and Atsuta, T. (1973), "Strength of Eccentrically Loaded Walls", International Journal of Solids and Structures, Vol.9, pp. 1283-1300,(1973).

6. Chen, W.F. and Atsuta, T. "Theory of Beam Columns", Volume1: In-Plane Behaviour and Design", McGraw-Hill Inc., 1976, 513 pages.

7. Cranston, W.B. and Roberts, J.J. (1976), "The Structural Behaviour of Concrete Masonry Reinforced and Unreinforced" The Structural Engineer, No. 11, Volume 54, November 1976.

8. CSA Standard CAN3-S304-M84 (1984) "Masonry Design for Buildings", Rexdale, Ontario, 69 pages.

9. Chwalla, E. (1934) "Theorie des aussermittig gedruckter Stabes

aus Baustahl" Der Stahlbau, Vol. 7, October and November 1934.

10. Drysdale, R.G., Sallam, S.E.A. and Karaluk, E. (1976) "Design of Masonry Walls and Columns for Combined Axial Load and Bending Moment" First Canadian Masonry Conference, Calgary, June 1976, pp. 394-408.

11. Drysdale, R.G. and Hamid, A.A. (1983), "Capacity of Block Masonry Under Eccentric Compression Loading", American Concrete Institute Journal, Vol. 80, No. 2, March-April 1983, pp. 102-108.

12. Ellis, J. S. (1958) "Plastic Behaviour of Compression Members" Journal of the Mechanics and Physics of Solids, Vol. 6, p 82, 1958.

13. Fattal, S.G. and Cattaneo, L.E. (1976), "Structural Performance of Masonry Walls Under Compression and Flexure" Building Science Series No. 73, National Bureau of Standards, Washington, June1976.

14. Galambos, T. V.(1968) "Structural Members and Frames", New York, Prentice-Hall, (1968).

15. Hamid, A.A (1978), "Behaviour Characteristics of Concrete Masonry", Ph.D Thesis, McMaster University, September 1978.

16. Hatzinikolas, M.A., Longworth, J. and Warwaruk, J. (1978) "Concrete Masonry Walls", Report No.70, Edmonton, September 1978.

17. Hatzinikolas, M.A., Longworth, J. and Warwaruk, J. (1978) "Experimental Data For Concrete Masonry Walls", Report No.71, Edmonton, September 1978.

18. Hatzinikolas, M.A., Longworth, J. and Warwaruk, J. (1980) "Failure Modes for Eccentrically Loaded Concrete Block Masonry Walls", ACI Journal No.17-28, July-August 1980, pp 258-263.

19. Hilsdorf, H.K. (1969) "Investigation into the Failure Mechanism of Brick Masonry loaded in Axial Compression" International Conference on Masonry Structural Systems, university of Texas, Austin, 1967 pp. 34-41.

20. Horne, M. R.(1956) "The Elastic Plastic Theory of Compression Member" Journal of the Mechanics and Physics of Solids, Vol. 4, p104, 1956.

21. Lind, N.C., (1975), "Newmark's Numerical Method" Solid Mechanics Division, University of Waterloo, University of Waterloo Press, 1975.

22. MacGregor, J.G., Breen, J.E and Pfrang, E.O. (1970)"Design of Slender Concrete Columns" Journal of American Concrete Institute 57, (1), 6, 1970.

23. MacGregor, J.G., Oelhafen, U.H. and Hage, S.E. (1975), "A Re-examination of the EI Values for Slender Columns" Reinforced Concrete Columns (SP-50), ACI, Detroit, Michigan 1975, pp 1-40.

24. MacGregor, J.G., Barter, S. L. (1966), "Long Eccentrically Loaded Concrete Columns Bent in Double Curvature" Symposium on Reinforced Concrete Columns (SP-13), ACI, Detroit, Michigan 1966, pp 139-156.

25. Nathan, N. D. (1972) "Slenderness of Prestressed Concrete Columns" PCI Journal, Vol. 17, No. 6, November/December, 1972, pp 45-57.

26. Nathan, N.D. (1985) "A Computer Program for Rational Analysis of Beam-columns. Research Report, Department of Civil Engineering, the University of British Columbia, 1985.

27. Newmark, N.M, (1942), "Numerical Procedure for Computing Deflections, Moments and Buckling Loads" Transactions of the American Society of Civil Engineers, paper no. 2202, May 1942.

28. Ojalvo, M. (1960) "Restrained Columns" Proceedings ASCE, Vol. 86, No. EM5, Proc. Paper 2615, pp. 1-11, October 1960.

29. Ojinaga, J.(1976), "The Ultimate Strength of Load Bearing Brick and Block Masonry Walls", M.Eng. thesis, Department of Civil Engineering, McGill University, Montreal, July 1976.

30. Ojinaga, J. and Tukstra, C.J(1980) "Design of Plain Masonry Walls", Canadian Journal of Civil Engineering, Vol.7, 1980, pp. 233-242.

31. Ojinaga, J. and Tukstra, C.J(1982) "Design of Reinforced Masonry Walls and Columns for Gravity Loads", Canadian Journal of Civil Engineering, Vol.9, 1982, pp. 84-95.

32. Risager, S. "The Buckling Load of Linear Elastic Wall without Tensile Strength", Proceedings of the Second International Brick Masonry Conference, Stoke-on-Trent, England, April 1970, pp 133-136.

33. Sahlin, S., (1971),"Structural Masonry", Englewood Cliffs, N.J., Prentice-Hall, Inc., 1971.

34. Shrive, N.G. (1982), "The Failure Mechanism of Face-shell bedded (Ungrouted and Unreinforced) Masonry" International Journal of Masonry Construction, Vol.2, No.3.

35. Structural Clay Products Institute "Recommended Practice for

Engineered Brick Masonry", Maclean, Virginia, November 1969.

36. Sahlin, S. (1965), "Diagrams of Critical Stress for Columns of Material without Tensile Strength" National Swedish Institute for Building Research, Report 16/65, Stockholm, Sweden, 1965.

37. Suwalski, P.D., Drysdale, R.G. (1986), "Influence of Slenderness on the Capacity of Block Walls" Proceedings of the Fourth Canadian Masonry Symposium, pp 122-135.

38. Von Karman, T. (1910) "Untersuchungen uber Knickfestigkeit" Mitteilungen uber Forschungsarbeiten auf dem Gebiete des Ingenieurwesens, No. 81, Berlin, (1910)

39. Yao,C. (1989) "An Alternate Basis for Concrete Masonry Under Eccentric Compression" Proceedings Fifth Canadian Masonry Symposium, June 1989, Vancouver B.C., pp 145-154.

40. Yokel, F.Y. (1971) "Stability and Load Capacity of Members with no Tensile Strength", Journal of the Structural Division, Proceedings of the ASCE, Vol.97, No. ST7, July 1971, Proc. Paper 8253, pp. 1913-1926.

41. Yokel, F.Y. and Dikkers, R.D.(1971) "Strength of Load Bearing Masonry Walls", Journal of the Structural Division, Proceedings of the ASCE, Vol.97, May 1971, pp. 1593-1609.

42. Young, B.W., (1973) "The in-plane failure of steel beam-columns", The Structural Engineer, London, England, volume 51, No. 1, January, 1973, pp. 27-35.

APPENDIX A
LISTING OF THE PROGRAM USING COLUMN DEFLECTION CURVE METHOD

```
      DIMENSION PX(100),XMX(100),XMOM(410),CURV(410)
      READ(5,1)FM1,XK,E0
1     FORMAT(1X,3F20.6)
      WRITE(6,1)FM1,XK,E0
      READ(5,2)T,B1,B2,T1,AS,ES,FY
      WRITE(6,1)T,B1,B2
      WRITE(6,59)T1,AS,ES,FY
59    FORMAT(1X,4F14.2)
2     FORMAT(1X,7F10.2)
      READ(5,3)FL,DRAT,DEC
      WRITE(6,3)FL,DRAT,DEC
3     FORMAT(3F15.4)
      CALL PM1(FM1,XK,E0,T,B1,B2,T1,AS,ES,FY,PO,PX,XMX,NPM)
      WRITE(6,27)PO
27    FORMAT(5X,'PURE AXIAL CAPACITY (KIPS) IS)',5X,F15.3)
      WRITE(6,13)
13    FORMAT(// 10X,'LOAD',10X,'MOMENT',//)
      DO 11 I=1,NPM
11    WRITE(6,4) PX(I),XMX(I)
4     FORMAT(5X,F12.3,5X,F12.3)
      DO 399 LL=1,19
      PS=LL*PO/20.0
      CALL CMC(FM1,XK,E0,T,B1,B2,T1,AS,ES,FY,PS,
      &XMOM,CURV,NPC)
      DO 45 KX=1,NPC
45    WRITE(6,6)CURV(KX),XMOM(KX)
6     FORMAT(2(4X,E12.4))
      CALL CDC(PS,FL,T,DRAT,DEC,XMOM,CURV,NPC)
399   CONTINUE
      STOP
      END
      SUBROUTINE PM1(FM1,XK,E0,T,B1,B2,T1,AS,ES,FY,PO,PX,
     &XMX,NPM)
      DIMENSION PX(100),XMX(100)
      TT=T-T1
      D=T/40.
      PO=FM1*XK*(2*T1*B1+(TT-T1)*B2)+FY*AS
      WRITE(6,72)PO
 72   FORMAT(5X,F15.3)
      N=40
      K=0
 10   K=K+1
      IF(K.LE.12)THEN
      BETA=(1.-K)*9.*T/11.+10*T
      ELSE
      BETA=T-D*K
      ENDIF
      PHI=E0/BETA
      X0=E0/PHI
      EST=E0-PHI*T/2.0
      BETAP=BETA*100.0/T
      IF(BETA.GT.T1) GO TO 11
      X1=BETA
      X2=0.0
      CALL CONCR(X1,X2,X0,XK,CONC,XCE,FM1)
      P1=CONC*B1
      XC1=BETA-XCE
      P2=0.0
      P3=0.0
      XC2=0.0
      XC3=0.0
      GO TO 99
 11   IF(BETA.GT.TT) GO TO 22
      X1=BETA
      X2=BETA-T1
      CALL CONCR(X1,X2,X0,XK,CONC,XCE,FM1)
      P1=CONC*B1
      XC1=BETA-XCE
      X3=0.0
      CALL CONCR(X2,X3,X0,XK,CONC,XCE,FM1)
      P2=CONC*B2
      XC2=BETA-XCE
      P3=0.0
      XC3=0.0
      GO TO 99
22    IF(BETA.GT.T)GO TO 33
      X1=BETA
      X2=BETA-T1
      CALL CONCR(X1,X2,X0,XK,CONC,XCE,FM1)
      P1=CONC*B1
      XC1=BETA-XCE
      X3=BETA-TT
      CALL CONCR(X2,X3,X0,XK,CONC,XCE,FM1)
      P2=CONC*B2
      XC2=BETA-XCE
      X4=0.0
      CALL CONCR(X3,X4,X0,XK,CONC,XCE,FM1)
      P3=CONC*B1
      XC3=BETA-XCE
      GO TO 99
33    X1=BETA
      X2=BETA-T1
      CALL CONCR(X1,X2,X0,XK,CONC,XCE,FM1)
      P1=CONC*B1
      XC1=BETA-XCE
      X3=BETA-TT
      CALL CONCR(X2,X3,X0,XK,CONC,XCE,FM1)
      P2=CONC*B2
      XC2=BETA-XCE
      X4=BETA-T
      CALL CONCR(X3,X4,X0,XK,CONC,XCE,FM1)
      P3=CONC*B1
      XC3=BETA-XCE
99    FS=ES*EST
```

```
      FSA=ABS(FS)
      IF(FSA.GT.FY)FS=FS*FY/FSA
      P4=FS*AS
      P=P1+P2+P3+P4
      XM=P1*(T/2.0-XC1)+P2*(T/2-XC2)+P3*(T/2-XC3)
      Y=XM/P
      NPM=K
      PX(NPM)=P
      XMX(NPM)=XM
      IF(P.LE.0.0)GO TO 100
      IF(K.LT.N)GO TO 10
100   RETURN
      END
      SUBROUTINE CONCR(X1,X2,X0,XK,CONC,XCE,FM1)
      X11=X1/X0
      X22=X2/X0
      CONC1=FM1*XK*X0*(X11*X11-X11**3/3.0)
      XCE1=X0*(2.0*X11/3.0-X11*X11/4.0)/(1.0-X11/3.)
      CONC2=FM1*XK*X0*(X22*X22-X22**3/3.0)
      XCE2=X0*(2.0*X22/3.0-X22*X22/4.0)/(1.0-X22/3.)
      CONC=CONC1-CONC2
      XCE=(CONC1*XCE1-CONC2*XCE2)/CONC
      RETURN
      END
      SUBROUTINE
     &CMC(FM1,XK,E0,T,B1,B2,T1,AS,ES,FY,PS,XMOM,CURV,KX)
      DIMENSION XMOM(410),CURV(410)
      DP=0.01*PS
      PHI1=1.0E-05
      DPHI=1.0E-05
      DE=0.0003
      WRITE(6,12)
12    FORMAT(5X,'FORCE P',4X,'DELTA P',6X,'PHI',6X,'DPHI',
     &6X,'DE')
      WRITE(6,13)PS,DP,PHI1,DPHI,DE
13    FORMAT(1X,5E12.3)
```

```
      WRITE(6,7)
    7 FORMAT(///5X,'PHI',7X,'MOMENT  KNM'//)
C
C     ESTIMATE THE STARTING STRAIN E1
C
      EC=1000.*FM1*XK
      AE=(2.0*T1*B1+(T-T1)*B2)*EC
      AE=AS*(ES-EC)+AE
      E1=PS/AE
C
C     WITH A CURVATURE PHI CALCULATE THE CORRESP  MOMENT
      KX=1
      M=0
  110 K=0
   10 IF(E1.LE.0.0)E1=1.E-6
      IF(PHI1.LE.0.0)PHI1=.5E-7
      BETA=E1/PHI1
      X0=E0/PHI1
      EST=E1-PHI1*T/2.0
      TT=T-T1
      IF(BETA.GT.T1) GO TO 11
      X1=BETA
      X2=0.0
      CALL CONCR(X1,X2,X0,XK,CONC,XCE,FM1)
      PP1=CONC*B1
      XC1=BETA-XCE
      PP2=0.0
      PP3=0.0
      XC2=0.0
      XC3=0.0
      GO TO 99
   11 IF(BETA.GT.TT) GO TO 22
      X1=BETA
      X2=BETA-T1
      CALL CONCR(X1,X2,X0,XK,CONC,XCE,FM1)
      PP1=CONC*B1
      XC1=BETA-XCE
      X3=0.0
      CALL CONCR(X2,X3,X0,XK,CONC,XCE,FM1)
      PP2=CONC*B2
      XC2=BETA-XCE
      PP3=0.0
      XC3=0.0
      GO TO 99
22    IF(BETA.GT.T)GO TO 33
      X1=BETA
      X2=BETA-T1
      CALL CONCR(X1,X2,X0,XK,CONC,XCE,FM1)
      PP1=CONC*B1
      XC1=BETA-XCE
      X3=BETA-TT
      CALL CONCR(X2,X3,X0,XK,CONC,XCE,FM1)
      PP2=CONC*B2
      XC2=BETA-XCE
      X4=0.0
      CALL CONCR(X3,X4,X0,XK,CONC,XCE,FM1)
      PP3=CONC*B1
      XC3=BETA-XCE
      GO TO 99
33    X1=BETA
      X2=BETA-T1
      CALL CONCR(X1,X2,X0,XK,CONC,XCE,FM1)
      PP1=CONC*B1
      XC1=BETA-XCE
      X3=BETA-TT
      CALL CONCR(X2,X3,X0,XK,CONC,XCE,FM1)
      PP2=CONC*B2
      XC2=BETA-XCE
      X4=BETA-T
      CALL CONCR(X3,X4,X0,XK,CONC,XCE,FM1)
      PP3=CONC*B1
      XC3=BETA-XCE
```

```
   99 FS=ES*EST
      FSA=ABS(FS)
      IF(FSA.GT.FY)FS=FS*FY/FSA
      PP4=FS*AS
      P=PP1+PP2+PP3+PP4
C
C     CHECK AXIAL FORCE
C
      DP1=P-PS
      ADP1=ABS(DP1)
      IF(ADP1.LE.DP)GO TO 50
C
C     CHECK STRAIN
C
      P1=DP1
      IF(K.NE.0) GO TO 140
      K=1
      E2=E1
      P2=P1
      E1=E1+DE
      GO TO 10
  140 IF(M.EQ.1)GO TO 45
      EE=E1-(E2-E1)*P1/(P2-P1)
      E2=E1
      E1=EE
      P2=P1
      IF(E1.LT.E0)GO TO 10
      M=1
      E1=E0
      PHI2=PHI1
      PHI1=PHI1+DPHI
      GO TO 10
   45 PHI3=PHI1-(PHI2-PHI1)*P1/(P2-P1)
      PHI2=PHI1
      PHI1=PHI3
      P2=P1
      GO TO 10
C
C     CALCULATE MOMENT
C
   50 XM=PP1*(T/2.0-XC1)+PP2*(T/2.-XC2)+PP3*(T/2.-XC3)
C
C     PRINT OUT PUT
C
      CURV(KX)=PHI1
      XMOM(KX)=XM
C     WRITE(6,6)CURV(KX),XMOM(KX),E1,BETA
C 6   FORMAT(4(2X,E12.4))
      PHI1=PHI1+DPHI
      IF(M.EQ.1)GO TO 111
      KX=KX+1
      IF(KX.GT.400) THEN
      WRITE(6,38)
   38 FORMAT(5X,'KX is GT 400 REVISE DIMENSION')
      GO TO 111
      ENDIF
      GO TO 110
  111 CONTINUE
      RETURN
      END
      SUBROUTINE CDC(PS,FL,T,DRAT,DEC,XMOM,CURV,NPC)
      DIMENSION ENDVAL(22,3),SLOPE(100),DEFL(100),CURVE(100)
      DIMENSION XMOM(410),CURV(410)
C
C     SET INITIAL VALUES
C
      DELTAX=T*DRAT
      DO 40 I=1,22
      DO 40 K=1,3
   40 ENDVAL(I,K)=0.0
      UMOM=0.0
      DO 50 I=1,NPC
   50 IF(XMOM(I).GT.UMOM) UMOM=XMOM(I)
      NLMAX=FL/DELTAX/2.+2.
      IX=0
      K=0
      BIGMOM=0.
      XMENDM=0.0
      WRITE(6,61)
   61 FORMAT(/,5X,'PS T DRAT FL DEC DELTAX  UMOM',/)
      WRITE(6,62)PS,T,DRAT,FL,DEC,DELTAX,UMOM
   62 FORMAT(/,5X,7(F6.2,1X))
C
C     RETURN HERE TO START A NEW CDC
C
  100 IX=IX+1
      WRITE(6,65)IX
   65 FORMAT(//,5X,'*****  CDC  NO.   *****',5X,I5,//)
      BIGML=BIGMOM
      BIGMOM=UMOM*(1.0-(IX-1.0)*DEC)
      SLOPE(1)=0.0
      DEFL(1)=BIGMOM/PS
      IY=0
      WRITE(6,66)
   66 FORMAT(//,8X,'NODE',5X,'DEFLECTION',10X,'SLOPE',9X,
     &'MOMENT',/)
C
C     RETURN HERE TO START A NEW SEGMENT OF CDC
C
  200 IY=IY+1
      FMOM=(DEFL(IY)+DELTAX*SLOPE(IY)/2.)*PS
      CALL RMCR(CURV,XMOM,NPC,FMOM,CURVE(IY),UMOM)
      IZ=IY+1
      DEFL(IZ)=DEFL(IY)+SLOPE(IY)*DELTAX-.5*CURVE(IY)
     &*DELTAX**2
      SLOPE(IZ)=SLOPE(IY)-CURVE(IY)*DELTAX
      WRITE(6,77)IY,DEFL(IY),SLOPE(IY),FMOM
   77 FORMAT(7X,I5,3(F12.4,3X))
```

```
C          CHECK IF THE LENGTH HAS BEEN EXCEEDED
C          OR CDC QUARTER WAVE HAS BEEN COMPLETED
C          OR  WHETHER NO. OF INCREMENTS EXCEED 100
C
           IF(IZ.EQ.NLMAX) GO TO 500
           IF(DEFL(IZ).LE.0.)GO TO 500
           IF(IZ.NE.100) GO TO 200
           WRITE(6,350)
      350  FORMAT(//,'IZ GT 100 REVISE DIMENSION')
      500  CONTINUE
C
C          FIND THE END VALUES ON THE CDC
           NODEL=FL/DELTAX/2.+1
           IF(NODEL.GT.IZ) GO TO 600
           IF(NODEL.LT.IZ) GO TO 550
           FMOM=(DEFL(NODEL)+DELTAX*SLOPE(NODEL)/2.)*PS
           CALL RMCR(CURV,XMOM,NPC,FMOM,CURVE(NODEL),UMOM)
      550  CONTINUE
           DELTEX=FL/2.-(NODEL-1)*DELTAX
           ENDVAL(IX,1)=DEFL(NODEL)+SLOPE(NODEL)*DELTEX-
           &.5*CURVE(NODEL)*DELTEX**2
           IF(ENDVAL(IX,1).LT.0.)ENDVAL(IX,1)=0.
           ENDVAL(IX,2)=SLOPE(NODEL)-CURVE(NODEL)*DELTEX
           ENDVAL(IX,3)=ENDVAL(IX,1)*PS
      600  CONTINUE
           WRITE(6,111)IX,ENDVAL(IX,1),ENDVAL(IX,2),ENDVAL(IX,3)
      111  FORMAT(//,10X,'END VALUES FOR CDC',I5,/,10X,'DEFLECTION
          &= ',5X ,F12.4,/,10X,'SLOPE=',5X,F12.4,/,10X,'MOMENT = ',5X,
          &F12.4)
           IF(ENDVAL(IX,1).GT.XMENDM)THEN
           XMENDM=ENDVAL(IX,1)
C          IF(ENDVAL(IX,1).GT.XMENDM)K=IX
           K=IX
           ENDIF
C          STOP IF STARTING MID-HEIGHT DEFLECTION IS REDUCED
C          TO ZERO
```

```
      IF(DEFL(1).GT.0.0) GO TO 100
      WRITE(6,122)XMENDM,K
 122  FORMAT(//,5X,'MAX.  END DEFLN. = ',3X,F12.3,'OCCURS FOR
     &.CDC.NO',I6)
1000  CONTINUE
      STOP
      END
      SUBROUTINE RMCR(CURV,XMOM,NPC,XXM,XPHI,UMOM)
      DIMENSION  XMOM(410),CURV(410)
      IF(XMOM(1).GT.XXM) THEN
      XPHI=CURV(1)*XXM/XMOM(1)
      GO TO 110
      ENDIF
      IF(XXM.GT.UMOM) THEN
      WRITE(6,138)  XXM
 138  FORMAT(/,5X,'MOMENT IS OUT OF RANGE OF M-PHI
     &RELATION',5X,F15.3)
      GO TO 110
      ENDIF
      J=2
 119  IF(XMOM(J).GE.XXM) THEN
      JJ=J-1
      XPHI=CURV(JJ)+(CURV(J)-CURV(JJ))*(XXM-XMOM(JJ))/
     &(XMOM(J)-XMOM(JJ))
      GO TO 110
      ENDIF
      J=J+1
      IF(J.LE.NPC) GO TO 119
 110  CONTINUE
      RETURN
      END
```

APPENDIX B

LISTING OF THE PROGRAM USING NEWMARK'S NUMERICAL METHOD

```
       DIMENSION PX(100),XMX(100),XMOM(1000),
     &CURV(1000),DEFL(21),XCURV(21),CONCUR(21),
     &XMMT(21),DISPL(21),RATIO(60),AVGSLO(22)
       READ(5,1)FM1,XK,E0
   1   FORMAT(1X,3F20.6)
       WRITE(6,1)FM1,XK,E0
       READ(5,2)T,B1,B2,T1,AS,ES,FY
       WRITE(6,1)T,B1,B2
       WRITE(6,59)T1,AS,ES,FY
   59  FORMAT(1X,4F14.2)
   2   FORMAT(1X,7F10.2)
       READ(5,3)FL,TETA
       WRITE(6,3)FL,TETA
   3   FORMAT(2F15.4)
       CALL PM1(FM1,XK,E0,T,B1,B2,T1,AS,ES,FY,PO,PX,XMX,NPM)
       WRITE(6,27)PO
   27  FORMAT(5X,'PURE AXIAL CAPACITY (KIPS) IS)',5X,F15.3)
C      WRITE(6,13)
   13  FORMAT(// 10X,'LOAD(KIPS)',10X,'MOMENT(KIPS-IN)',//)
C      DO 11 I=1,NPM
C  11  WRITE(6,4) PX(I),XMX(I)
   4   FORMAT(5X,F12.3,5X,F12.3)
       DO 399 LL=1,19
       PS=LL*PO/20.0
       CALL CMC(FM1,XK,E0,T,B1,B2,T1,AS,ES,FY,PS,
     &XMOM,CURV,NPC)
C      DO 45 KX=1,NPC
C  45  WRITE(6,6)CURV(KX),XMOM(KX)
C  6   FORMAT(2(4X,E12.4))
C      WRITE(6,674)
   674 FORMAT(//,2X,'ENDMOMENT',3X,'II',20X,'DEFLECTIONS AT
     &NODES',/, 14X,'1   3   5   7   9   11   13   15   17   19   21',//)
     &XMOMIN=(B1*T**3-(B1-B2)*(T-2.0*T1)**3)/12.0
       ECM=2.0*FM1*XK/E0
       UMOM=0.0
       DO 50 I=1,NPC
   50  IF(XMOM(I).GT.UMOM)UMOM=XMOM(I)
```

```
      ENDMOM=0.0
      DENDMO=UMOM/50.0
  200 II=0
      ENDMOM=ENDMOM+DENDMO
      CALL YELAST(PS,ENDMOM,TETA,ECM,XMOMIN,DEFL,FL)
C     WRITE(6,702)(DEFL(I),I=1,21)
  150 CONTINUE
      II=II+1
      DO 35 KI=1,21
   35 DISPL(KI)=DEFL(KI)
C     FIND MOMENTS
      DO 36 I=1,21
      X=(I-1)*FL/20.0
   36 XMMT(I)=PS*DEFL(I)+ENDMOM-(1.0-TETA)*ENDMOM*X/FL
      IF(TETA.EQ.-1.0)THEN
      DINIM=PS*FL/1000.0
      DO 437 I=1,21
      X=(I-1)*22.0/(7.0*20.00)
  437 XMMT(I)=XMMT(I)+DINIM*SIN(X)
      ENDIF
      MATF=0
C     FIND CURVATURES
      DO 52 I=1,21
      CALLRMCR(CURV,XMOM,NPC,XMMT(I),XCURV(I),
     &UMOM,MATF)
      IF(MATF.EQ.1)THEN
      WRITE(6,41)PS,ENDMOM,XMMT(I),UMOM
   41 FORMAT(2X,4(F10.2,1X))
C     WRITE(6,672)ENDMOM,I
  672 FORMAT(//,5X,'MATERIAL FAILED FOR ENDMOM=',2X,F15.3,
     &2X,'AT NODE NO. ',2X,I5//)
      GO TO 999
      END IF
   52 CONTINUE
C     FIND CONCENTRATION OF CURVATURES
      CALL CONCEN(XCURV,CONCUR,FL)
C     MID INTERVEL SLOPE IS ASSUMED TO GET APROXIMATE
C     DEFLECTIONS
      SUM=0.00
      DO 911 I=1,21
  911 SUM=SUM+ABS(CONCUR(I))
      SUM=SUM/2.0
      IF(TETA.LT.0.0)SUM=SUM/2.0
      DO 72 J=1,21
      AVGSLO(J)=SUM
   72 SUM=AVGSLO(J)-CONCUR(J)
C     APPROXIMATE DEFLECTIONS
      SUM=0.0
      DO 81 J=1,21
      DEFL(J)=SUM
   81 SUM=DEFL(J)+AVGSLO(J+1)*FL/20.0
C     CORRECTED DEFLECTIONS
      WRONG=DEFL(21)
      DO 91 J=1,21
   91 DEFL(22-J)=DEFL(22-J)-((21-J)/20.)*WRONG
C     SLOPES ALONG THE MEMBER
      DO 403 J=1,20
      STD=DEFL(J)*DEFL(J+1)
      IF(STD.GE.0.0)THEN
      AVGSLO(J)=(ABS(DEFL(J+1))-ABS(DEFL(J)))*20.0/FL
      ELSE
      AVGSLO(J)=(ABS(DEFL(J+1))+ABS(DEFL(J)))*20.0/FL
      ENDIF
  403 CONTINUE
      AVGSLO(21)=AVGSLO(20)
C     WRITE(6,702)(AVGSLO(I),I=1,21)
  702 FORMAT(2X,21(F12.5,2X))
C     PRINT DEFLECTIONS
C     WRITE(6,675)ENDMOM,II,(DEFL(I),I=1,21)
675   FORMAT(/,2X,F7.3,2X,I2,2X,21(F10.3,2X),/)
C     CHECK ON CONVERGENCE OF THE DEFLECTIONS
      SUM1=0.0
      SUM2=0.0
      DO 102 J=1,21
      SUM1=SUM1+ABS(DISPL(J))
  102 SUM2=SUM2+ABS(DEFL(J))
      RATIO(II)=SUM1/SUM2
C     WRITE(6,649)II,SUM1,SUM2,RATIO(II)
  649 FORMAT(5X,I5,3(5X,F12.4))
      IF(II.LT.3)GO TO 150
      IF(II.GT.50)GO TO 901
      IF(RATIO(II)-RATIO(II-1).LT.-0.01)GO TO 901
      IF(RATIO(II).GT.0.99.AND.RATIO(II).LT.1.01)GO TO 200
      IF(SUM2.GT.SUM1.AND.RATIO(II).GE.RATIO(II-1)) GO TO 150
      IF(SUM2.LT.SUM1.AND.RATIO(II).LE.RATIO(II-1)) GO TO 150
  901 WRITE(6,42)PS,ENDMOM,UMOM
```

```
42   FORMAT(2X,2(F10.2,1X),11X,F10.2)
46   FORMAT(2X,'DEFLNS. DO NOT CONVERGE FOR
    &ENDMOMENT=',5X,F8.3)
999  CONTINUE
399  CONTINUE
     STOP
     END
     SUBROUTINE CONCEN(XCURV,CONCUR,FL)
     DIMENSION XCURV(21),CONCUR(21)
     DO 62 I=1,21
     IF(I.GT.1.AND.I.LT.21) THEN
     CONCUR(I)=FL*(XCURV(I-1)*2.+20.*XCURV(I)+
    &2.*XCURV(I+1))/480.0
     END IF
     IF(I.EQ.1)CONCUR(I)=FL*(7.0*XCURV(1)+
    &6.*XCURV(2)-XCURV(3))/480.
     IF(I.EQ.21)CONCUR(I)=FL*(7.0*XCURV(21)+
    &6.*XCURV(20)-XCURV(19))/480.
62   CONTINUE
     RETURN
     END
     SUBROUTINE YELAST(PS,ENDMOM,TETA,ECM,XMOMIN,
    &DEFL,FL)
     DIMENSION DEFL(21)
     DO 32 I=1,21
     X=(I-1)*FL/20.0
32   DEFL(I)=ENDMOM*X/(6.*ECM*XMOMIN*FL)*
     &((1.-TETA)*X*X-3.*X*FL+(2.+TETA)*FL*FL)
     RETURN
     END
     SUBROUTINE PM1(FM1,XK,E0,T,B1,B2,T1,AS,ES,FY,PO,PX,
    &XMX,NPM)
     DIMENSION  PX(100),XMX(100)
     TT=T-T1
     D=T/40.
     PO=FM1*XK*(2*T1*B1+(TT-T1)*B2)+FY*AS
C    WRITE(6,72)PO
72   FORMAT(5X,F15.3)
     N=40
     K=0
10 K=K+1
     IF(K.LE.12)THEN
     BETA=(1.-K)*9.*T/11.+10*T
```

```
      ELSE
      BETA=T-D*K
      ENDIF
      PHI=E0/BETA
      X0=E0/PHI
      EST=E0-PHI*T/2.0
      BETAP=BETA*100.0/T
      IF(BETA.GT.T1) GO TO 11
      X1=BETA
      X2=0.0
      CALL CONCR(X1,X2,X0,XK,CONC,XCE,FM1)
      P1=CONC*B1
      XC1=BETA-XCE
      P2=0.0
      P3=0.0
      XC2=0.0
      XC3=0.0
      GO TO 99
11    IF(BETA.GT.TT) GO TO 22
      X1=BETA
      X2=BETA-T1
      CALL CONCR(X1,X2,X0,XK,CONC,XCE,FM1)
      P1=CONC*B1
      XC1=BETA-XCE
      X3=0.0
      CALL CONCR(X2,X3,X0,XK,CONC,XCE,FM1)
      P2=CONC*B2
      XC2=BETA-XCE
      P3=0.0
      XC3=0.0
      GO TO 99
22    IF(BETA.GT.T)GO TO 33
      X1=BETA
      X2=BETA-T1
      CALL CONCR(X1,X2,X0,XK,CONC,XCE,FM1)
      P1=CONC*B1
      XC1=BETA-XCE
      X3=BETA-TT
      CALL CONCR(X2,X3,X0,XK,CONC,XCE,FM1)
      P2=CONC*B2
      XC2=BETA-XCE
      X4=0.0
      CALL CONCR(X3,X4,X0,XK,CONC,XCE,FM1)
      P3=CONC*B1
      XC3=BETA-XCE
      GO TO 99
 33   X1=BETA
      X2=BETA-T1
      CALL CONCR(X1,X2,X0,XK,CONC,XCE,FM1)
      P1=CONC*B1
      XC1=BETA-XCE
      X3=BETA-TT
      CALL CONCR(X2,X3,X0,XK,CONC,XCE,FM1)
      P2=CONC*B2
      XC2=BETA-XCE
      X4=BETA-T
      CALL CONCR(X3,X4,X0,XK,CONC,XCE,FM1)
      P3=CONC*B1
      XC3=BETA-XCE
 99   FS=ES*EST
      FSA=ABS(FS)
      IF(FSA.GT.FY)FS=FS*FY/FSA
      P4=FS*AS
      P=P1+P2+P3+P4
      XM=P1*(T/2.0-XC1)+P2*(T/2-XC2)+P3*(T/2-XC3)
      Y=XM/P
      NPM=K
      XMX(NPM)=XM
      IF(P.LE.0.0)GO TO 100
      IF(K.LT.N)GO TO 10
100   RETURN
      END
      SUBROUTINE CONCR(X1,X2,X0,XK,CONC,XCE,FM1)
      X11=X1/X0
      X22=X2/X0
      CONC1=FM1*XK*X0*(X11*X11-X11**3/3.0)
      XCE1=X0*(2.0*X11/3.0-X11*X11/4.0)/(1.0-X11/3.)
      CONC2=FM1*XK*X0*(X22*X22-X22**3/3.0)
      XCE2=X0*(2.0*X22/3.0-X22*X22/4.0)/(1.0-X22/3.)
      CONC=CONC1-CONC2
      XCE=(CONC1*XCE1-CONC2*XCE2)/CONC
      RETURN
      END
      SUBROUTINE CMC(FM1,XK,E0,T,B1,B2,T1,AS,ES,FY,PS,
     &XMOM,CURV,KX)
      DIMENSION XMOM(1000),CURV(1000)
      DP=0.01*PS
      PHI1=1.0E-05
      DPHI=1.0E-05
      DE=0.0003
C     WRITE(6,12)
 12   FORMAT(5X,'FORCE P',4X,'DELTA P',6X,'PHI',6X,'DPHI',6X,'DE')
C     WRITE(6,13)PS,DP,PHI1,DPHI,DE
 13   FORMAT(1X,5E12.3)
C     WRITE(6,7)
  7   FORMAT(///5X,'CURVATURE',7X,'MOMENT  KIP-IN'//)
C
C     ESTIMATE THE STARTING STRAIN E1
C
      EC=2.0*FM1*XK/E0
      AE=((B1*T)-(B1-B2)*(T-2.0*T1))*EC
      AE=AS*(ES-EC)+AE
      E1=PS/AE
C
C     WITH A CURVATURE PHI CALCULATE THE CORRESP
C     MOMENT
      KX=1
      M=0
 110  K=0
 10   IF(E1.LE.0.0)E1=1.E-6
      IF(PHI1.LE.0.0)PHI1=.5E-7
      BETA=E1/PHI1
      X0=E0/PHI1
      EST=E1-PHI1*T/2.0
      TT=T-T1
      IF(BETA.GT.T1) GO TO 11
      X1=BETA
      X2=0.0
      CALL CONCR(X1,X2,X0,XK,CONC,XCE,FM1)
      PP1=CONC*B1
      XC1=BETA-XCE
      PP2=0.0
      PP3=0.0
      XC2=0.0
      XC3=0.0
      GO TO 99
 11   IF(BETA.GT.TT) GO TO 22
      X1=BETA
      X2=BETA-T1
      CALL CONCR(X1,X2,X0,XK,CONC,XCE,FM1)
      PP1=CONC*B1
      XC1=BETA-XCE
      X3=0.0
      CALL CONCR(X2,X3,X0,XK,CONC,XCE,FM1)
      PP2=CONC*B2
      XC2=BETA-XCE
      PP3=0.0
      XC3=0.0
      GO TO 99
22    IF(BETA.GT.T)GO TO 33
      X1=BETA
      X2=BETA-T1
      CALL CONCR(X1,X2,X0,XK,CONC,XCE,FM1)
      PP1=CONC*B1
      XC1=BETA-XCE
      X3=BETA-TT
      CALL CONCR(X2,X3,X0,XK,CONC,XCE,FM1)
      PP2=CONC*B2
      XC2=BETA-XCE
      X4=0.0
      CALL CONCR(X3,X4,X0,XK,CONC,XCE,FM1)
      PP3=CONC*B1
      XC3=BETA-XCE
      GO TO 99
33    X1=BETA
      X2=BETA-T1
      CALL CONCR(X1,X2,X0,XK,CONC,XCE,FM1)
      PP1=CONC*B1
      XC1=BETA-XCE
      X3=BETA-TT
      CALL CONCR(X2,X3,X0,XK,CONC,XCE,FM1)
      PP2=CONC*B2
      XC2=BETA-XCE
      X4=BETA-T
      CALL CONCR(X3,X4,X0,XK,CONC,XCE,FM1)
      PP3=CONC*B1
      XC3=BETA-XCE
99    FS=ES*EST
      FSA=ABS(FS)
      IF(FSA.GT.FY)FS=FS*FY/FSA
      PP4=FS*AS
      P=PP1+PP2+PP3+PP4
```

```
C
C      CHECK AXIAL FORCE
C
       DP1=P-PS
       ADP1=ABS(DP1)
       IF(ADP1.LE.DP)GO TO 50
C
C      CHECK STRAIN
C
       P1=DP1
       IF(K.NE.0) GO TO 140
       K=1
       E2=E1
       P2=P1
       E1=E1+DE
       GO TO 10
  140  IF(M.EQ.1)GO TO 45
       EE=E1-(E2-E1)*P1/(P2-P1)
       E2=E1
       E1=EE
       P2=P1
       IF(E1.LT.E0)GO TO 10
       M=1
       E1=E0
       PHI2=PHI1
       PHI1=PHI1+DPHI
       GO TO 10
   45  PHI3=PHI1-(PHI2-PHI1)*P1/(P2-P1)
       PHI2=PHI1
       PHI1=PHI3
       P2=P1
       GO TO 10
C
C      CALCULATE MOMENT
C
   50  XM=PP1*(T/2.0-XC1)+PP2*(T/2.-XC2)+PP3*(T/2.-XC3)
       CURV(KX)=PHI1
       XMOM(KX)=XM
       PHI1=PHI1+DPHI
       IF(M.EQ.1)GO TO 111
       KX=KX+1
       IF(KX.GT.1000) THEN
       WRITE(6,38)
  38  FORMAT(5X,'KX IS GT 1000 REVISE DIMENSION')
      GO TO 111
      ENDIF
      GO TO 110
 111  CONTINUE
      RETURN
      END
      SUBROUTINE RMCR(CURV,XMOM,NPC,XXM,XPHI,UMOM,MATF)
      DIMENSION  XMOM(1000),CURV(1000)
      JSA=0
      IF(XXM.LT.0.0)THEN
      XXM=ABS(XXM)
      JSA=-1
      ENDIF
      IF(XMOM(1).GT.XXM) THEN
      XPHI=CURV(1)*XXM/XMOM(1)
      GO TO 110
      ENDIF
      IF(XXM.GT.UMOM) THEN
C     WRITE(6,138)  XXM,UMOM
C 138 FORMAT(/,5X,'MOMENT IS OUT OF  M-PHI-RANGE',
     &2(5X,F15.3))
      MATF=1
      GO TO 110
      ENDIF
      J=2
 119  IF(XMOM(J).GE.XXM) THEN
      JJ=J-1
      XPHI=CURV(JJ)+(CURV(J)-CURV(JJ))*(XXM-XMOM(JJ))/
     &(XMOM(J)-XMOM(JJ))
      GO TO 110
      ENDIF
      J=J+1
      IF(J.LE.NPC) GO TO 119
 110  CONTINUE
      IF(JSA.EQ.-1)XPHI=-XPHI
      RETURN
      END
```